AD-A185 149 TECHNICAL PAPERS PRESENTED AT THE DEFENSE NUCLEAR AGENCY GLOBAL EFFECTS R..(U) DOD NUCLEAR INFORMATION AND ANALYSIS CENTER SANTA BARBARA CA.. 15 MAY 86 1/3

UNCLASSIFIED DASIAC-TN-86-29-VOL-1 DNA001-82-C-0274 F/G 15/6.4 NL

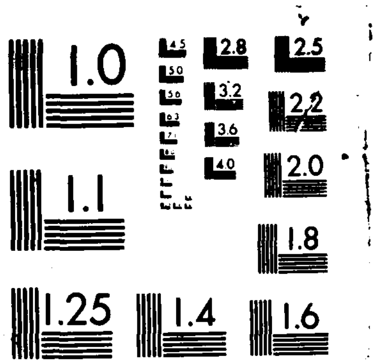

MICROCOPY RESOLUTION TEST CHART
NATIONAL BUREAU OF STANDARDS-1963-A

DASIAC-TN-86-29-V1

TECHNICAL PAPERS PRESENTED AT THE DEFENSE NUCLEAR AGENCY GLOBAL EFFECTS REVIEW

Volume I

Kaman Tempo
Alexandria Office
Huntington Building
2560 Huntington Avenue
Alexandria, VA 22303-1410

15 May 1986

Technical Report

CONTRACT No. DNA 001-82-C-0274

THIS WORK WAS SPONSORED BY THE DEFENSE NUCLEAR AGENCY
UNDER RDT&E RMSS CODE B331086466 P99QMXDC00003 H2590D.

Prepared for
Director
DEFENSE NUCLEAR AGENCY
Washington, DC 20305-1000

DISTRIBUTION LIST UPDATE

This mailer is provided to enable DNA to maintain current distribution lists for reports. We would appreciate your providing the requested information.

☐ Add the individual listed to your distribution list.

☐ Delete the cited organization/individual.

☐ Change of address.

NAME: ____________________

ORGANIZATION: ____________________

OLD ADDRESS	CURRENT ADDRESS

TELEPHONE NUMBER: (   ) ____________________

SUBJECT AREA(s) OF INTEREST:

DNA OR OTHER GOVERNMENT CONTRACT NUMBER: ____________________

CERTIFICATION OF NEED-TO-KNOW BY GOVERNMENT SPONSOR (if other than DNA)

SPONSORING ORGANIZATION: ____________________

CONTRACTING OFFICER OR REPRESENTATIVE: ____________________

SIGNATURE: ____________________

CUT HERE AND RETURN

Director
Defense Nuclear Agency
ATTN: [redacted] TITL
Washington, DC 20305-1000

Director
Defense Nuclear Agency
ATTN: [redacted] TITL
Washington, DC 20305-1000

UNCLASSIFIED
SECURITY CLASSIFICATION OF THIS PAGE

REPORT DOCUMENTATION PAGE

1a REPORT SECURITY CLASSIFICATION: UNCLASSIFIED	1b RESTRICTIVE MARKINGS
2a SECURITY CLASSIFICATION AUTHORITY: N/A since Unclassified	3 DISTRIBUTION / AVAILABILITY OF REPORT: Approved for public release; distribution is unlimited.
2b DECLASSIFICATION / DOWNGRADING SCHEDULE: N/A since Unclassified	
4 PERFORMING ORGANIZATION REPORT NUMBER(S)	5 MONITORING ORGANIZATION REPORT NUMBER(S): DASIAC-TN-86-29-V1
6a NAME OF PERFORMING ORGANIZATION: Kaman Tempo; 6b OFFICE SYMBOL (If applicable)	7a NAME OF MONITORING ORGANIZATION: Director, Defense Nuclear Agency
6c ADDRESS (City, State, and ZIP Code): Alexandria Office, Huntington Building, 2560 Huntington Avenue, Alexandria, VA 22303-1410	7b ADDRESS (City, State, and ZIP Code): Washington, DC 20305-1000
8a NAME OF FUNDING / SPONSORING ORGANIZATION; 8b OFFICE SYMBOL (If applicable)	9 PROCUREMENT INSTRUMENT IDENTIFICATION NUMBER: DNA 001-82-C-0274
8c ADDRESS (City, State, and ZIP Code)	10 SOURCE OF FUNDING NUMBERS

PROGRAM ELEMENT NO	PROJECT NO	TASK NO	WORK UNIT ACCESSION NO
62715H	P99QMXD	C	DH008684

11 TITLE (Include Security Classification)
TECHNICAL PAPERS PRESENTED AT THE DEFENSE NUCLEAR AGENCY GLOBAL EFFECTS REVIEW
Volume 1

12 PERSONAL AUTHOR(S)
Various

13a TYPE OF REPORT	13b TIME COVERED	14 DATE OF REPORT (Year, Month, Day)	15 PAGE COUNT
Technical Report	FROM 860225 TO 860512	860515	268

16 SUPPLEMENTARY NOTATION
This work was sponsored by the Defense Nuclear Agency under RDT&E RMSS Code B331086466 P99QMXDC00003 H2590D.

17 COSATI CODES			18 SUBJECT TERMS (Continue on reverse if necessary and identify by block number)
FIELD	GROUP	SUB-GROUP	
04	01		Nuclear War
15	06		Global Climate Effects

19 ABSTRACT (Continue on reverse if necessary and identify by block number)

This document contains technical papers presented at the Defense Nuclear Agency Review of Global Effects held at NASA Ames Research Center 25-27 February 1986.

20 DISTRIBUTION / AVAILABILITY OF ABSTRACT: ☐ UNCLASSIFIED/UNLIMITED ☒ SAME AS RPT ☐ DTIC USERS	21 ABSTRACT SECURITY CLASSIFICATION: UNCLASSIFIED
22a NAME OF RESPONSIBLE INDIVIDUAL: Sandra E. Young	22b TELEPHONE (Include Area Code): (202) 325-7042; 22c OFFICE SYMBOL: DNA/CSTI

DD FORM 1473, 84 MAR — 83 APR edition may be used until exhausted. All other editions are obsolete.

SECURITY CLASSIFICATION OF THIS PAGE
UNCLASSIFIED

PREFACE

The Defense Nuclear Agency has collected and printed the attached papers from the February 25-27 1986 Global Effects review as a service to the community. The Defense Nuclear Agency takes this opportunity to express its gratitude to the numerous participants in the Global Effects review.

The technical papers enclosed include all those which were received by DNA prior to the closing date of 28 April 1986. Where papers are missing their place is occupied by the abstract received prior to the meeting.

The inclusion of a paper in this proceeding does not necessarily imply endorsement of the results of the research reported or conclusions which might be drawn from that research. It is the opinion of the Defense Nuclear Agency that, while good progress is being made in improving our understanding of Global Effects, the results to date are tentative and preliminary and should not be used for planning beyond the planning of future research.

TABLE OF CONTENTS

		Page
PREFACE		iii
SECTION 1	Fuel Bed Database Compilation	1
1.	Urban Area Analysis and Smoke Production - Anno, Bush, Dore, Small	2
2.	A Critical Examination of Methods of Estimating the Spatial Distribution and Magnitudes of Urban Fuel Loadings - Simonett	23
3.	Estimates of Total Combustible Material in NATO and Warsaw Pact Countries - Bing	24
SECTION 2	Smoke Source Term	43
4.	Smoke Emission and Properties - Mulholland	44
5.	Source Term Research Program at Sandia National Laboratories - Zail, Nowlan, Keltner, Bergeron	83
6.	Measurements of the Radiative Properties of Smoke Emissions from Vegetative Fuels: Relationship of this Data to Desired Information on the Properties of Urban Smoke Emissions - Patterson	116
7.	Wildland Fires and Nuclear Winters: Selected Reconstructions of Historic Large Fires - Pyne, Omi	146
8.	Progress in Developing the Smoke Source Term for "Nuclear Winter" Studies: Major Uncertainties - Penner	147
9.	Supermicron Wind Suspended Particles and Firestorm Plume Coagulation - Porch, Penner	173
10.	High Reliability Fire-Start Mechanism - Martin	182
11.	Collision Formation Kinetics and Optical Properties of Submicrometer, Post Detonation Aerosols - Marlow	193
SECTION 3	Dust Source Term	204
12.	Radiative Properties of Dust for Input to Dust Source Terms for Models of the Global Effects of a Nuclear Exchange - Patterson	205
13.	Micro-Analytical Techniques for Characterizing the Optical Properties of Soil Aerosols - Kinsey, Muleski, Coveney	220
14.	Overview of DNA's Nuclear Dust Re-Analysis Program - Rawson	238

SECTION 1

FUEL BED DATABASE COMPILATION

URBAN AREA ANALYSIS AND SMOKE PRODUCTION

G. ANNO

B. BUSH

M. DORE

R.D. SMALL

GLOBAL EFFECTS PROGRAM MEETING

February 26-27, 1986

PSR
EATON

URBAN AREA ANALYSIS AND SMOKE PRODUCTION

- DEFINE URBAN AREA LIMITS
- IDENTIFY POTENTIAL TARGETS
- COLOCATE URBAN/WEAPON IGNITION AREAS
- CHARACTERIZE URBAN AREAS
- SPECIFY FUEL LOADINGS
- ESTIMATE SMOKE GENERATION
- CALCULATE URBAN FIRE PLUMES

PSR
EATON

DEFINITION OF URBAN AREAS USING CENSUS DATA

- 1982 CENSUS OF POPULATION AND HOUSING
- URBAN AREA DEFINED AS:

  -- ALL PLACES $\geq$ 25,000, AND

  -- ALL PLACES $\geq$ 2,500 AND $\geq$ 1000 PEOPLE/MI^2

  (CENSUS DEFINES URBAN AREA AS $\geq$ 50,000 AND $\geq$ 1000 PEOPLE/MI^2
- 1000 PEOPLE/MI^2 EQUIVALENT TO AMERICAN SUBURBAN-RURAL AREAS

PSR
EATON

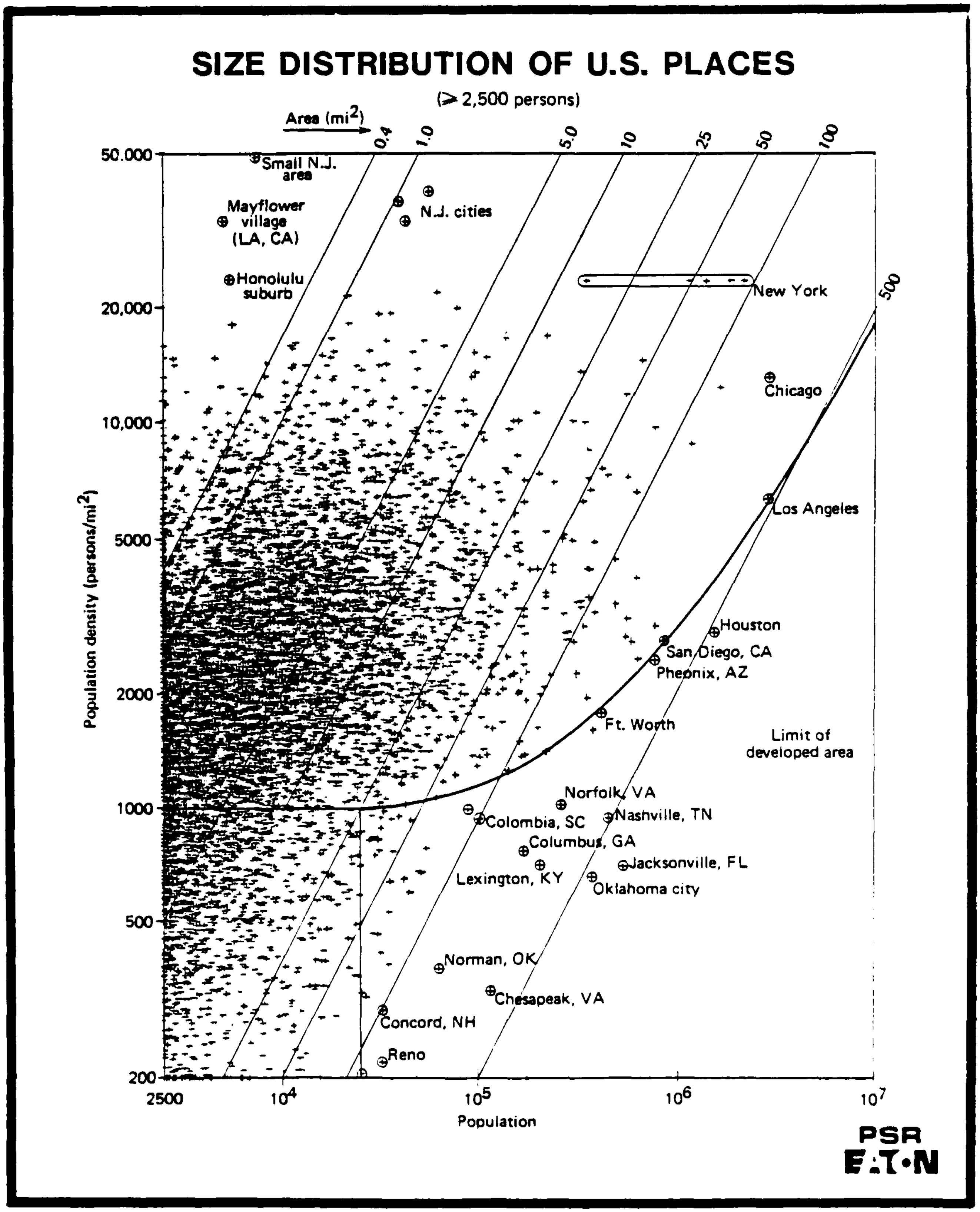
SIZE DISTRIBUTION OF U.S. PLACES
(≥ 2,500 persons)
Area (mi²)
0.4
1.0
5.0
10
25
50
100
500
Small N.J. area
Mayflower village (LA, CA)
N.J. cities
Honolulu suburb
New York
Chicago
Los Angeles
Houston
San Diego, CA
Pheonix, AZ
Ft. Worth
Limit of developed area
Norfolk, VA
Colombia, SC
Nashville, TN
Columbus, GA
Jacksonville, FL
Lexington, KY
Oklahoma city
Norman, OK
Chesapeak, VA
Concord, NH
Reno
Population density (persons/mi²)
50,000
20,000
10,000
5000
2000
1000
500
200
2500
10^4
10^5
10^6
10^7
Population
PSR
EATON

TARGET-URBAN AREA COLOCATION

- "URBAN" TARGETS CONSIDERED INCLUDE:
  - -- MILITARY FACILITIES, REFINERIES, POWER STATIONS, POLITICAL CENTERS, PORTS, TRANSPORTATION, ...
- WEAPON IGNITION AREA: $\leq$XX KM RADIUS
- EQUIVALENT CIRCULAR AREA REPRESENTATION
  - -- URBAN AREA PLACES
  - -- GENERATE PERIPHERAL LIMITS
  - -- ACCOUNT FOR CIRCLE OVERLAP
- MANY POTENTIAL TARGETS OUTSIDE BUILT-UP AREAS

PSR
EATON

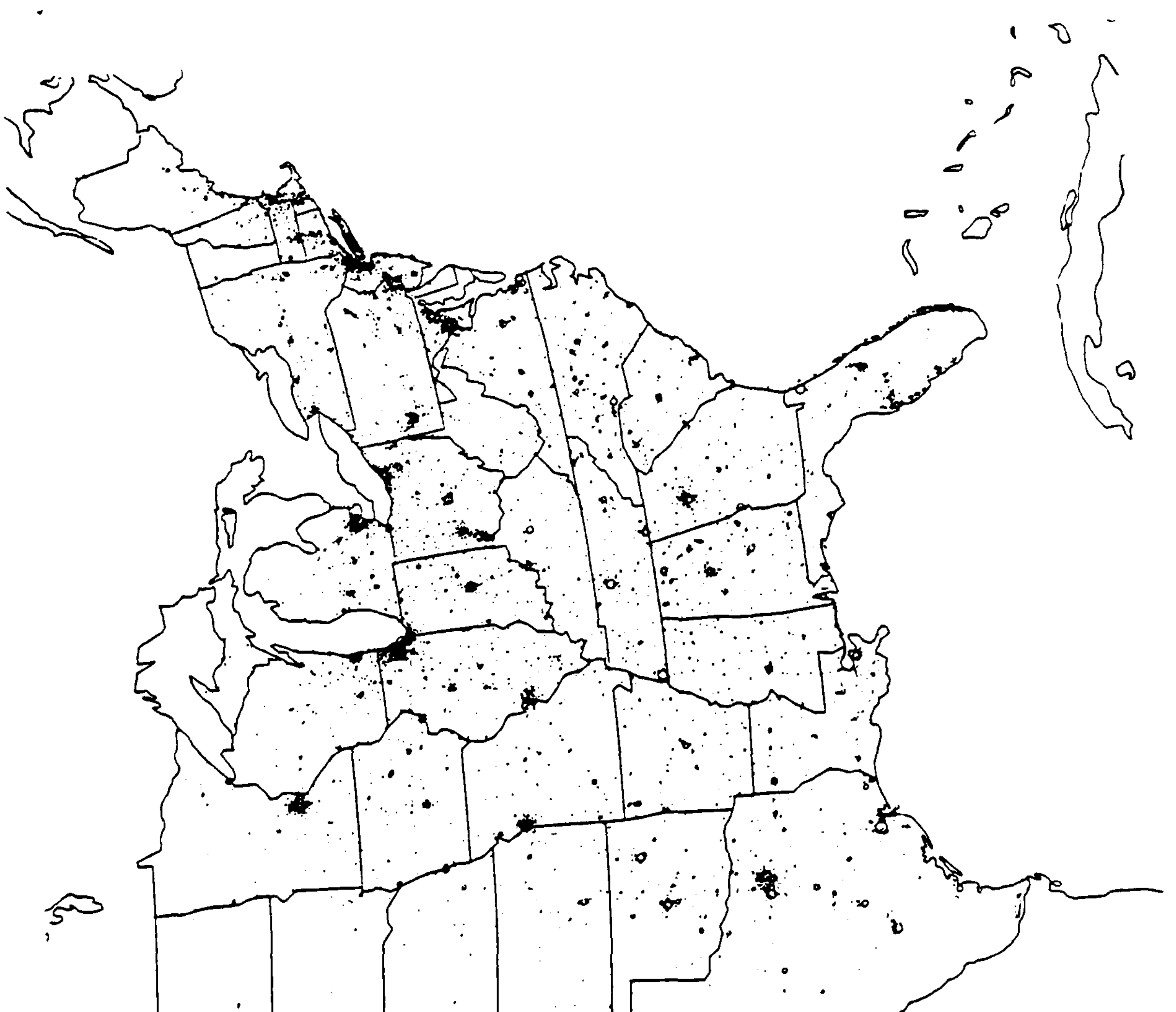

07

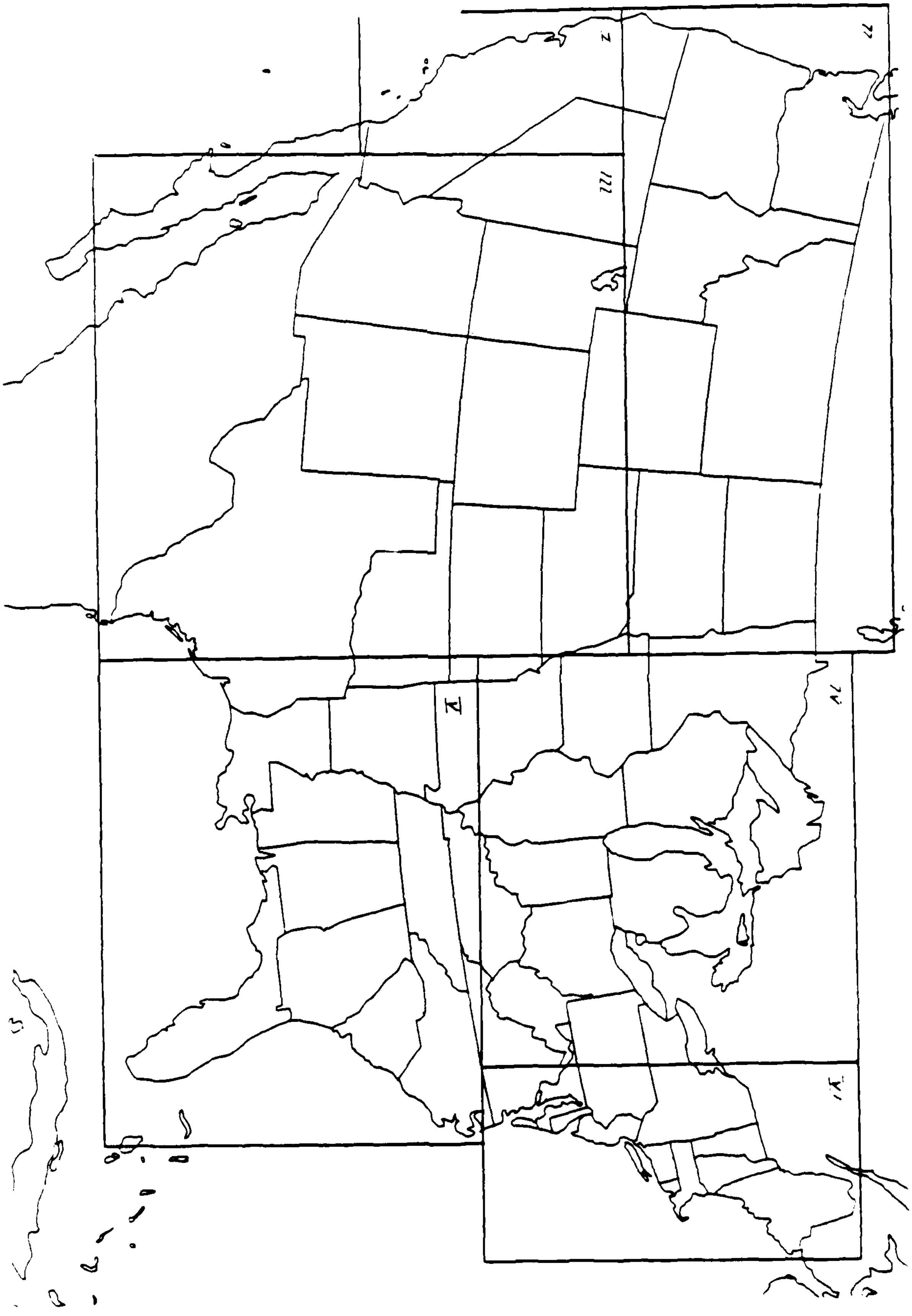


11

URBAN GEOGRAPHICAL ANALYSIS

- CITIES ARE DIFFERENT
  - -- U.S.
  - -- EUROPEAN
  - -- SOVIET
- LAND USE PARAMETERS
  - -- IDENTIFY DIFFERENCES
- 6, 7, 8 CLASS REPRESENTATIONS OF 106 U.S. CITIES
- LAND USE CORRELATES REGIONALLY

PSR
EATON

THREE URBAN LAND CLASSIFICATIONS

6-CLASS LAND USE	8-CLASS LAND USE	LUDA LAND USE*
SINGLE FAMILY RESIDENTIAL	SINGLE FAMILY RESIDENTIAL	11. RESIDENTIAL
MULTIPLE FAMILY RESIDENTIAL	MULTIPLE FAMILY RESIDENTIAL	12. COMMERCIAL, SERVICES
COMMERCIAL	COMMERCIAL	13. INDUSTRIAL
INDUSTRIAL	INDUSTRIAL	14. TRANSPORTATION, COMMUNICATION, UTILITIES
STREETS	TRANSPORTATION	15. INDUSTRIAL AND COMMERCIAL COMPLEXES
PUBLIC, SEMI-PUBLIC	EDUCATION	16. MIXED URBAN
	STREETS	17. OTHER URBAN
	PUBLIC, SEMI-PUBLIC	

*LUDA (LAND USE DEVELOPED AREA), ANDERSON ET AL., 1976.

PSR
E.T.N

PSR
E:T·N

6-Class Breakdown

Geographic Region	WE	NW	SW	NO	SO	NE
Number of Cities	8	3	10	17	7	13
Political Area per Developed Area						
Mean	1.41	1.37	1.91	1.35	1.74	1.19
Standard Deviation	.37	.25	.64	.17	.54	.12
S. D. of the Mean	.13	.14	.20	.42	.20	.30
Single Family Area per Developed Area						
Mean	37.4	38.9	35.6	35.0	40.3	26.4
Standard Deviation	5.0	1.5	6.4	8.0	9.1	8.8
S. D. of the Mean	1.8	0.9	2.0	1.9	3.5	2.4
Multiple Family Area per Developed Area						
Mean	9.25	2.69	2.71	4.74	3.66	10.01
Standard Deviation	9.07	.59	2.45	3.16	2.22	4.71
S. D. of the Mean	3.21	.34	.78	.77	.84	1.31
Commercial Area per Developed Area						
Mean	6.08	4.73	5.17	5.17	7.09	7.87
Standard Deviation	2.16	.71	1.49	2.33	2.77	2.86
S. D. of the Mean	.76	.41	.47	.57	.11	.79
Industrial Area per Developed Area						
Mean	5.93	4.80	6.09	12.00	5.92	9.14
Standard Deviation	2.36	1.80	2.67	7.98	2.76	4.37
S. D. of the Mean	.83	1.04	.84	1.94	1.04	1.21
Street Area per Developed Area						
Mean	22.9	33.8	24.7	25.0	24.0	21.2
Standard Deviation	4.8	3.0	5.4	4.72	7.8	3.8
S. D. of the Mean	1.7	1.7	1.7	1.14	3.0	1.[illegible]
Semi-Public Area per Developed Area						
Mean	18.4	15.1	25.7	18.1	19.0	25.3
Standard Deviation	8.3	2.3	8.7	11.8	7.5	9.[illegible]
S. D. of the Mean	3.0	1.3	2.7	2.9	2.[illegible]	2.[illegible]

LAND USE IN THREE CITIES

LUDA LAND USE*	PERCENT OF URBAN LAND USE		
	LOS ANGELES	HARTFORD	MIAMI
11. RESIDENTIAL	60.8	70.3	68.4
12. COMMERCIAL AND SERVICES	14.8	15.5	16.6
13. INDUSTRIAL	11.3	4.8	2.0
14. TRANS., COMM., UTIL.	1.6	1.1	3.1
17. OTHER, OPEN	9.0	8.2	9.9

*LUDA (LAND USE DEVELOPED AREA)

PSR
E:T·N

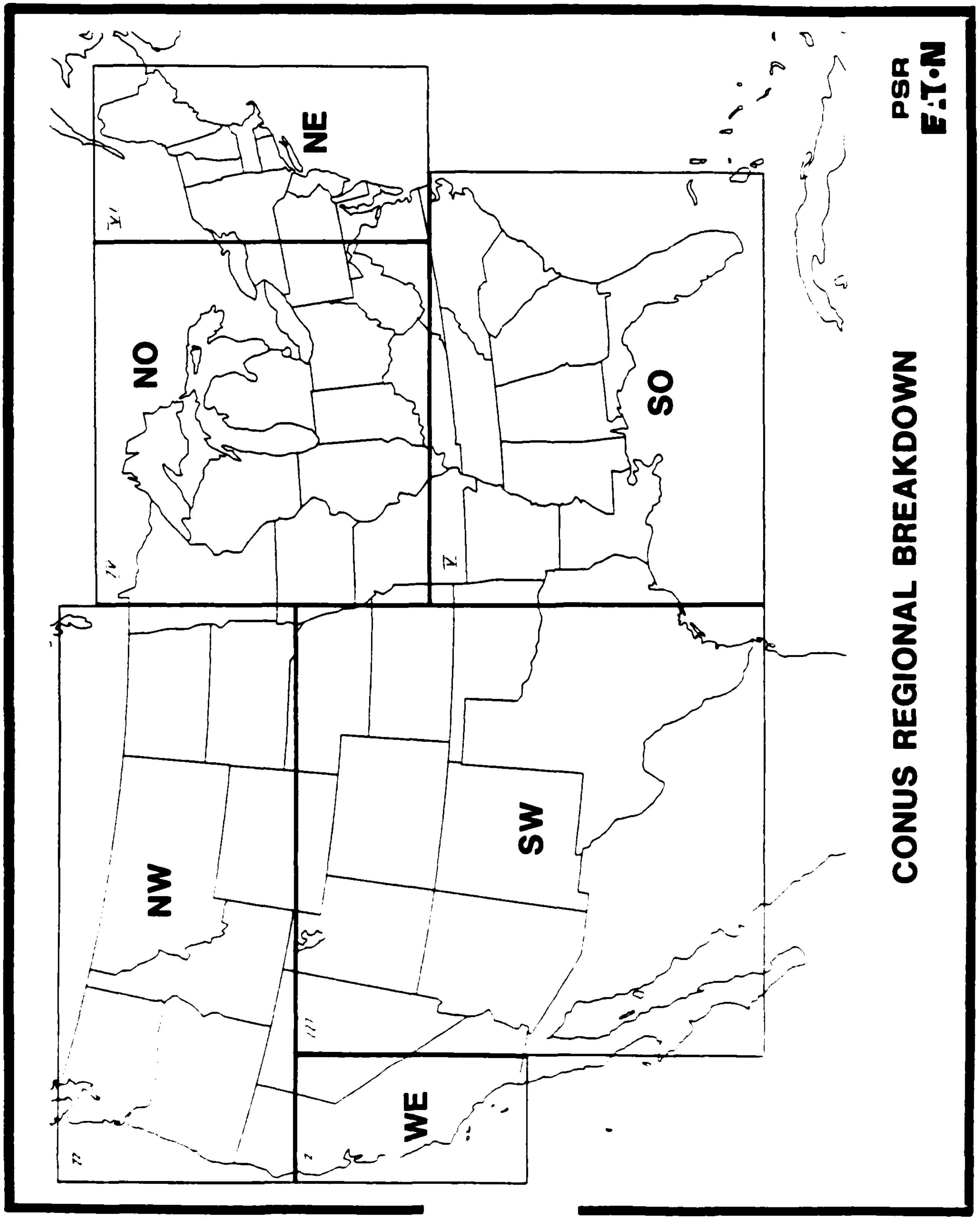
CONUS REGIONAL BREAKDOWN
NE
NO
SO
NW
SW
WE
PSR
EATON

URBAN LAND USAGE FOR NON-INDUSTRIAL PURPOSES IN THE USSR AND U.S.

LAND USE	PERCENT LAND USED USSR	U.S.
POPULATION > 250,000		
RESIDENTIAL	42.2	45.8
COMMERCIAL AND PUBLIC	17.3	15.9
STREETS	20.2	28.9
PARKS	20.3	9.9
POPULATION 100,000-250,000		
RESIDENTIAL	50.0	46.7
COMMERCIAL AND PUBLIC	15.3	15.9
STREETS	16.5	31.0
PARKS	18.2	6.0
POPULATION 50,000-100,000		
RESIDENTIAL	58.1	41.0
COMMERCIAL AND PUBLIC	14.2	15.0
STREETS	11.7	26.8
PARKS	17.0	7.2

SOURCE: FRENCH AND HAMILTON, 1979.

PSR EATON

LAND USE IN U.S. CITIES

- URBAN STRCUTURE DEFINED USING LUDA (USGS) CLASSES
- REPRESENTATIVE CITY FROM EACH CONUS REGION CONSIDERED IN DETAIL
- TARGET COLOCATED AREAS ANALYZED

PSR
EATON

PSR
EATON

URBAN AREA FUEL LOAD INVENTORY

- RESIDENTIAL (11)
  - -- SINGLE FAMILY DETACHED
  - -- SINGLE FAMILY ATTACHED, PLEXES, ROWHOUSES
  - -- MULTIUNIT (APARTMENTS, CONDOS, DORMITORIES)
  - -- MOBILE HOMES AND TRAILERS (PARKS)
- INDUSTRIAL (13)
  - -- MANUFACTORING AND ASSEMBLY
  - -- MILLING AND FABRICATION
  - -- WAREHOUSING AND WHOLESALE
  - -- GAS STORAGE AND DISTRIBUTION
  - -- CHEMICAL PRODUCTION AND STORAGE
  - -- FOOD PROCESSING AND STORAGE
- COMMERCIAL (12)
  - -- RETAIL SALES
  - -- WAREHOUSING
  - -- OFFICE BUILDINGS
  - -- HOTELS AND MOTELS
  - -- RECREATION AND ENTERTAINMENT

PSR
EATON

URBAN AREA FUEL LOAD INVENTORY (CONTINUED)

- SERVICES (12)
  - -- SCHOOLS AND INSTITUTIONS
  - -- HEALTH CARE FACILITIES
  - -- OFFICE BUILDINGS (LOCAL, STATE, GOVERNMENT)
  - -- MILITARY FACILITIES
- TRANSPORTATION, COMMUNICATION, AND UTILITIES (14)
  - -- AIRPORTS AND FUEL STORAGE
  - -- DOCKS, WAREHOUSING, AND FUEL STORAGE
  - -- BUS AND RAIL TERMINALS
  - -- SHIPYARDS
- OPEN AND VEGETATION
  - -- PARK AND URBAN VEGETATION (17)
  - -- URBAN PERPERTUAL VEGETATION AND AGRICULTURE (21,22,24)
- VEHICLES AND FUEL (XX)
  - -- AUTOMOBILES AND TRUCKS
  - -- BUSES AND TRAINS
  - -- BOATS AND SHIPS
  - -- AIRCRAFT
- OTHER (YY)

EXAMPLE BURNABLE FUEL LOAD ESTIMATE: SUBURBAN-RURAL SINGLE FAMILY RESIDENCE

- 1000 PEOPLE/MI^2 (1.56 PEOPLE/ACRE)
- 2.5 PEOPLE/FAMILY (U.S. AVERAGE)

1 HOUSE PER 1.6 ACRE

- FLOOR LOAD: 12 LB/FT^2 (6 GM/CM^2)
- 2000 FT^2 HOUSE

(0.17 G/CM^2)

PSR
EATON

CONCLUSIONS

- EQUIVALENT CIRCLE AREAS APPROXIMATE URBAN AREAS WELL
- NOT ALL CITIES SIMILAR
- 6 CLASS LAND USE APPROPRIATE
- REGIONAL CORRELATION FOR U.S. CITIES
- EUROPEAN, SOVIET CITIES DIFFERENT
- TARGET COLOCATED AREA LAND USE IMPORTANT

PSR EATON

A CRITICAL EXAMINATION OF METHODS OF ESTIMATING THE SPATIAL DISTRIBUTION AND MAGNITUDES OF URBAN FUEL LOADINGS

David S. Simonett
Department of Geography
University of California
Santa Barbara, CA 93106

This study was undertaken because the plume height and dynamics of mass urban fires following a nuclear exchange may be sensitive to the magnitudes and spatial distribution of urban fuel loadings. Methods now used to make loading estimates involve gross approximations, such as a simple decrease in loadings from an urban center, and have uncertainties in magnitudes of a factor of 5 or more for different cities, in the aggregate, with more-than-order-of-magnitude uncertainties applying to details of the spatial distribution within cities.

We review the weaknesses of current methods and examine alternative, more detailed, methods, including aerial photo interpretation, censuses of housing, population and industry, business directories, land use maps and other data. Preliminary results are presented with emphasis on aerial photographic methods for calculating fuel loadings for 1000 x 1000 ft cells of San Jose and vicinity, California.

Procedures are described for estimating the following items for each cell, which are then used with typical residential and business fuel loadings from the literature to derive fuel loadings in Kg/M^2 on a cell-by-cell basis:

1) Number of buildings by type (residential: single family, mobile home, apartments; commercial; school-institutional; offices; light-industrial, industrial).

2) Average building base dimension by building type.

3) Building height (percentage of buildings within a cell with 1,2, 3, . . ., 20 stories).

4) Average fuel load per building type (derived from an extensive literature search).

Besides these parameters for fuel load calculation, a number of items of importance for the study of fire spread and plume dynamics were also obtained through air photo interpretation:

1) Building density (percentage of the cell covered by buildings).

2) Built-up-ness (proportion of the total area contiguously covered with structures).

3) Average spacing between buildings.

4) Proportion of organic/synthetic components in fuel load (from the literature).

5) Nearest neighbor distances between structures.

6) Openness Index (proportion of cell occupied by water, vegetation, bare ground, or superhighways).

7) Presence or absence of fire-breaks (organized open areas capable of stopping fire spread).

ESTIMATES OF TOTAL COMBUSTIBLE MATERIAL IN NATO AND WARSAW PACT COUNTRIES

GEORGE F. BING

LAWRENCE LIVERMORE NATIONAL LABORATORY

FEBRUARY 26, 1986

WAR SCENARIOS AND TARGETS

- POSSIBLE NUCLEAR EXCHANGES
  - NUMBER AND YIELD OF WEAPONS

- TARGETS
  - COUNTRIES
  - TARGET TYPES AND NUMBERS
  - RELATION TO BUILT-UP AREAS
  - ASSOCIATED COMBUSTIBLE MATERIAL

HOW OTHERS ESTIMATE SMOKE INJECTION

- THE 1984 NATIONAL ACADEMY OF SCIENCES STUDY IS TYPICAL.
- ASSUMES A BASELINE EXCHANGE BETWEEN NATO AND WARSAW PACT.
- TOTAL YIELD 6500 MEGATONS.
- 1500 MEGATONS (3500 WARHEADS) ARE USED AGAINST COUNTERVALUE TARGETS AND START FIRES IN URBAN AREAS.
- FIRES ARE IGNITED FOR THERMAL FLUENCES ≥ 20 CAL/CM^2.
- 1/3 OF THERMAL FLUENCE AREA IS OVERLAP.

HOW OTHERS ESTIMATE SMOKE INJECTION (CONTINUED)

- SMOKE PRODUCTION IS ESTIMATED BY THE PRESCRIPTION:

$$E = Y_F A_0 M_0 F_B \epsilon$$

WHERE:

Y_F = TOTAL EFFECTIVE YIELD = 1000 MEGATONS

A_0 = AREA PER MEGATON WITH FLUENCE $\geq$ 20 CAL/CM^2 = 250 KM^2

M_0 = AVERAGE COMBUSTIBLE MATERIAL DENSITY = 4 GRAM/CM^2

10,000 Tg

F_B = FRACTION OF IGNITED MATERIAL BURNED = 0.75

ϵ = GRAMS OF SMOKE INJECTED/GRAM OF FUEL BURNED = 0.02 = 2%

E = TOTAL URBAN SMOKE INJECTED INTO THE ATMOSPHERE = 150 x 10^{12} GRAMS = 150 TERAGRAMS

- ESTIMATED UNCERTAINTY RANGE: 20 - 450 TERAGRAMS.

$\frac{2}{3} \times 3 + \frac{1}{3} \times 6 = 4\%$

60% prompt scavenged

net = 2%

TWO ESTIMATES BY CRUTZEN, ET. AL OF COMBUSTIBLE MATERIAL IN BUILDINGS

ESTIMATE 1. 300 CITIES OF POPULATION $\gtrsim 10^5$ PEOPLE AND AREA OF $\sim$ 250,000 KM^2 ATTACKED WITH 2000 WEAPONS OF TOTAL YIELD 800 MT. (AVERAGE YIELD 0.4 MT).

AVERAGE COMBUSTIBLE LOADING TAKEN AS 4 GM/CM^2.

TOTAL MASS EXPOSED TO IGNITION CONDITIONS (20 CAL/CM^2 OR MORE) IS

$$2.5 \times 10^{15}\ CM^2 \times 4\ GM/CM^2 = 10^{16}\ GM = 10^4\ TERAGRAMS.$$

HALF THE EXPOSED MASS, 5000 TERAGRAMS, ASSUMED BURNED. 300 CITIES IS $\sim$ 30% OF ALL CITIES OVER 10^5 PEOPLE IN DEVELOPED WORLD. ALL SUCH CITIES WOULD CONTAIN 33,000 TERAGRAMS. SMALLER URBAN AND RURAL PLACES OF THE DEVELOPED WORLD WOULD CONTAIN A COMPARABLE MASS FOR A TOTAL OF $\sim$ 60,000 TERAGRAMS. NATO AND THE WARSAW PACT COUNTRIES REPRESENT ABOUT 85% OF THE DEVELOPED WORLD.

TWO ESTIMATES BY CRUTZEN, ET. AL OF COMBUSTIBLE MATERIAL IN BUILDINGS

ESTIMATE 2. ANNUAL PRODUCTION (1974) OF SAWN WOOD IN DEVELOPED WORLD WAS 2.5×10^{14} G. ASSUME ALL GOES TO BUILDINGS WITH 50 YEAR AVERAGE LIFETIME. TOTAL COMBUSTIBLE LOAD THEN

$$\sim 1.3 \times 10^{16} \text{ G} = 13{,}000 \text{ TERAGRAMS}$$

70% OF POPULATION LIVE IN CITIES WITH TOTAL COMBUSTIBLE LOAD

$$\sim 0.9 \times 10^{16} \text{ G}$$

30% OF URBAN AREAS DESTROYED BY FIRE

$$\sim 0.3 \times 10^{16} \text{ G}$$

PAPER AND CELLULOSES MAKE THE AVAILABLE BURNABLE MATERIAL IN THE ATTACKED CITIES

$$\sim 0.4 \times 10^{16} \text{ G}$$

HALF BURNS

2000

$$\sim 0.2 \times 10^{16} \text{ G} = \text{TERAGRAMS}$$

ESTIMATE 2 IS 40% OF ESTIMATE 1.

HOW MUCH COMBUSTIBLE MATERIAL IS IN TYPICAL URBAN AND SUBURBAN AREAS?

- WE HAVE COMPILED AVAILABLE U.S. DATA ON TOTAL FLOOR SPACE IN RESIDENTIAL AND NONRESIDENTIAL BUILDINGS AND ON AVERAGE COMBUSTIBLE LOADING PER UNIT AREA IN ORDER TO ESTIMATE TOTAL COMBUSTIBLE MATERIAL IN U.S. BUILDINGS.

- WE HAVE ALSO ESTIMATED HOW MUCH CRUDE OIL, PETROLEUM PRODUCTS, ASPHALT AND SYNTHETICS IS STORED OR ACCUMULATED IN THE UNITED STATES.

- ESTIMATES HAVE ALSO BEEN MADE FOR THE SOVIET UNION AND FOR THE OTHER NATO AND WARSAW PACT COUNTRIES.

TABLE 8. Summary of Estimates of Total Primary Combustible Materials in the NATO and Warsaw Pact Countries in 1984-1985.

Countries	Combustible Mass (Teragrams)			
	Residential Buildings	Nonresidential Buildings	Crude Oil & Other Petroleum Stocks	Rubber in Tires*
United States	1,485	634	162	10
Other 15 NATO Countries	2,522	1,076	194	7
Soviet Union	285	753	158	1 (1.3)
Other Six Warsaw Pact Countries	116	307	34	1 (0.9)
Totals	4,408	2,770	548	19

* Automobiles and other vehicles contain substantial combustible material in addition to their tires. An estimate of their gasoline or diesel fuel supply is included in the "other petroleum stocks" above. Plastics and synthetic fabrics used in vehicles are included in the estimates of the total inventories of these products in Table 9 below.

Table I. Estimated Total Combustible Weight in US Residential Buildings (1982)

Household Type	Number of Units (millions)	Heated Area sq. ft. (billions)	Combustible Density lb/ft^2	Total Combustible Weight lb. billions	percent
Single-family detached	53.8	92.3	25	2310	79.6
Single-family attached	3.9	5.9	25	150	5.1
Buildings with 2 to 4 units	10.1	10.4	25	260	9.0
Buildings with 5 or more units	12.2	9.6	13	120	4.3
Mobile homes	3.7	3.2	18	60	2.0
All Households	83.8	121.4	(23.9)	2,900 (1,316 teragrams)	100.0

Table 2. Nonresidential Buildings in the United States - Number and Area - 1980

Type *	Number (Thousands)	Average Area/ Building (Thousand Sq. Ft.)**	Total Area (Billion Sq. Ft.)
Assembly	448	11.2	5.02
Automobile sales, service	401	4.5	1.80
Education	161	36.2	5.83
Food Sales	366	5.1	1.87
Health Care	44	38.5	1.69
Industrial	243	29.4	7.14
Lodging	101	19.9	2.01
Office	600	13.6	8.16
Residential	347	9.0	3.12
Retail/Services	714	10.7	7.64
Warehouse and Storage	430	14.1	6.06
Other	237	13.2	3.13
Vacant	146	8.7	1.27
Total	4,238	12.9	54.75

*See Appendix B for definitions of building types.
**Average areas for each building type are given in Statistical Abstract for 1982-83, Table 1375, pg 764.

Table C-1. Comparison of Estimates of Combustible Loading of Nonresidential Buildings

Building Type	Fuel Loading Per Unit Area of Floor Space (lb/ft^2): UCRL-15544 (1983)	FEMA (1982)	IITRI (1965)	NBS (1942,1957)
Residential				
Single-Family				
Frame or Brick	10-20	10-20	23,24,27	---
Fire Resistive	5-10	---	---	---
Residential				
Multi-Family Hi-Rise				
Tenement Apartments	10-30	3-5	10,15,17 21, 24	10 (avg. of 13)
Garden Apartments (fire resistant)	3-5	---	---	---
Nonresidential				
Public	5-10	---	---	7.5, 7.8, 10, 16
Office & Commercial				
Hi-Rise	10-40	10-40	20, 21, 22, 25	10.9, 11.8, 21.2
Industrial Park	10-30	---	---	---
Industrial	5-30	0-30	35	7.2, 7.3, 10.9, 13.9, 16.5, 24.4, 26.3, 38.4
Warehouse	20-80	20-80	---	20.1, 80.9

Table 3. Total Combustible Material in Nonresidential Buildings in the United States in 1980

Building Type	Area (billion sq. ft.)	Combustible Loading lb/ft^2 Average	Combustible Loading lb/ft^2 Range	Total (billion lbs.)	Percent
Residential (Apartment-like)					
Residential	3.12				
Lodging	2.01				
Health Care	1.69				
	6.82	20	10-30	136	10.8
Office and Commercial					
Automobile Sales & Service	1.80				
Office	8.16				
Retail/Services	7.64				
Food Sales	1.87				
Other	3.13				
Vacant	1.27				
	23.87	25	10-40	597	47.4
Public					
Assembly	5.02				
Education	5.83				
	10.85	7.5	5-10	81	6.4
Industrial	7.14	20	10-30	143	11.4
Warehouses & Storage	6.06	50	20-80	303	24.0
Totals	54.75	(23)	-----	1,260 (572 teragrams)	100%

Table 4. The Population of NATO and Warsaw Pact Nations in 1985

Country	Population (millions)	Urban Fraction (percent)
NATO		
United States	234.5	74
Belgium	9.9	95
Canada	26.4	75
Denmark	5.2	83
France	54.3	73
Germany (West)	60.1	94 (est)
Greece	9.6	65
Iceland	.2	89
Italy	57.8	67 (est)
Luxembourg	.3	68
Netherlands	14.4	51
Norway	4.1	70
Portugal	10.2	26
Spain	39.0	54
Turkey	51.1	44
United Kingdom	55.6	77
NATO without U.S., Total	398.2	
Warsaw Pact		
Soviet Union	278.2	64
Bulgaria	9.2	64
Czechoslovakia	15.7	73
Germany (East)	16.9	76
Hungary	10.9	54
Poland	37.6	59
Romania	23.2	50
Warsaw Pact without USSR, Total	113.5	

TABLE 9. Estimates of Asphalt, Plastic and Synthetic Fiber in the Structures and Contents of NATO and Warsaw Pact Buildings

Countries	Combustible Mass (Teragrams)				
		Petrochemical Products			
	All Buildings	Roof Asphalt	Plastics	Synthetic Fiber	Percent Petrochemical Products
United States	2,119	147	150	25	15.2
Other 15 NATO Countries	3,598	104	140	18	7.3
Soviet Union	1,038	59	30	9	9.4
Other Six Warsaw Pact Countries	423	25	23	4	12.3
Totals	7,178	335	343	56	10.2

ESTIMATE BY CRUTZEN, ET. AL, OF WORLD PETROLEUM STOCKS

PRIMARY PETROLEUM STOCKS OF OECD NATIONS
420 TERAGRAMS

SECONDARY STOCKS RANGE FROM 40 TO 100% OF PRIMARY STOCKS
168-420 TERAGRAMS

FOR TOTAL OECD STOCKS OF
588-840 TERAGRAMS

OECD USES 60% OF WORLD OIL. WORLD STOCKS ARE THUS
980-1400 TERAGRAMS

IN ADDITION, ABOUT 100 TERAGRAMS ARE IN TANKERS AT SEA.

GRAND TOTAL OF WORLD PETROLEUM STOCKS IS THUS ABOUT
1080-1500 TERAGRAMS = $1.1\text{-}1.5 \times 10^{15}$ GRAMS

CRUTZEN ET. AL ASSUME ABOUT 400 TERAGRAMS OF STORED PETROLEUM BURN IN A NUCLEAR WAR OR 27-36% OF ESTIMATED WORLD STOCKS.

Table 5. Petroleum Types in US Primary Stocks in 1983[13]

Item	Millions of Barrels
Crude oil in Strategic Reserve	379
Other Crude Oil Stocks	343
Gasoline	222
Jet Fuel	39
Distillate Fuel Oil	140
Residual Fuel Oil	49
Ethane and Liquified Gases	101
Unfinished Oils	107
Other Products	72
Total	1,453

Table 6. Estimated Petroleum Storage Capacity of U.S. Secondary and Consumer Segments in 1978[14]

Segment			Capacity (millions of barrels)
Secondary Distribution System			
Petroleum Bulk Stations			73
Gasoline Service Stations			75
Fuel Oil Dealers			16
Consumer Segment			
Electric Utilities			120
U.S. Military			41
Transportation:	Cars	48 million bbl.	77
	Trucks	29 million bbl.	
Residential Buildings			87
			489
Other: including Federal, State, and Local Governments and for Commercial and Industrial Consumers			?
Total		more than	500

COMBUSTIBLE INVENTORY SUMMARY (TERAGRAMS)

COUNTRIES	BUILDINGS	PERCENT ASPHALT AND SYNTHETICS	CRUDE OIL AND OTHER PETROLEUM STOCKS
UNITED STATES	2,120	15%	160
OTHER 15 NATO COUNTRIES	3,600	7%	190
SOVIET UNION	1,040	10%	160
OTHER SIX WARSAW PACT COUNTRIES	420	12%	30
TOTAL	7,180	10%	540

CONCLUSIONS

- COMBUSTIBLE INVENTORIES IN NATO AND WARSAW PACT COUNTRIES ARE HALF OR LESS OF THOSE IMPLIED IN PREVIOUSLY PUBLISHED STUDIES.

- IF ALL THE COMBUSTIBLES WERE EXPOSED TO IGNITION CONDITIONS 70 TO 200 TERAGRAMS OF SMOKE WOULD BE INJECTED INTO THE ATMOSPHERE.

- IN A "REALISTIC" WAR PERHAPS ONE-QUARTER OF THIS SMOKE WOULD BE INJECTED INTO THE ATMOSPHERE.

SECTION 2

SMOKE SOURCE TERM

SMOKE EMISSION AND PROPERTIES

GEORGE MULHOLLAND

NATIONAL BUREAU OF STANDARDS

OVERVIEW

1. COMPUTER SIMULATION OF SOOT AGGLOMERATION

   (R. MOUNTAIN, H. BAUM)

2. AGGLOMERATE STRUCTURE OF SOOT PRODUCED BY A LAMINAR DIFFUSION FLAME

   (R. SAMSON, E. STEEL)

3. SMOKE EMISSION/PROPERTIES FOR BUOYANCY DOMINATED TURBULENT DIFFUSION FLAMES

   (G. KLOUDA)

Mulholland & Baum

OVERVIEW OF COMPUTATIONAL METHOD

1. Initial Condition - 500 particles placed at random in 3-D box; particle velocity chosen consistent with Boltzmann distribution

   (periodic boundary conditions)

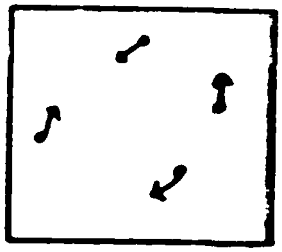

2. Equation of Motion - Langevin equation (stochastic, differential equation)

$$m_0 \frac{d\vec{v}}{dt} = \underbrace{-m_0 \beta \vec{v}}_{\text{friction term}} + \vec{F} \longleftarrow \text{stochastic force}$$

3. Aggregation Condition - particles assumed to stick whenever the separation of the centers of two particles becomes a unit distance or less

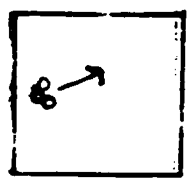

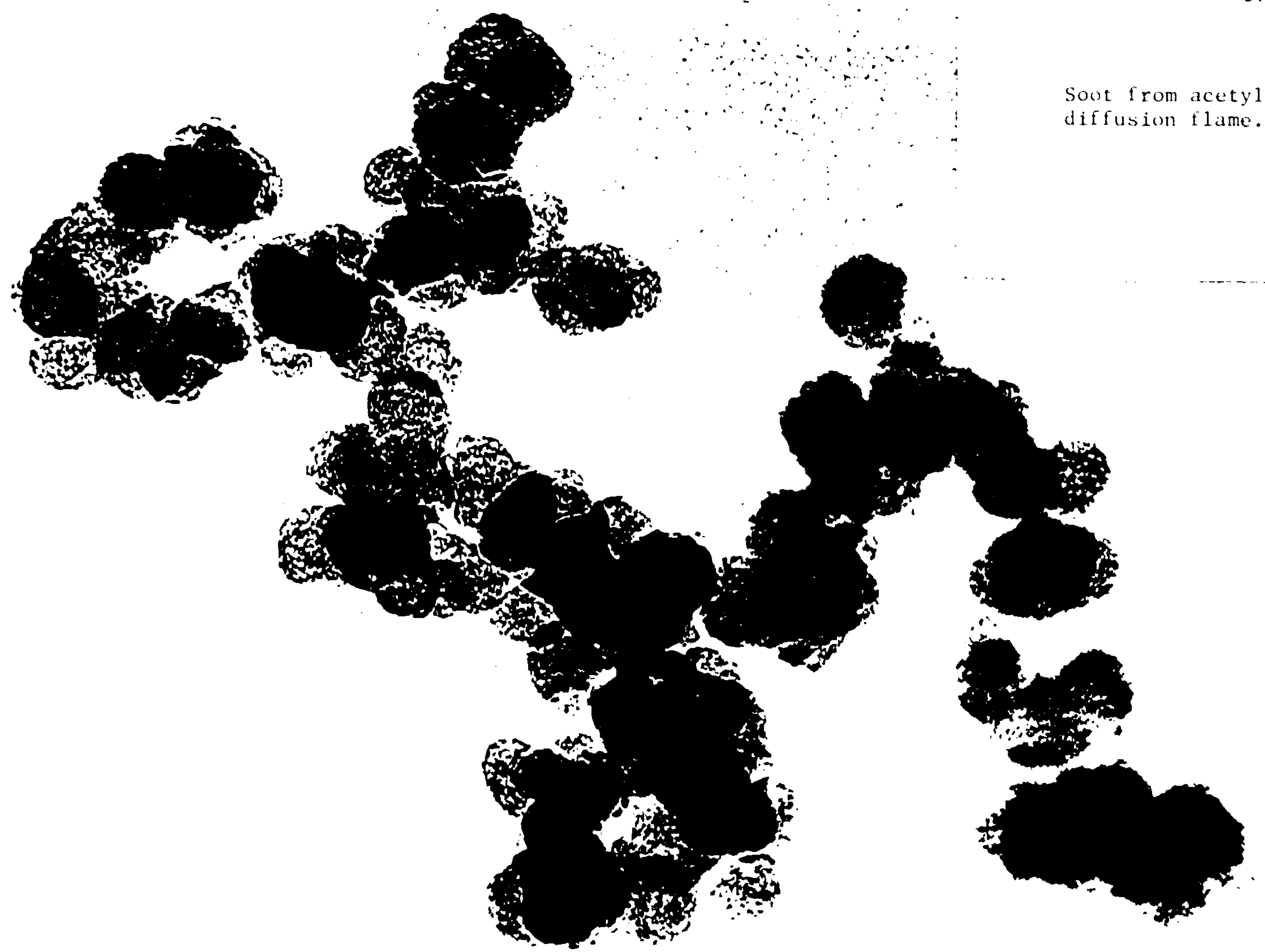

Soot from acetylene laminar diffusion flame.

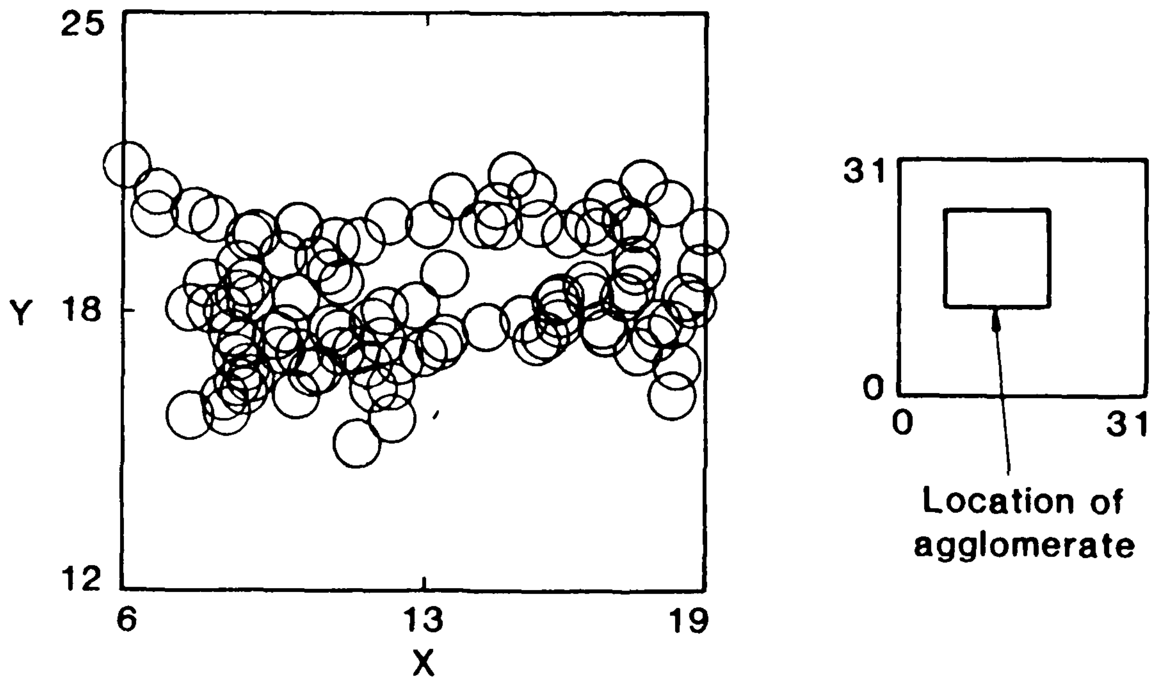

Fig 1

DIMENSIONALITY OF CLUSTER

mass $\sim \ell^{D}$

examples

(1) Compact cluster 

mass $\sim \ell^{3}$

(2) Straight chain 

mass $\sim \ell$

For cluster - cluster aggregation

$N \sim R_g^{1.75}$

Originally found in Monte Carlo computer simulation by Meakin

Observed by Forrest and Witten for iron, zinc, and silicon dioxide aggregates

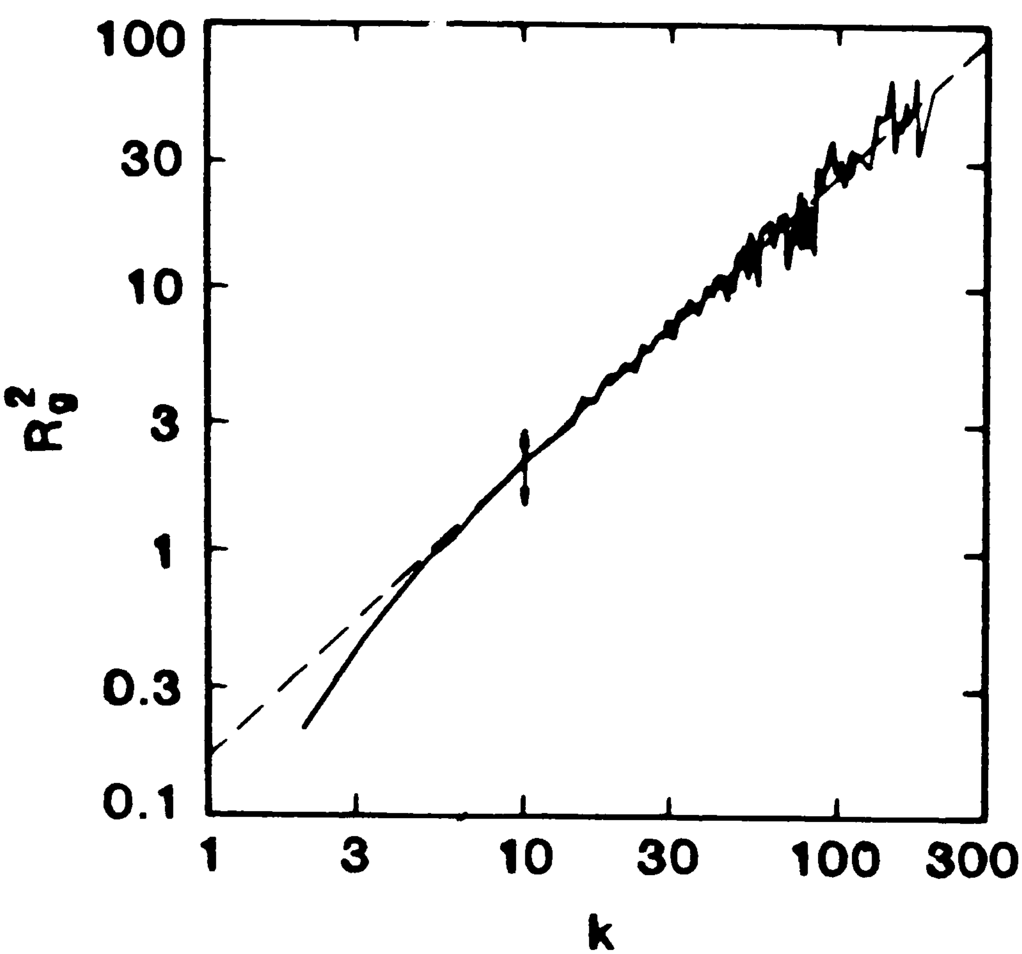

fig 2

Rg as a function of k

Mulholland simulation ten run average

$\rho = 0.05$, $\beta\tau = 0.2$

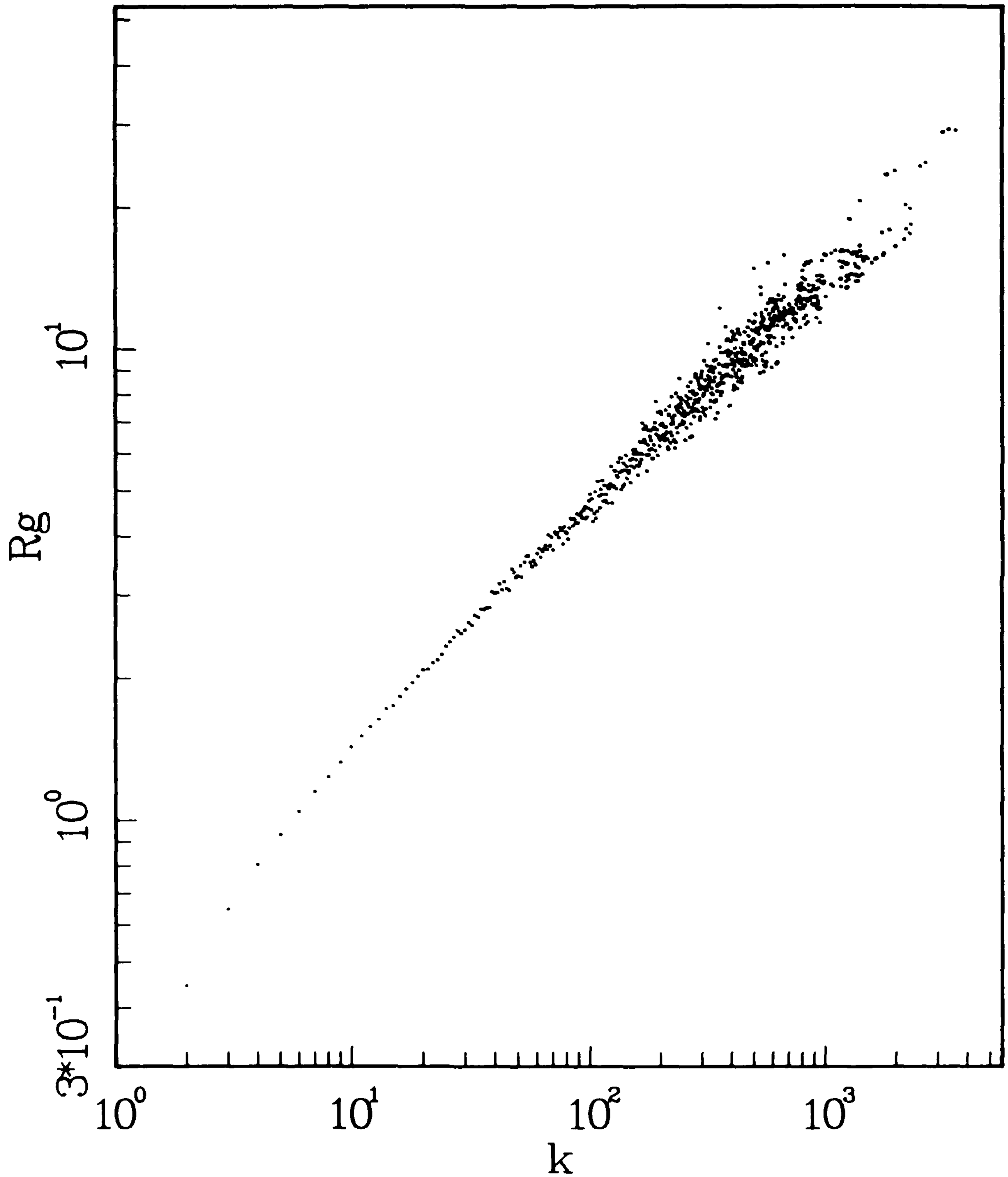

Volume distribution at 400 time steps
Mulholland simulation ten run average
$\rho = 0.05$, $\beta\tau = 0.2$

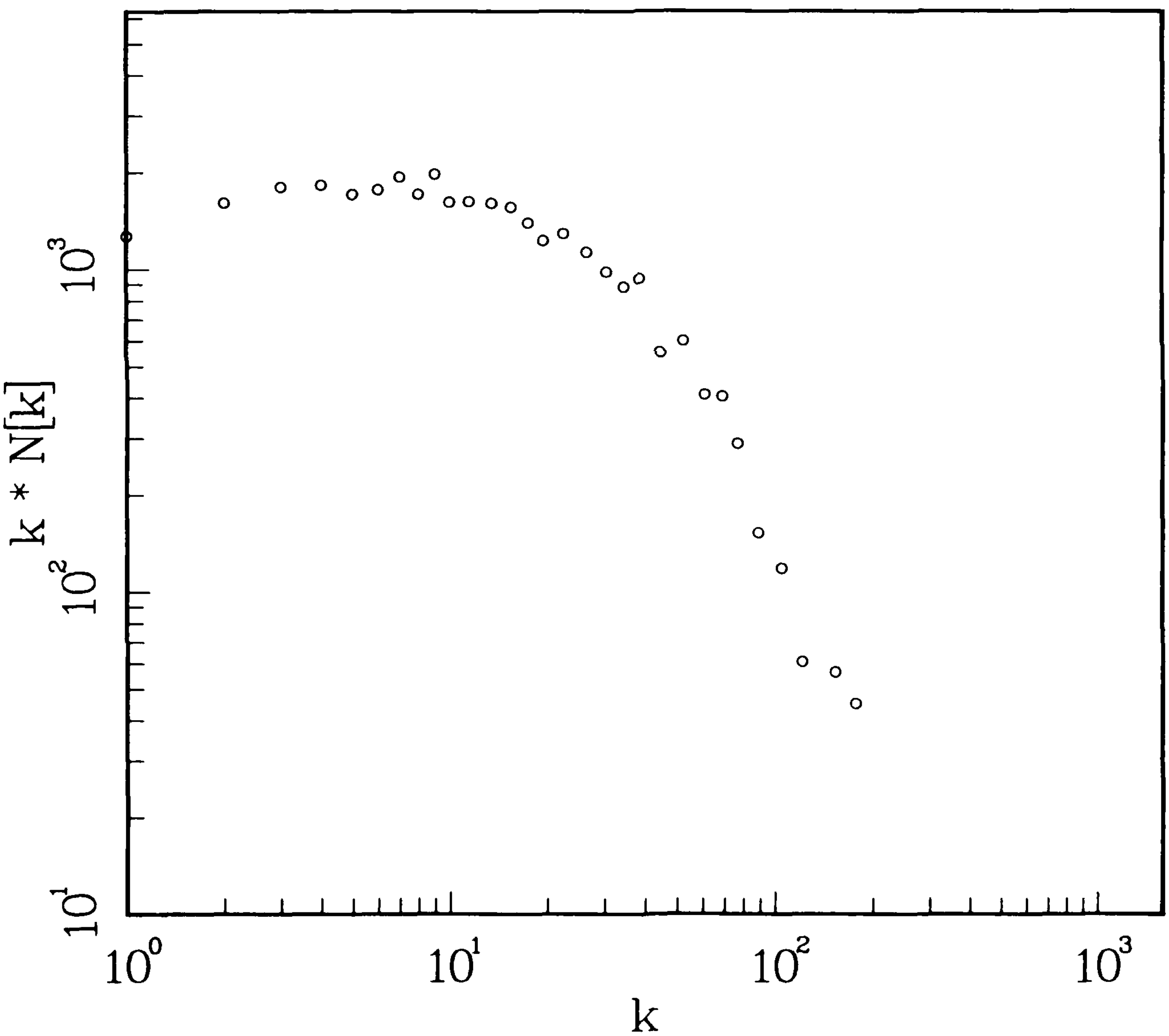

Volume distribution at 1400 time steps
Mulholland simulation ten run average
$\rho = 0.05$, $\beta\tau = 0.2$

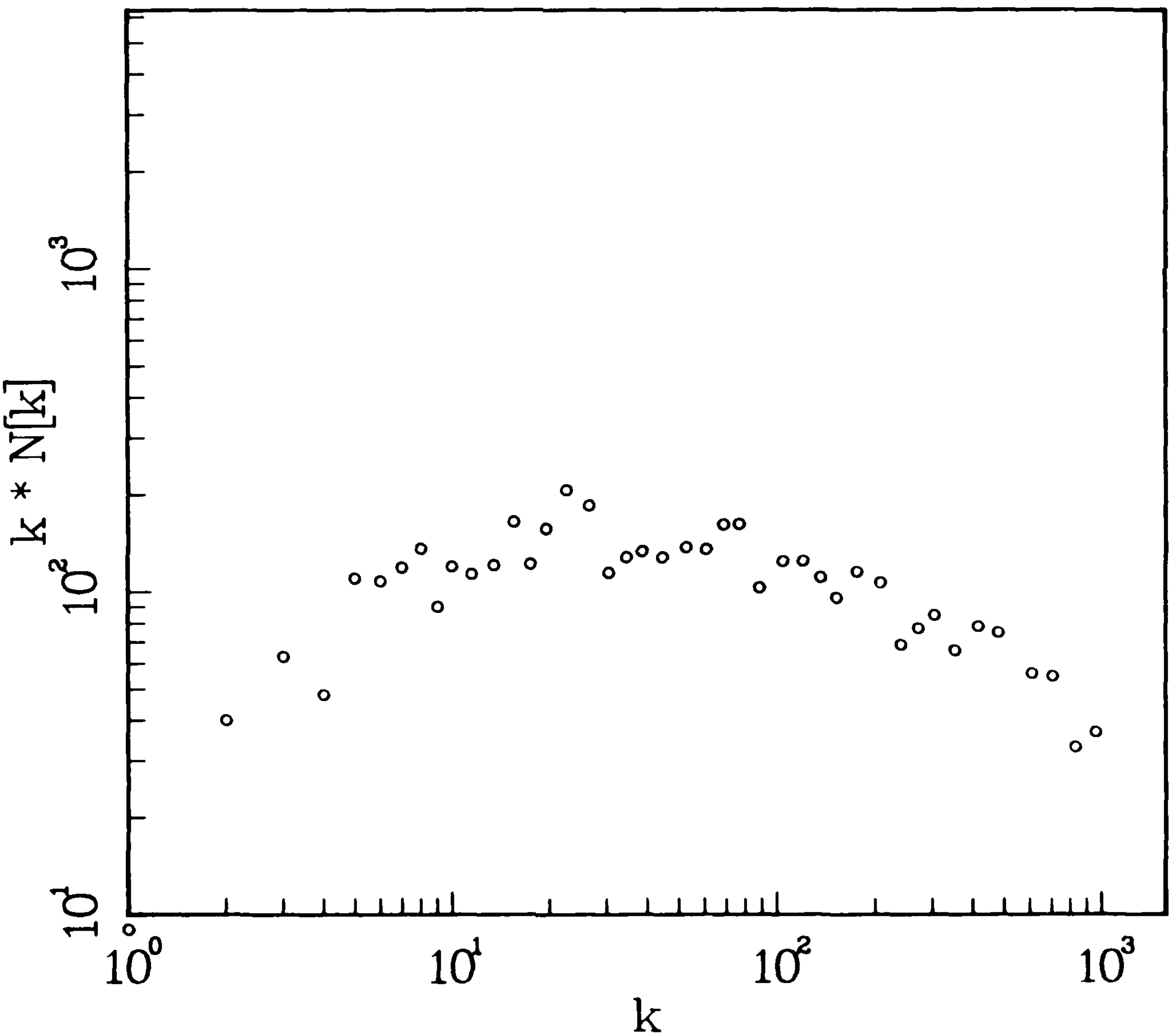

SCALING VARIABLES FOR DISCRETE SIZE DISTRIBUTION

$n_k = \psi(\eta)\, N(t)/\bar{k}$ number distribution

$k = \eta \bar{k} = \eta N_0/N(t)$ number of spheres contained in a cluster

$k\, n_k = \eta\, \psi(\eta)\, N(t)$ volume distribution

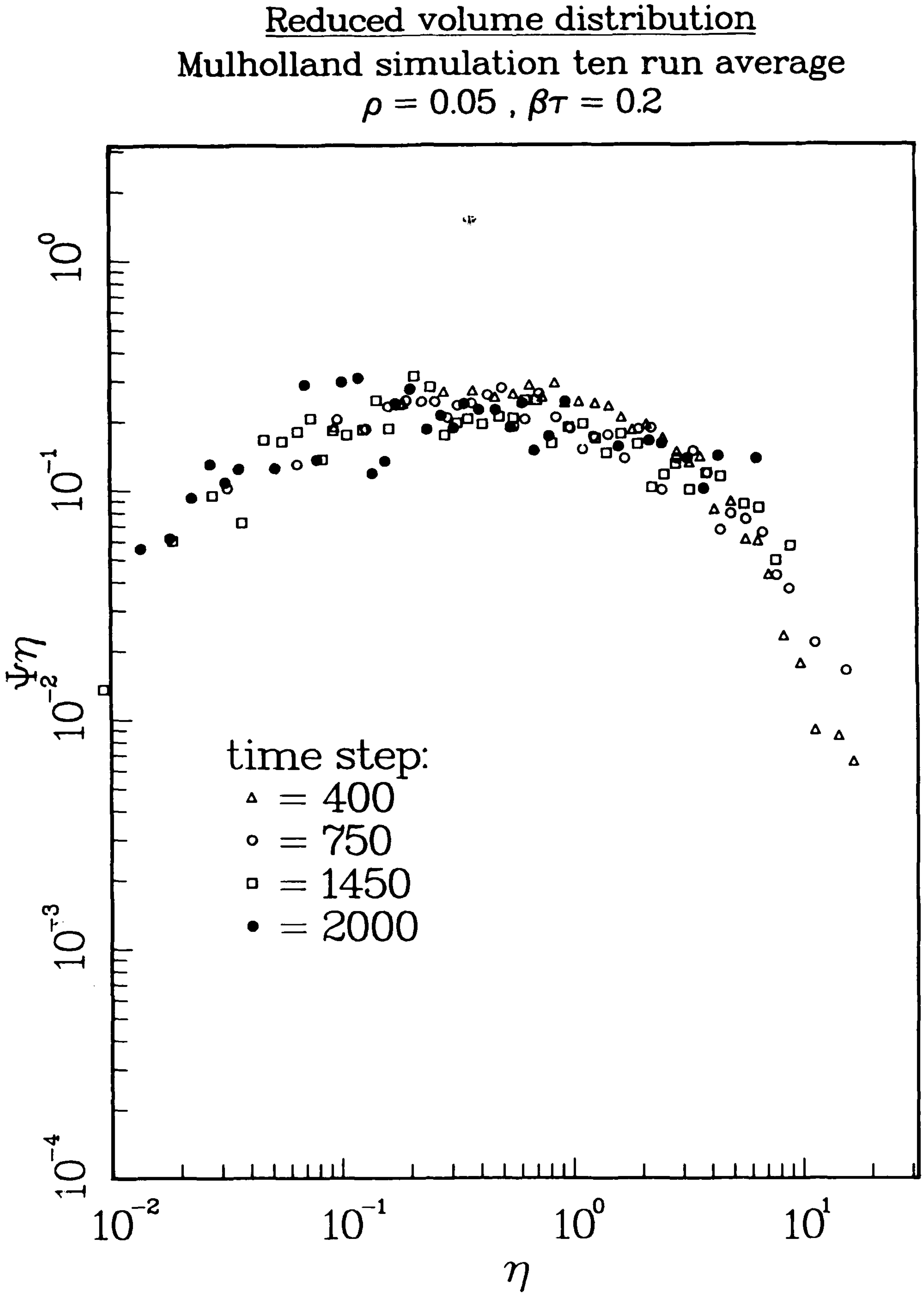
Reduced volume distribution
Mulholland simulation ten run average
$\rho = 0.05$, $\beta\tau = 0.2$
10^{0}
10^{-1}
10^{-2}
10^{-3}
10^{-4}
$\Psi\eta$
10^{-2}
10^{-1}
10^{0}
10^{1}
η
time step:
= 400
= 750
= 1450
= 2000

LAMINAR COANNULAR DIFFUSION BURNER

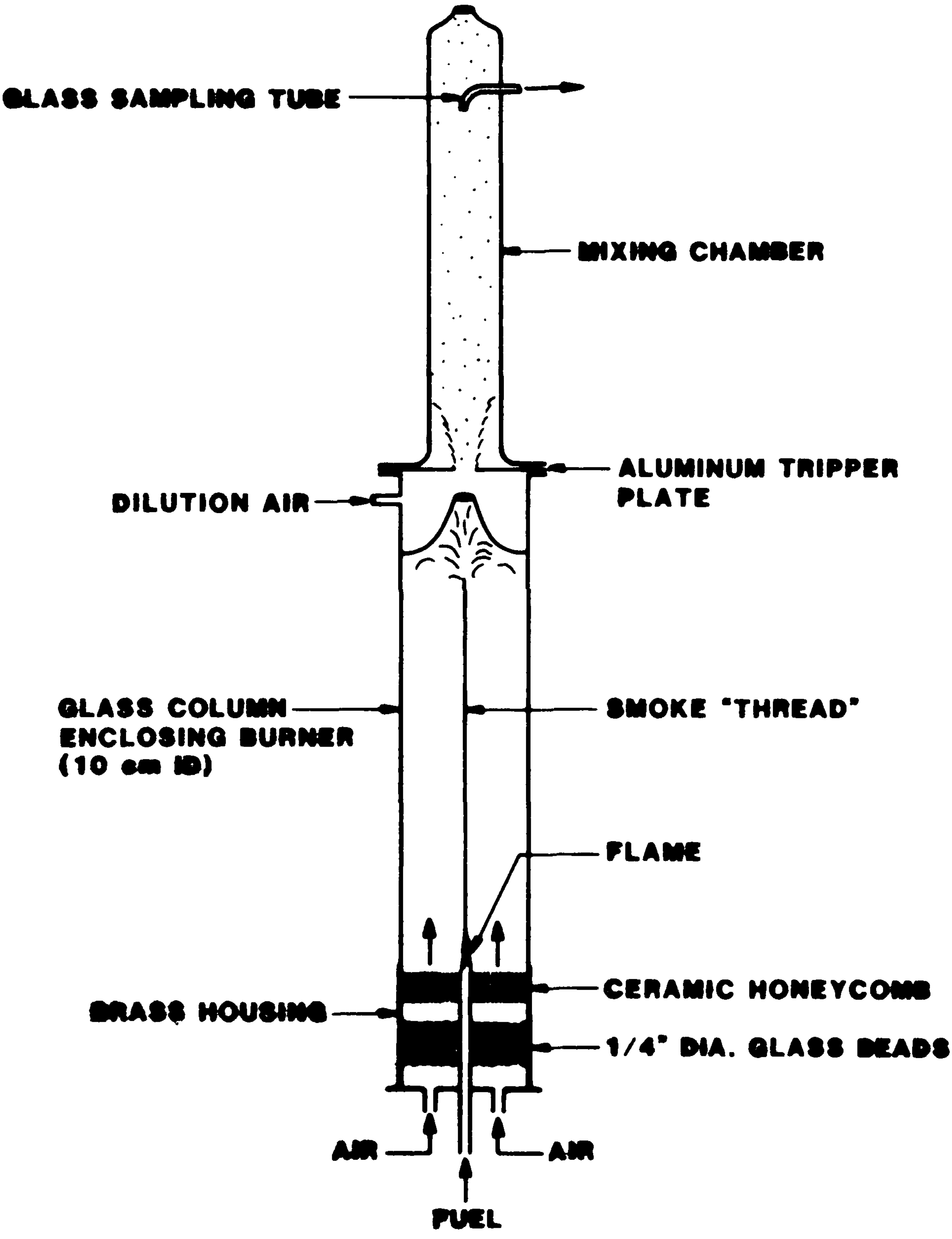

Particle Counting Method

Experimental Data

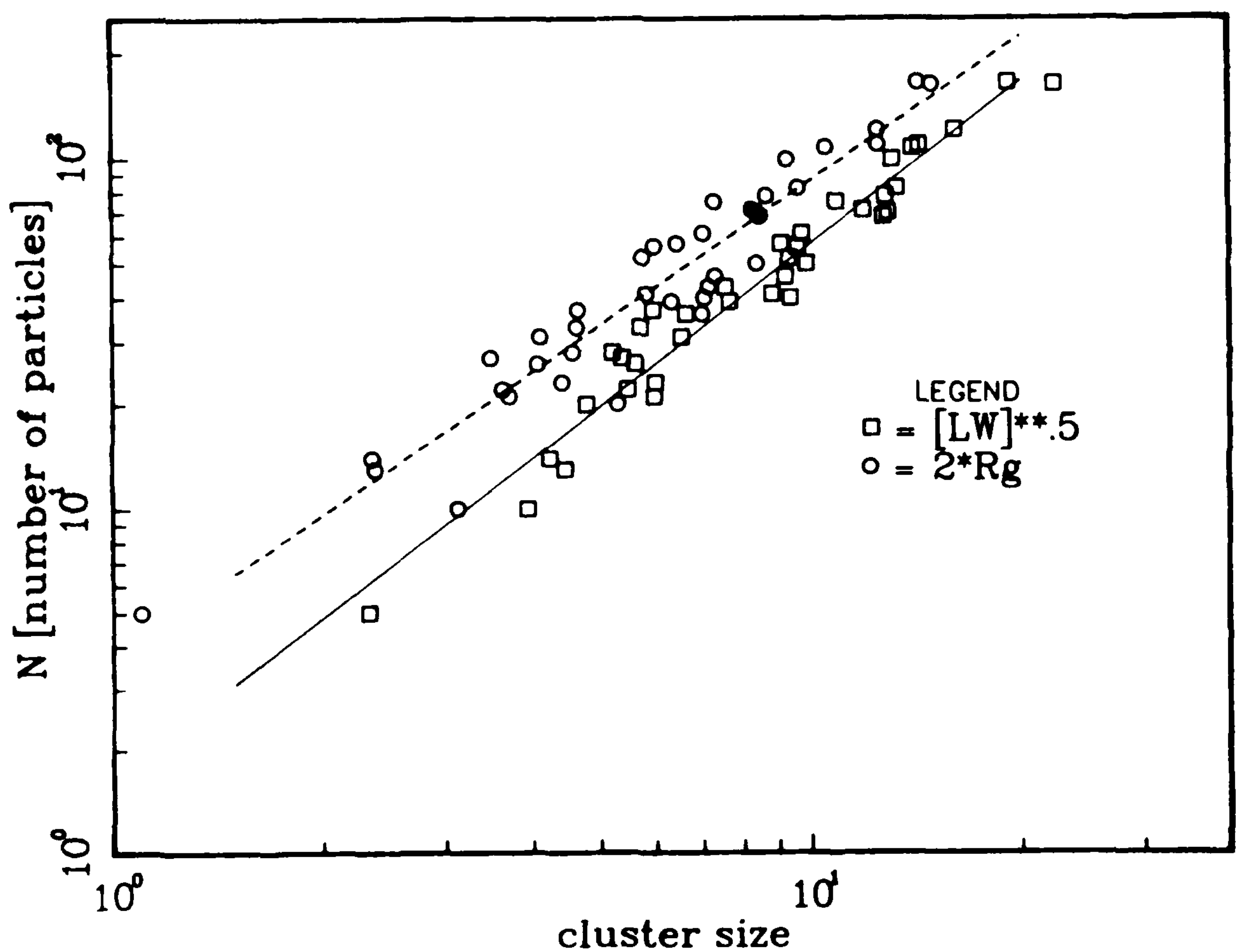

Particle Counting Method

Comparison of simulations with experimental data

simulation k vs Rg fit of projections

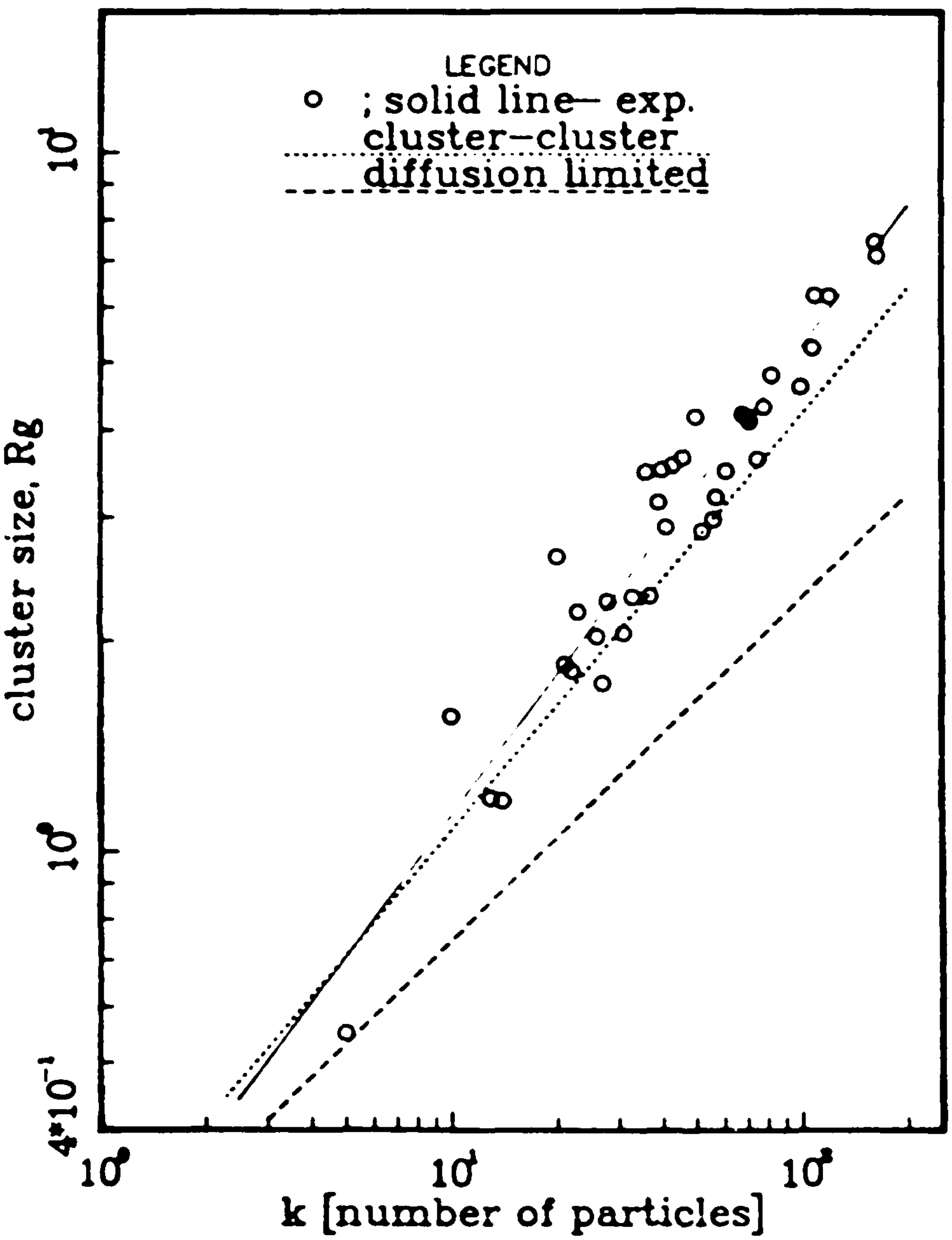

CALCULATION OF FRACTAL DIMENSION D FOR LARGE AGGLOMERATES

1. Display TEM negative on TV monitor
2. Create an array corresponding to all "occupied" pixels (LISPIX software)
3. Calculate the pair correlation function

$$C(r) \sim \sum_{r_0} \frac{\langle \rho(\vec{r}_0)\, \rho(\vec{r}_0 + \vec{r}) \rangle}{r} \overset{?}{\sim} r^{D-d}$$

4. (2nd method) Calculate the number of squares with edge length ε required to cover the entire agglomerate

$$N \sim (1/\varepsilon)^{D}$$

(100 times faster on Cyber 205)

Pair Correlation function vs. radius

Long range effects of cluster shape on c[r]
r in pixel spacings

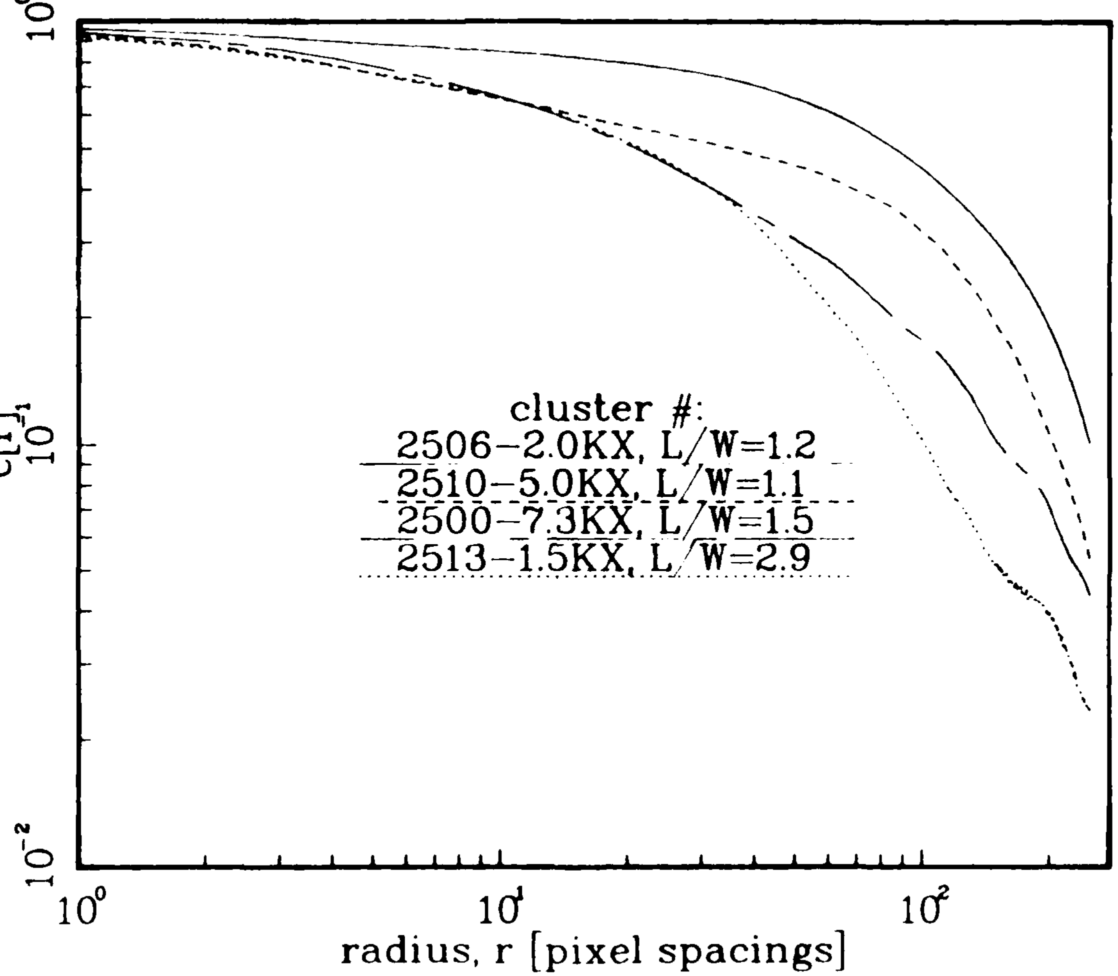

SUMMARY OF SOOT STRUCTURE RESULTS

AGGLOM SIZE, μm	FRACT. DIMEN.	METHOD	$\frac{LENGTH}{WIDTH}$
0.065 - 0.80	1.49	R_g vs N	1.68 ± 0.50
	1.61	$(LW)^{1/2}$ vs N	
5.5 - 40	1.87	Pair Corr. Funct	1.80 ± 0.66
	1.83	Covering method	

SMOKE CONVERSION FACTOR

ε = MASS OF SMOKE PRODUCED/MASS OF FUEL CONSUMED

FLUX METHOD

$$\varepsilon_1 = \frac{\text{MASS ON FILTER}}{\text{MASS LOSS OF SAMPLE}} \quad \frac{\dot{M}_{air}\ (\text{STACK})}{\dot{M}_{air}\ (\text{FILTER})}$$

CARBON BALANCE METHOD

$$\varepsilon_2 = \frac{M_S \quad (\text{C FRACT OF FUE}}{(M_S + M_C\,(CO_2) + M_C\,(CO))} \quad \frac{1}{(\text{C FRACT OF FUE}}$$

LIGHT EXTINCTION COEFFICIENTS

$K \equiv$ EXTINCTION COEFFICIENT AT $\lambda = 633$ nm, m^{-1}

$$I/I_o = e^{-KL}$$

[illegible] MASS CONC OF SMOKE, m^2/g

[illegible] LOSS RATE OF SAMPLE / STACK FLOW)

FACILITY FOR MONITORING SMOKE EMISSION/PROPERTIES

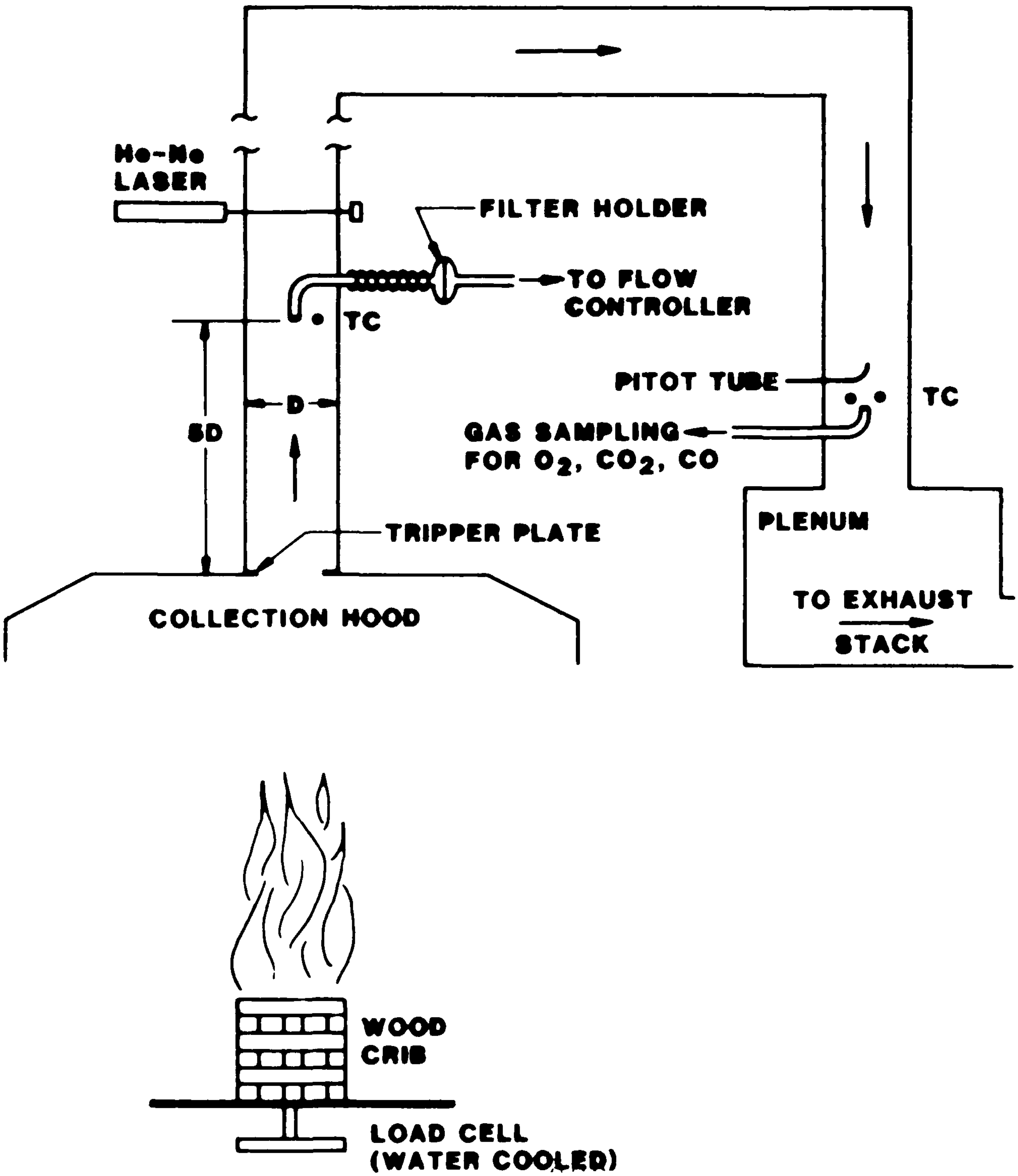

3-FILTER, ALL GLASS, SMOKE COLLECTION SYSTEM

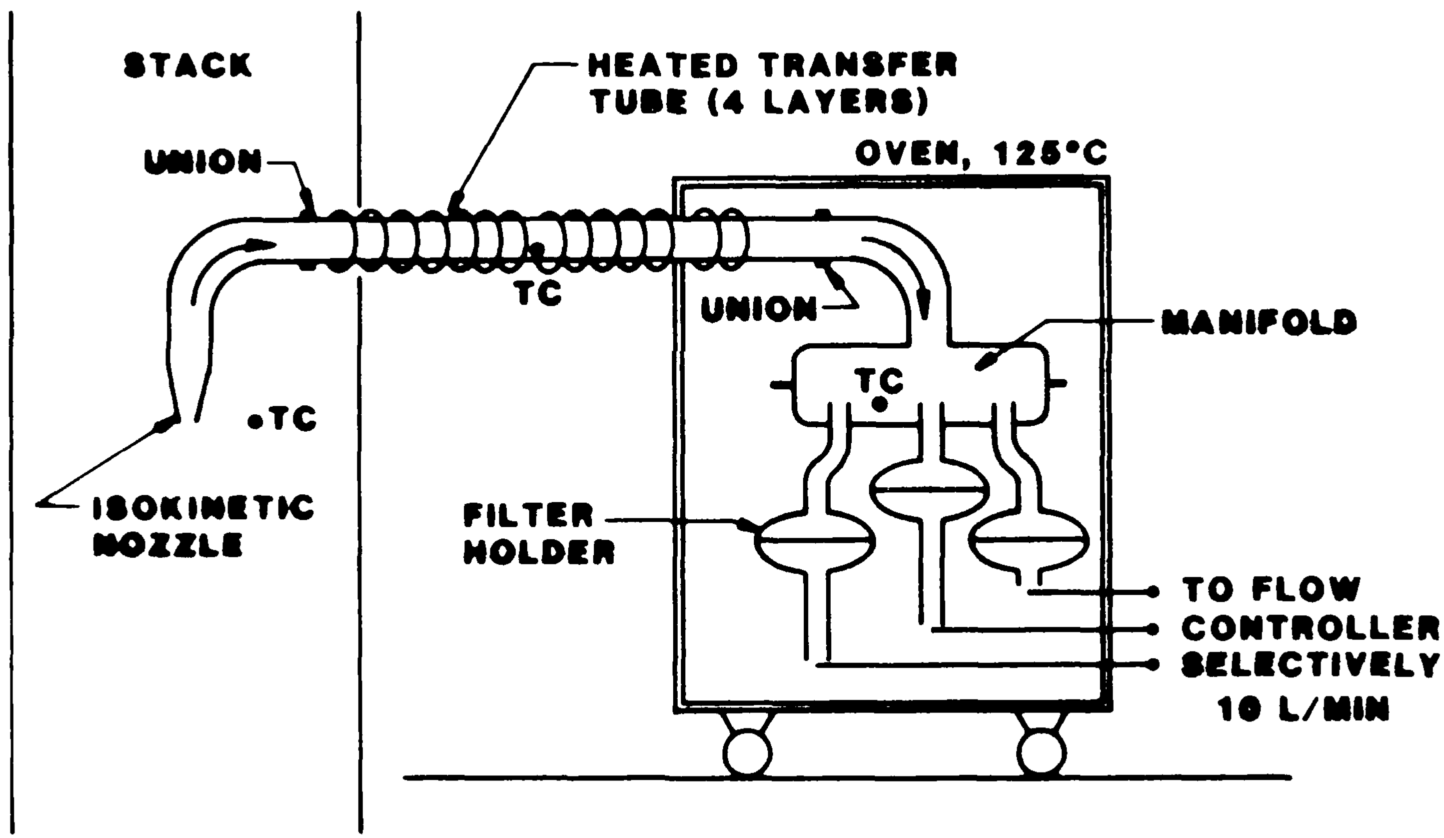

Oxygen Concentration in Pipe — 3 Wood "Cribs"

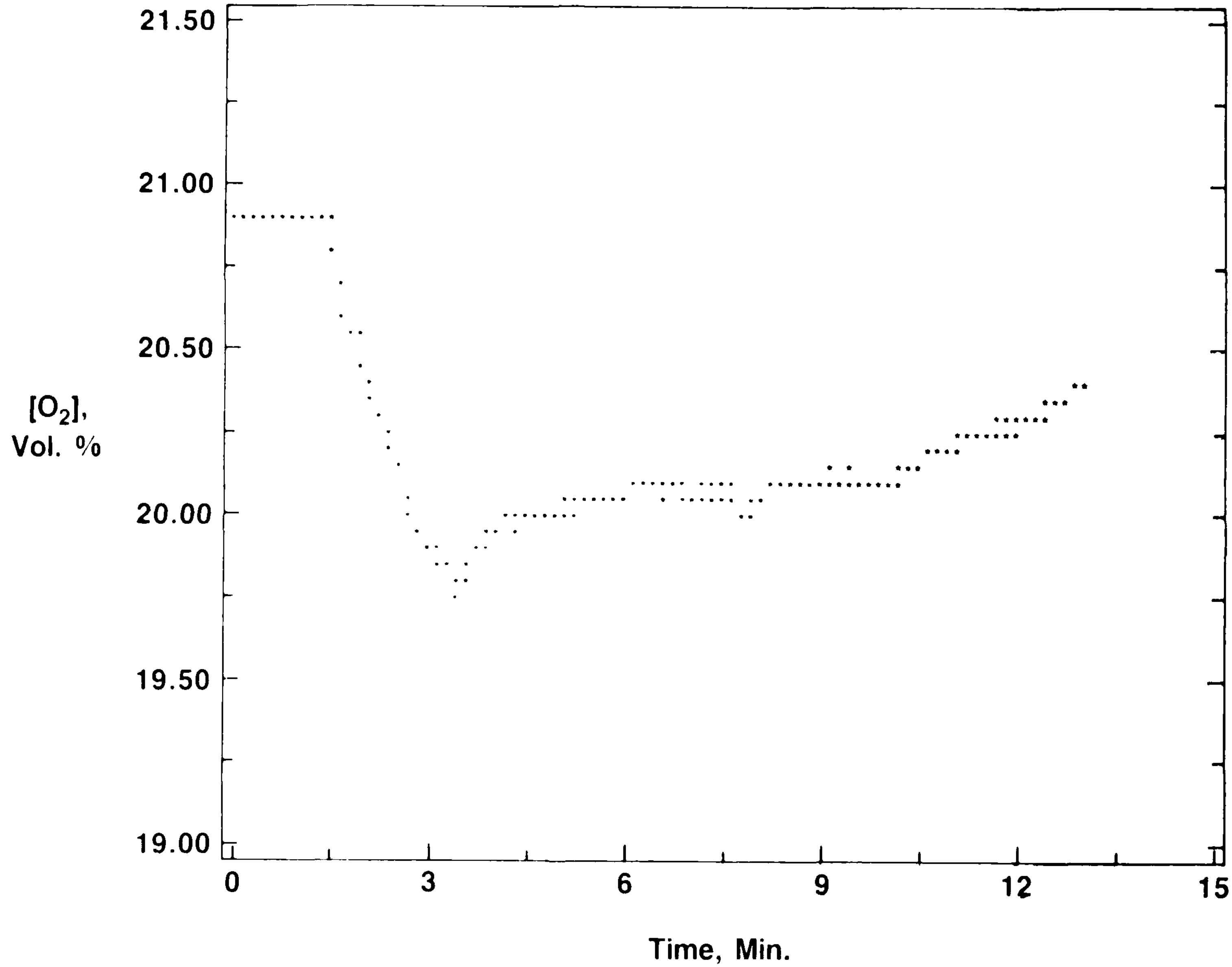

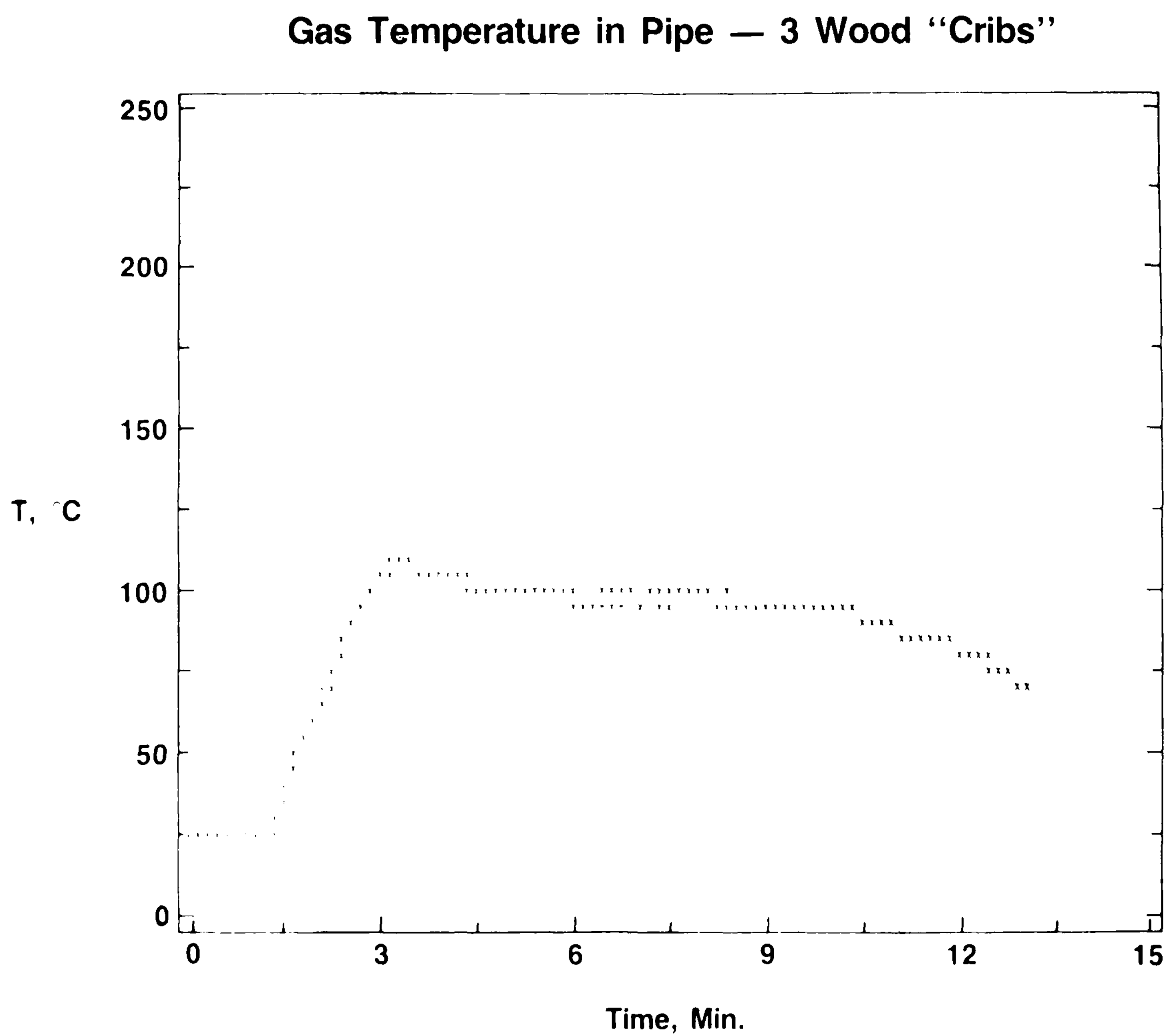

Gas Temperature in Pipe — 3 Wood "Cribs"
T, °C
250
200
150
100
50
0
0
3
6
9
12
15
Time, Min.

Gas Velocity Through Pipe — 3 Wood "Cribs"

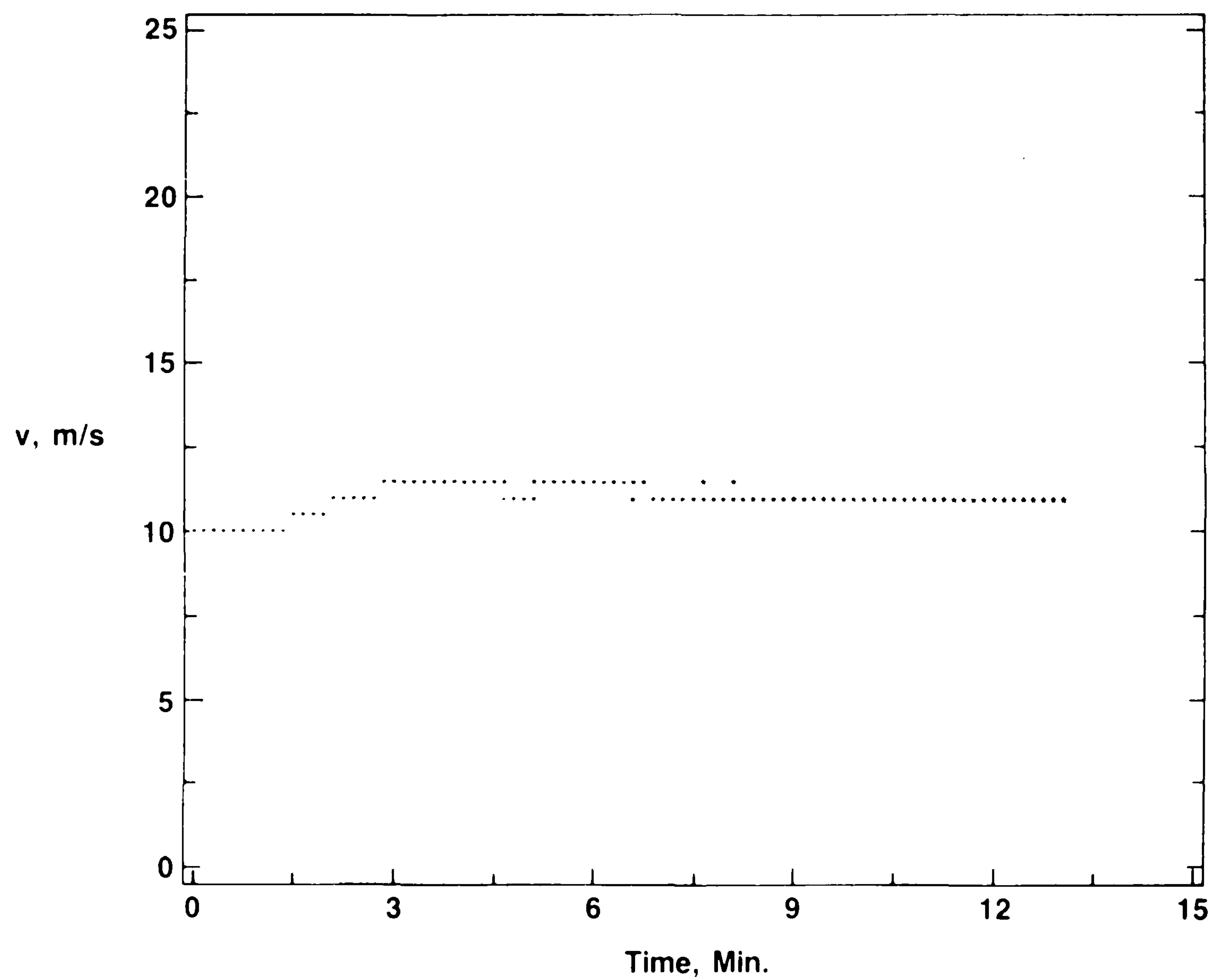

Rate of Mass Loss and Rate of Heat Release — 3 Wood "Cribs"

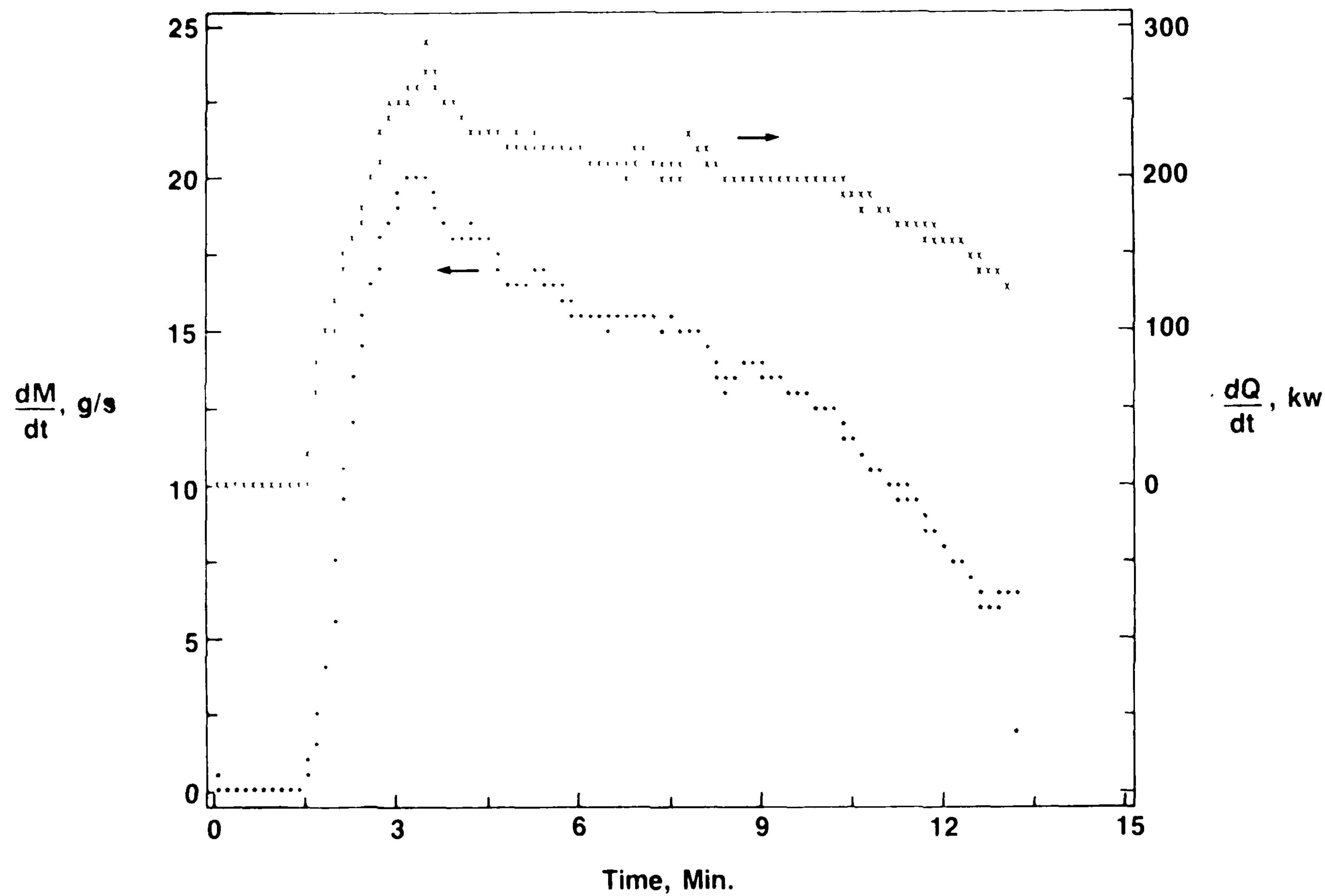

Rate of Mass Loss and Smoke Extinction Coefficient — 3 Wood "Cribs"

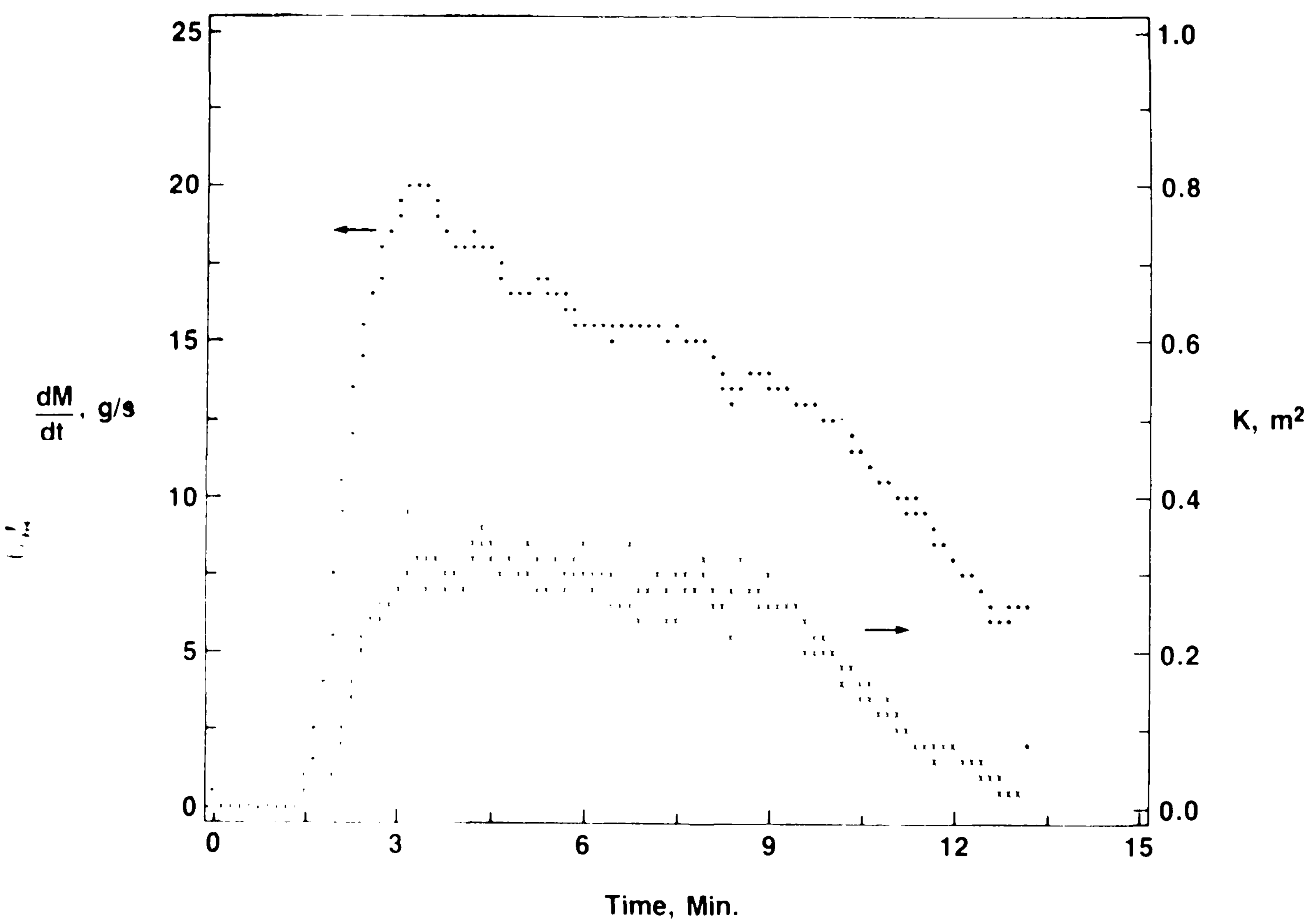

CO_2 and CO Concentrations — 3 Wood "Cribs"

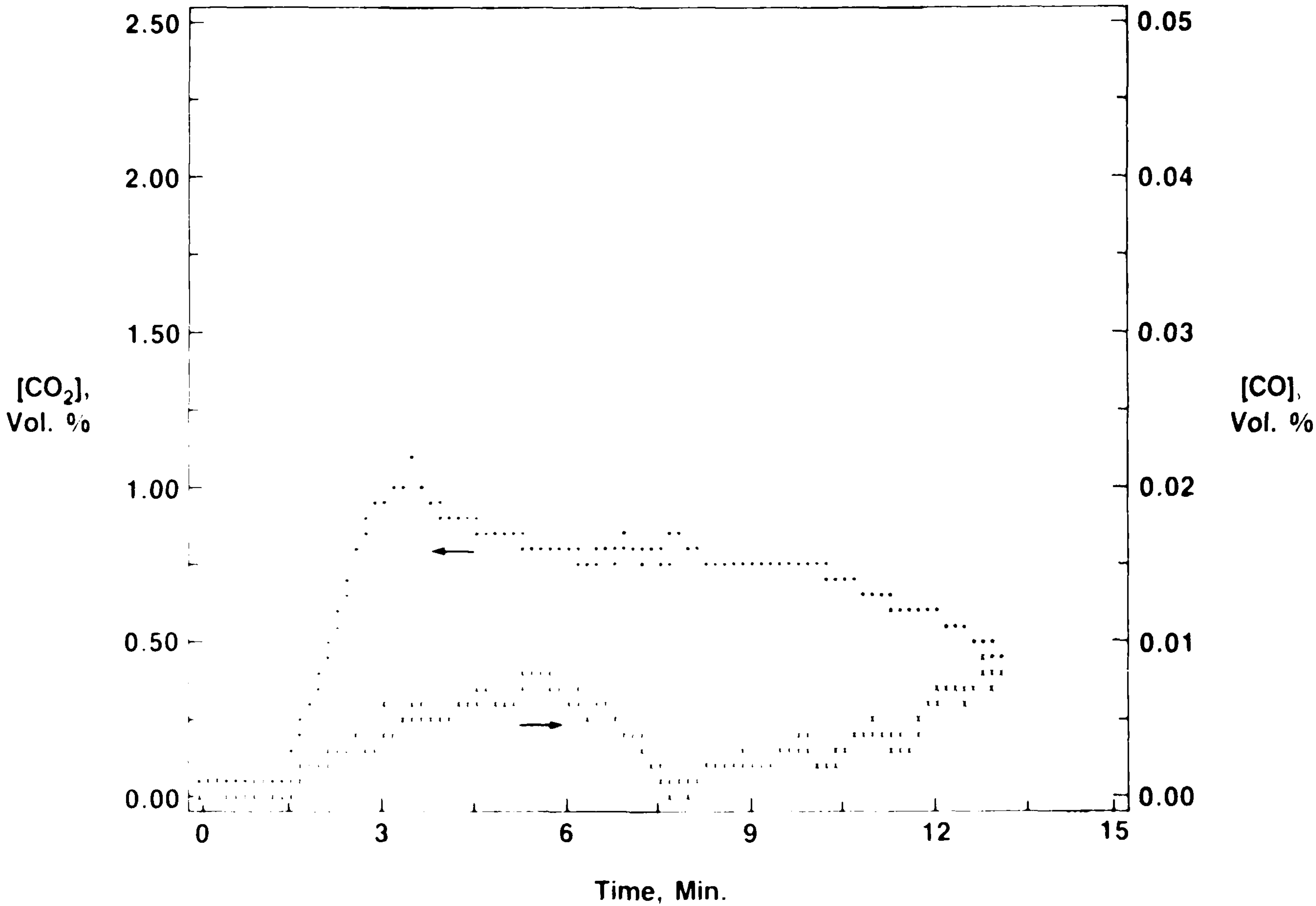

Specific Extinction Coefficient Relative to Fuel — 3 Wood "Cribs"

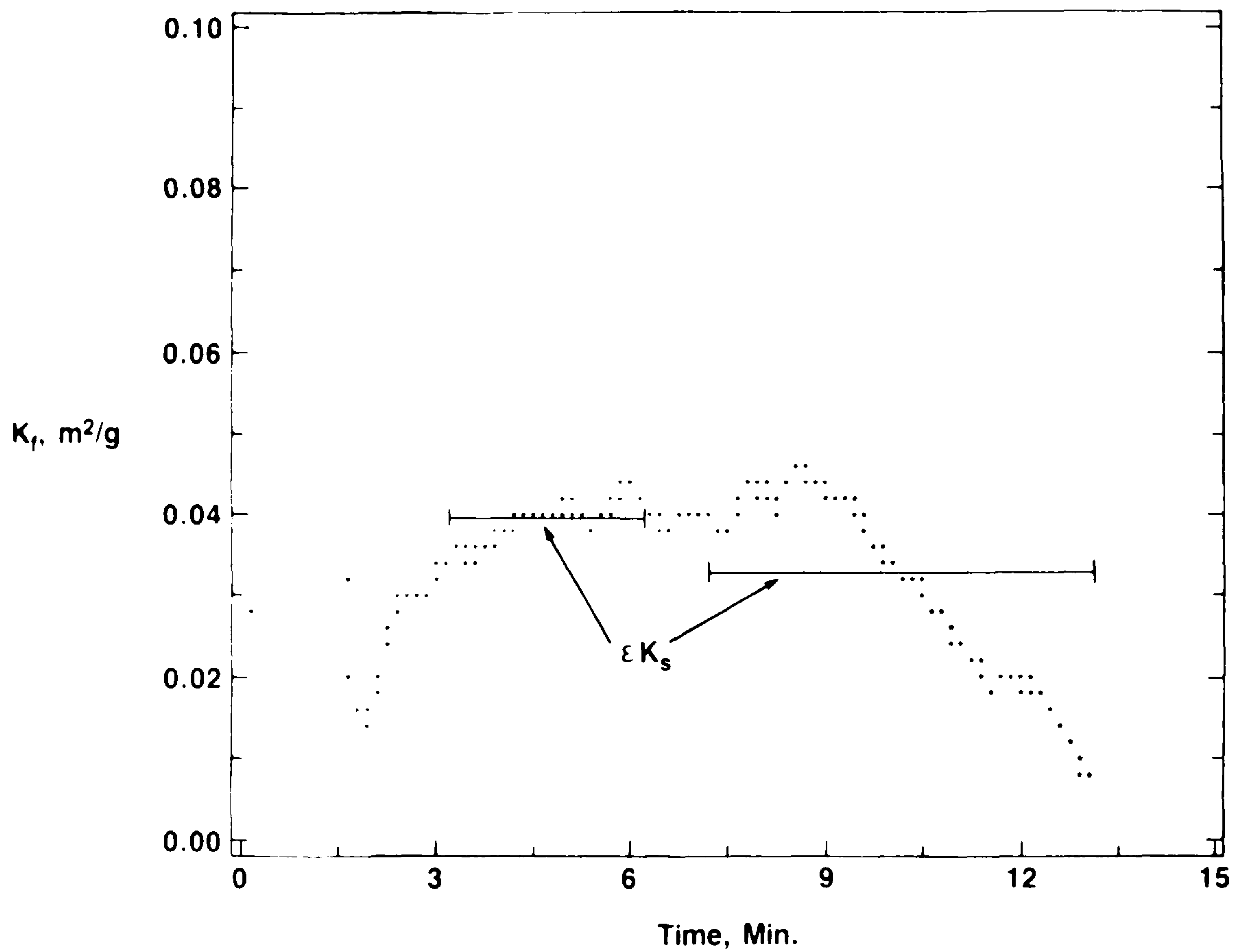

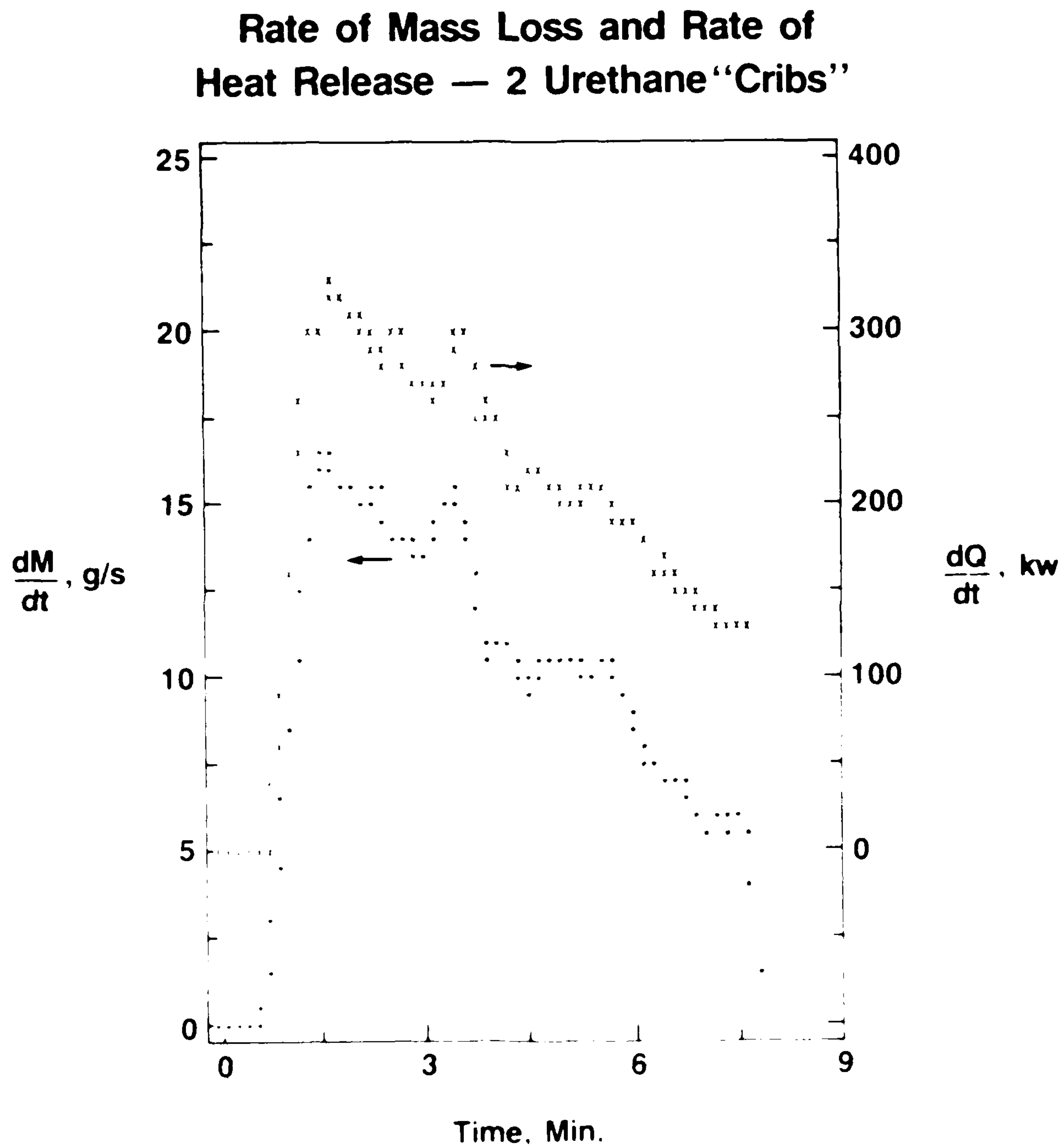
Rate of Mass Loss and Rate of
Heat Release — 2 Urethane "Cribs"
25
20
15
10
5
0
400
300
200
100
0
$\frac{dM}{dt}$, g/s
$\frac{dQ}{dt}$, kw
0
3
6
9
Time, Min.

CO_2 and CO Concentrations — 2 Urethane "Cribs"

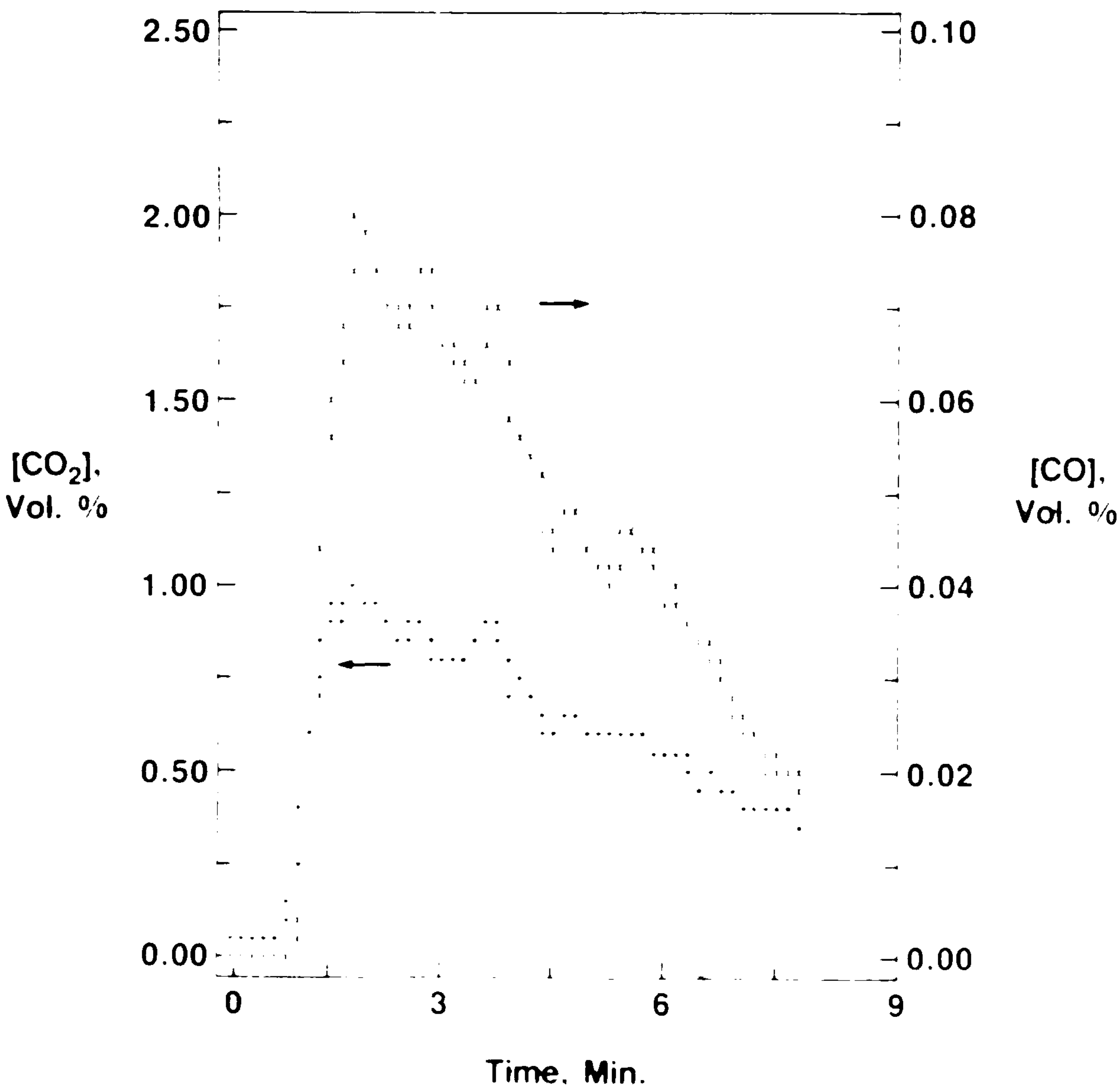

Rate of Mass Loss and Smoke Extinction Coefficient — 2 Urethane "Cribs"

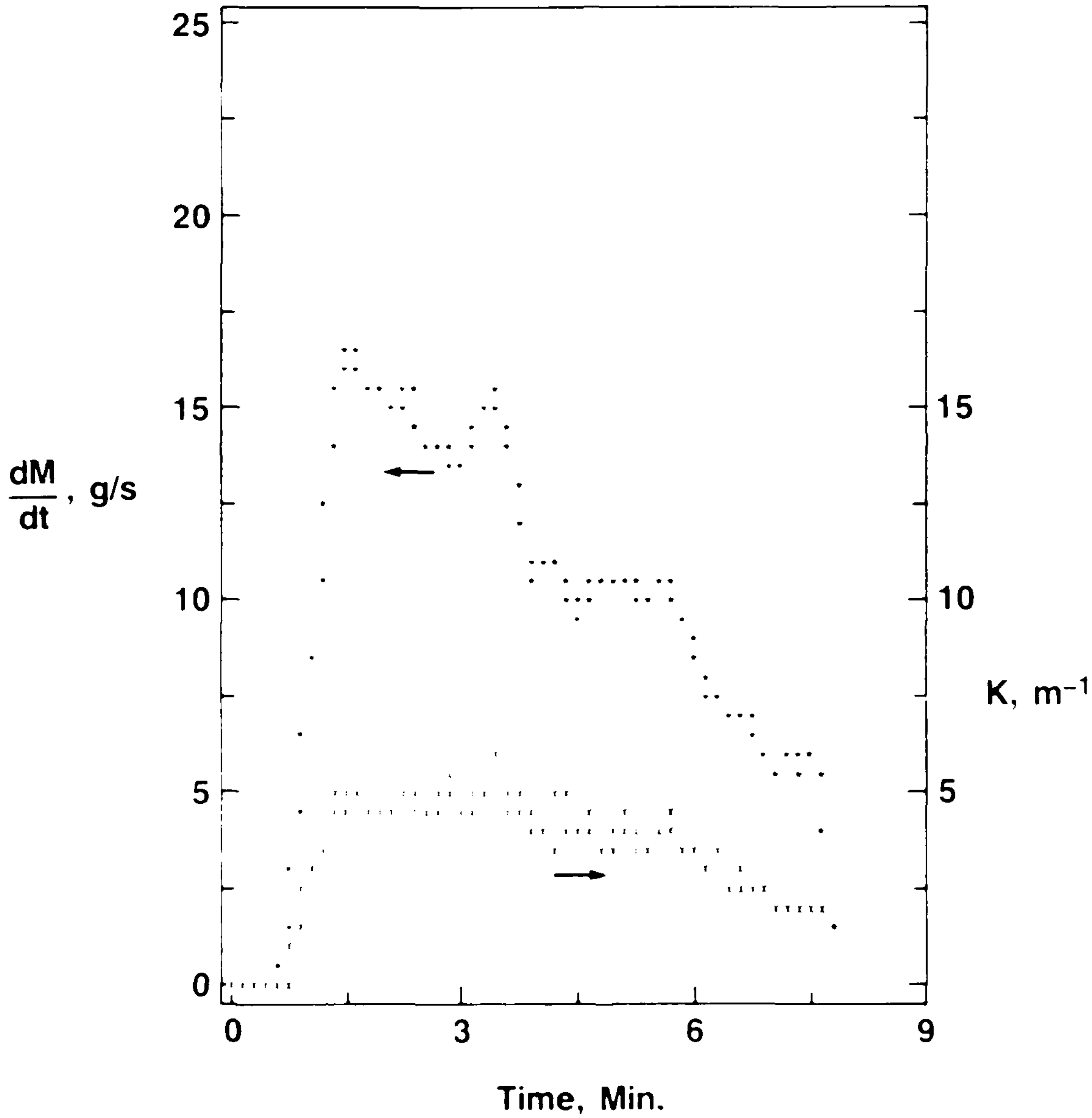

Specific Extinction Coefficient Relative to Fuel — 2 Urethane "Cribs"

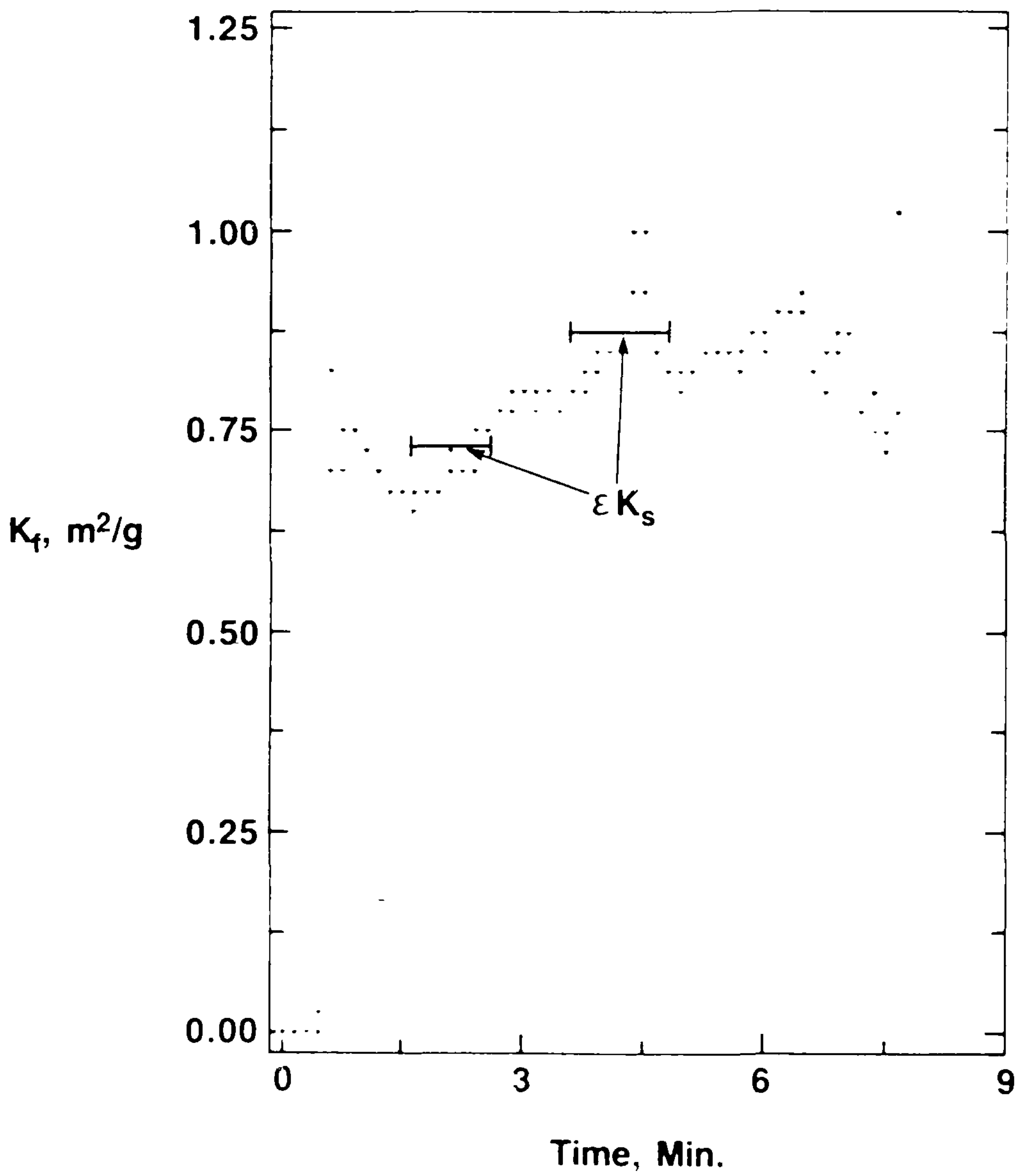

TEST CASE - PROPANE

EXP. #	FUEL FLOW RATE, g/s	ε_1 (10^{-2})	ε_2 (10^{-2})	K m^{-1}	K_s m^2/g
6	2.37	0.37	0.40	0.107	13.62 *
	(100 kW)	0.61	0.61	0.104	8.05
		0.62	0.60	0.103	8.00
AVG		0.61			8.02
1	3.68	1.69		0.221	8.07
	(175 kW)	1.49		0.195	8.04
		1.37		0.141	4.91 *
AVG		1.59			8.06
2	4.87	1.90		0.329	7.97
	(250 kW)	1.72		0.309	8.31
		1.75		0.307	8.14
AVG		1.79			8.14
3 & 4	8.12	2.07	2.04	0.473	7.06
	(350 kW)	1.76	1.77	0.433	7.47
		1.60	1.73	0.421	8.10
		1.61	1.60	0.439	8.77
		1.25	1.25	0.424	10.72 *
		1.71	1.74	0.392	7.37
AVG		1.75 ± 0.19			7.75 ± 0.68
GRAND AVG					7.95 ± 0.45

TIME DEPENDENCE OF SMOKE

PROPERTIES

FUEL	TIME MIN.	MASS LOSS RATE, g/s	$\varepsilon_1 (10^{-2})$	$\varepsilon_2 (10^{-2})$	$\frac{C(OUT)}{C(IN)}$	K_s m^2/g
HEPTANE	3	5.4	1.29	1.29	0.97	8.30
50 cm pool	7	6.0	1.31	1.30	1.01	8.13
WOOD	3	19.4	0.42	0.59	0.72	9.50
3 "cribs"	7	11.9	0.43	0.52	0.84	7.55
POLYURETH.	2	15.8	8.96	10.00	0.90	8.14
2 "cribs"	5	7.9	11.00	11.82	0.93	7.77

"ELEMENTAL CARBON" ANALYSIS

OF SMOKE

FUEL		% ELEMENTAL CARBON CARY	KLUUDA	K_s m^2/g
PROPANE		45	44	795
		76	74	
HEPTANE		66	85	817
		75	100	
WOOD	2 min	75	93	936
	7 min	82	95	774
POLYURETHANE				
	1 min	86	87	847
	5 min	85	92	777

* Blank not subtracted

SUMMARY OF RESULTS ON SMOKE EMISSION

AND LIGHT EXTINCTION COEFFICIENT

FUEL	FIRE SIZE kW	ε (10^{-2})	K_s m^2/g, $\lambda = 633$ nm
PROPANE	100	0.61	8.02
	350	1.75 ± 0.19	7.75 ± 0.45
HEPTANE	70	0.92 ± 0.06	7.64 ± 0.47
	250	1.21 ± 0.10	8.17 ± 0.74
WOOD	50	0.36	8.49 early time
	250	0.43 ± 0.01	8.55 average
POLYURETH.	125	8.44 ± 0.55	8.57 ± 0.78
	300	10.08 ± 1.17	8.17 ± 0.38

$\sigma_v = \underline{8.33}$ $\sigma_v = 5.8$

$\sigma_D = \frac{1}{D}\sigma_v$ $\sigma_{D_1} = 1.92$

unpaired object $\underline{\sigma_D = 2.78}$ $\underline{\sigma_{D_2} = 3.2}$

agglomerate $\underline{\sigma_{D_1} = 4.62}$

43 mm = 1 decade

7

radio

$\sigma_v = \frac{2.5}{.4} = \frac{4}{.005} = \sqrt{\frac{2.5}{.05}}$

$= 6.25 = 8 = 7.07$

$\sigma_v \simeq 7.0$

$\sigma_d = \frac{1}{D}\sigma_v$

unpaired object $\sigma_d = 2.3$

agglomerate $\underline{\sigma_{d_1} = 3.9}$
with $D_f = 1.8$

Source Term Research Program at Sandia National Laboratories

B.D. Zail, S.P. Nowlan, N.R Keltner, & K.D. Bergeron
Sandia National Laboratories

SNL PROGRAM

- EXPERIMENTAL PLANS AND CURRENT STATUS
- MODELING
- RELATED DATA

(SS/NW18 2/86)

NUCLEAR WINTER SOURCE TERM

SNL EXPERIMENTAL PLANS

- LAB SCALE
- ROOM SCALE
- INTERMEDIATE POOL FIRES
- LARGE POOL FIRES
- SCHEDULED FOREST BURNS

(SS/NW 7/85)

LAB SCALE EXPERIMENTS

- ONGOING FUNDAMENTAL STUDIES OF SOOT PRODUCTION AS PART OF COMBUSTION RESEARCH PROGRAM
- COMPARISON OF SOOT PRODUCTION BY DIFFERENT LIQUID FUELS UNDER IDENTICAL CONDITIONS
- GOAL: CLASSIFY MAJOR LIQUID FUELS INTO GROUPS WITH SIMILAR SOOT PRODUCTION PROPERTIES TO REDUCE NUMBER OF TESTS REQUIRED IN LARGER FACILITIES

(SS/NW2 7/85)

Room Scale

Nuclear Winter

Fire Testing at SNLA

Room Fire Test Facility

- 24'x25'x18' Earth sheltered bunker
- Fully enclosed
- Controlled forced ventilation system
  (0 to 3000 CFM)
- Fully instrumented for fire testing
- Easily accessed exhaust stack
  at "ground level"
- Capable of withstanding fires up
  to 2-MW in intensity

The effects of the following parameters on the burning behavior will be investigated

- Fuel type
- Pool size, fire intensity
- Oxygen availability
- Smoke recirculation
- Ambient humidity

AD-A185 149 TECHNICAL PAPERS PRESENTED AT THE DEFENSE NUCLEAR AGENCY GLOBAL EFFECTS R..(U) DOD NUCLEAR INFORMATION AND ANALYSIS CENTER SANTA BARBARA CA.. 15 MAY 86 2/3

UNCLASSIFIED DASIAC-TN-86-29-VOL-1 DNA001-82-C-0274 F/G 15/6.4 NL

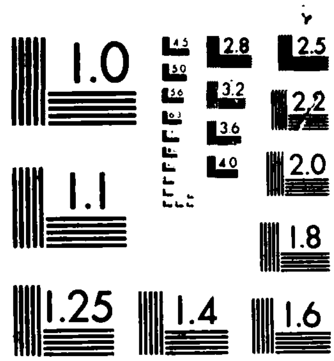

MICROCOPY RESOLUTION TEST CHART
NATIONAL BUREAU OF STANDARDS 1963 A

Fuels to be tested:

JP-4 Jet fuel

Heptane

Gasoline

Pool fire sizes:

0.1 to 1.0 Square meters

50 to 2000 kW

	"Traditional" Fire Characteristics															
	Mass Rel. Rate	Heat Rel. Rate			Burn Effic.			Oxy. Avail.		CO Production	CO/2 Prod.	Carbon Distr.	Plume Vel.	Plume Temp.	Plume Radia.	Smoke Radia.
Oxygen Monitor		●			●			●								
Carbon Monoxide Monitor							●			●		●				
Carbon Dioxide Monitor			●			●	●				●	●				
Hydrocarbon Monitor												●				
Load Platform	●			●	●	●										
Velocity Probes		●	●					●		●	●		●			
Radiometers/Calorimeters															●	●
Thermocouples														●		

Measuring traditional fire characteristics

	Smoke Characteristics									
	Light Extinc.	Light Scatt.	Light Absorb.	Mass Gen. Rt.	Part. Size				Part. Shape	Compos./Size
Optical Density Meters	●		●		●					
Cascade Impactors						●				
Cyclone Separator							●			●
Diffusion Battery								●		
Filters/Pumps				●						
Nephelometer		●	●							
Electrostatic Precipitator									●	

Measuring smoke production characteristics

INTERMEDIATE POOL FIRE EXPERIMENTS

- MEASUREMENT OF AEROSOL EMISSIONS FROM REGULATORY JP–4 FIRES
- AEROSOL PROPERTIES
- DEVELOPMENT OF TRACER TECHNIQUE FOR EMISSION FACTOR MEASUREMENTS
- CHECK OF TRACER TECHNIQUE AGAINST ARRAY TECHNIQUE IN PLUMES

(SS/NW4 7/85)

LARGE POOL FIRES

- 30' X 60' POOL (170 m)
- 0.5 – 2.0 HR DURATION
- 15,000 GAL/HR OF JP–4 (TYPICALLY)
- DESIGNED FOR REGULATORY FIRES

(SS/NW13 7/85)

LARGE POOL FIRES

- NOW
- SUMMER 1986
- FY 87 (?)

(SS/NW5 7/85)

GOALS OF EFFORT ON FEBRUARY/MARCH 1986 FIRE:

- o TECHNIQUE DEVELOPMENT
- o EXPLORATORY MEASUREMENTS

(SS/NW15 2/86)

FEBRUARY/MARCH 1986 POOL FIRE

- TRACER IN FUEL/FUEL SAMPLING
- SINGLE POINT PLUME SAMPLING AT 300 m WITH 4kg BALLOON PAYLOAD
- VERTICAL VELOCITY MEASUREMENTS AT BALLOON
- AIRCRAFT AEROSOL AND GAS SAMPLING IN DOWNWIND PLUME CROSS-SECTION (SNL/DRI)
- INFLOW MEASUREMENTS WITH LASER ANEMOMETER ARRAY (LLNL)
- SUPPORTING WIND SPEED, TEMPERATURE, AND HUMIDITY PROFILES

(SS/NW7 7/85)

BALLOON SAMPLING

- AEROSOL SAMPLING ON QUARTZ, TEFLON, AND NUCLEOPORE MEDIA AT 2 DIFFERENT FLOW RATES
- GAS SAMPLING

(SS/NW14 2/86)

AIRCRAFT INSTRUMENTATION FOR FEBRUARY/MARCH 1986 POOL FIRE

- WING–MOUNTED LASER PARTICLE–SIZING PROBES FOR 0.5–45 AND 25–1550 μm
- WING–MOUNTED TEMPERATURE AND DEW POINT SENSORS
- 100 L PROTOTYPE "GULP" BAG SAMPLER
- FILTER SAMPLING FROM EACH SEQUENTIAL GULP ON QUARTZ, TEFLON, AND NUCLEOPORE MEDIA THROUGHOUT FIRE
- GAS SAMPLING FROM EACH GULP
- CN MEASUREMENTS ON EACH GULP (DRI)
- POSITION, ALTITUDE, AND AIR SPEED MEASUREMENTS
- DATA ACQUISITION SYSTEM

(SS/NW16A 2/86)

PLANNED AIRCRAFT INSTRUMENTATION FOR SUMMER 1986 POOL AND FOREST FIRE EXPERIMENTS

- EXTERNALLY–MOUNTED LASER PARTICLE–SIZING PROBES FOR 0.12–3, 0.5–45, AND 25–1550 μm
- WING–MOUNTED TEMPERATURE AND DEW POINT SENSORS
- FORMVAR PARTICLE REPLICATOR (DRI)
- INTEGRATING NEPHELOMETER
- REAL TIME CO2 MONITOR (?)
- 6–WAVELENGTH AUTOTRACKING SUN PHOTOMETER (NASA/SNL)
- 1,000 L "GULP" BAG SAMPLER
- FILTER SAMPLING FROM EACH SEQUENTIAL GULP ON QUARTZ, TEFLON, AND NUCLEOPORE MEDIA THROUGHOUT FIRE; CYCLONE PRE–SEPARATOR (?)

(CONTINUED)

(SS/NW16A 2/86)

PLANNED AIRCRAFT INSTRUMENTATION (continued)

- GAS SAMPLING FROM EACH GULP
- CN AND CCN MEASUREMENTS ON EACH GULP (DRI)
- NEPHELOMETER MEASUREMENTS ON EACH GULP
- DIFFERENTIAL MOBILITY PARTICLE SPECTROMETER MEASUREMENTS COVERING .01–1.0 μm ON EACH GULP
- POSITION, ALTITUDE, AND AIR SPEED MEASUREMENTS
- DATA ACQUISITION SYSTEM

(SS/NW17)

INFORMATION TO BE OBTAINED ON RESPECTIVE FUELS FROM LARGE POOL FIRE AND FOREST FIRE EXPERIMENTS

- o GROSS AEROSOL EMISSION FACTORS*
- o EXTINCTION EMISSION FACTORS*
- o ABSORPTION AND SCATTERING EMISSION FACTORS*
- o VOLATILE AND NON-VOLATILE CARBON EMISSION FACTORS*
- o GASEOUS SPECIES EMISSION FACTORS*
- o PARTICLE SIZE DISTRIBUTIONS, 0.01–1550 μm
- o SPECIFIC ABSORPTION COEFFICIENTS
- o SPECIFIC SCATTERING COEFFICIENTS
- o SPECIFIC EXTINCTION COEFFICIENTS
- o PARTICLE MORPHOLOGY
- o CCN/CN RATIO VS. TRAVEL TIME

*BASED ON MULTIPLE TRACER TECHNIQUES

(SS/NW20 2/86)

SUMMARY

AT A SCALE:

LAB–SIZE

- o CLASSIFICATION OF LIQUID HYDROCARBON FUELS
- o RELATE EMISSION FACTORS AND OPTICAL CHARACTERISTICS TO FLAME CONDITIONS

ROOM–SIZE/INTERMEDIATE POOL FIRES

- o INFLUENCE OF BOUNDARY CONDITIONS ON AEROSOL FORMATION (e.g. O_2 AVAILABILITY, RADIATIVE ENVIRONMENT, RECYCLED COMBUSTION PRODUCTS)
- o EFFECT OF BURNING CONDITIONS AND FUEL CONFIGURATIONS
- o ACCURATE MEASUREMENT OF BURN RATE, SMOKE EVOLUTION, AND AEROSOL CHARACTERISTICS
- o INVESTIGATION OF VALIDITY OF ASSUMPTIONS REGARDING TRACER TECHNIQUES (INCLUDING CARBON)

LARGE–SCALE

- o FIRE–INDUCED FLOW FIELD DATA
- o EMISSION FACTOR, OPTICAL, AND METEOROLOGICAL CHARACTERISTICS OF AEROSOLS AT THIS SCALE
- o DOWN–PLUME AEROSOL BEHAVIOR

ACROSS SCALE:

- o SCALING FEASIBILITY
- o DATA BASE FOR MODELS AND EXTRAPOLATION

(SS/NW19 2/86)

AEROSOL DYNAMICS MODELING

A Two-component Aerosol Distribution and Processes Affecting its Evolution

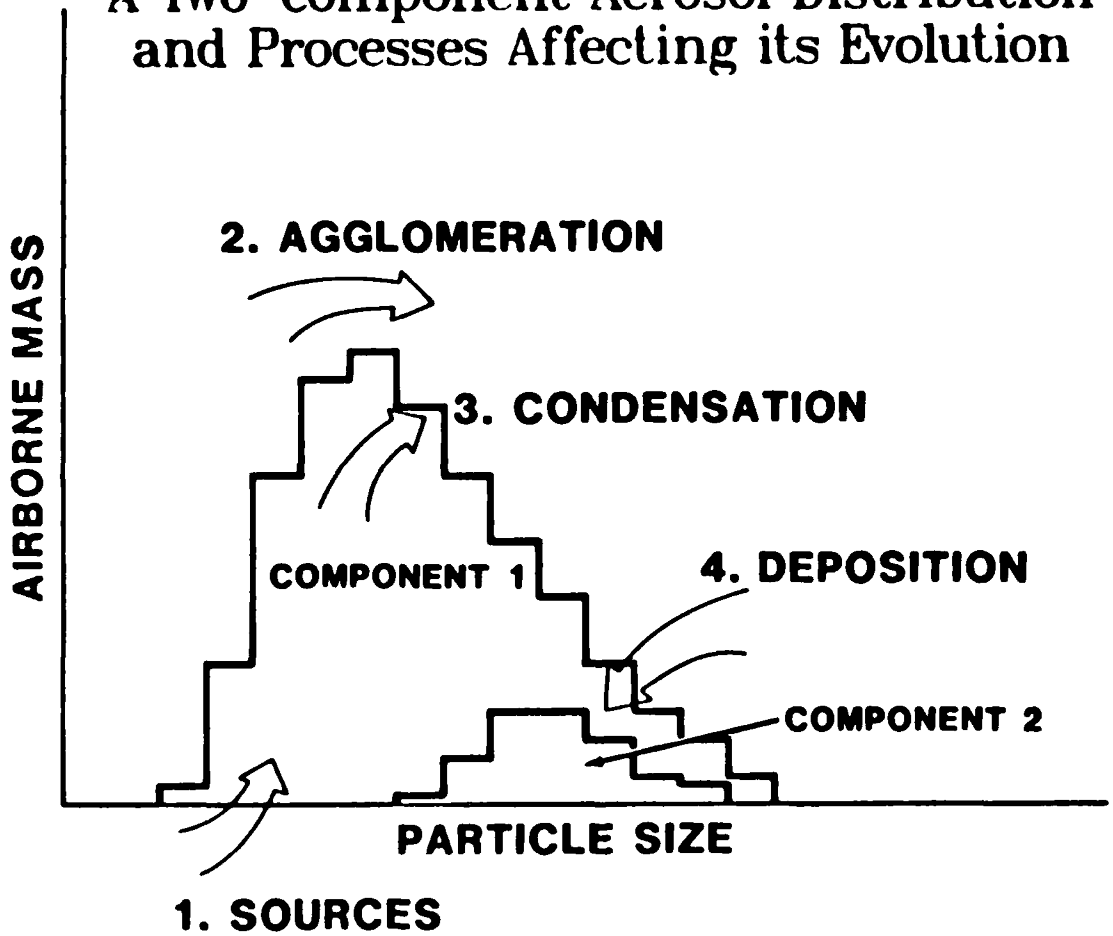

ABCOVE Aerosol Validation Experiments

* Dry aerosol tests performed at HEDL

* Specifically designed for "blind" code validation

* Earlier AB5 test provided strong validation of CONTAIN for single component aerosols

* More recent AB6, AB7 tests involved two aerosol components, NaI and NaOx

* AB7 was run as a refinement of AB6 to eliminate some experimental problems (e.g., NaI vaporization)

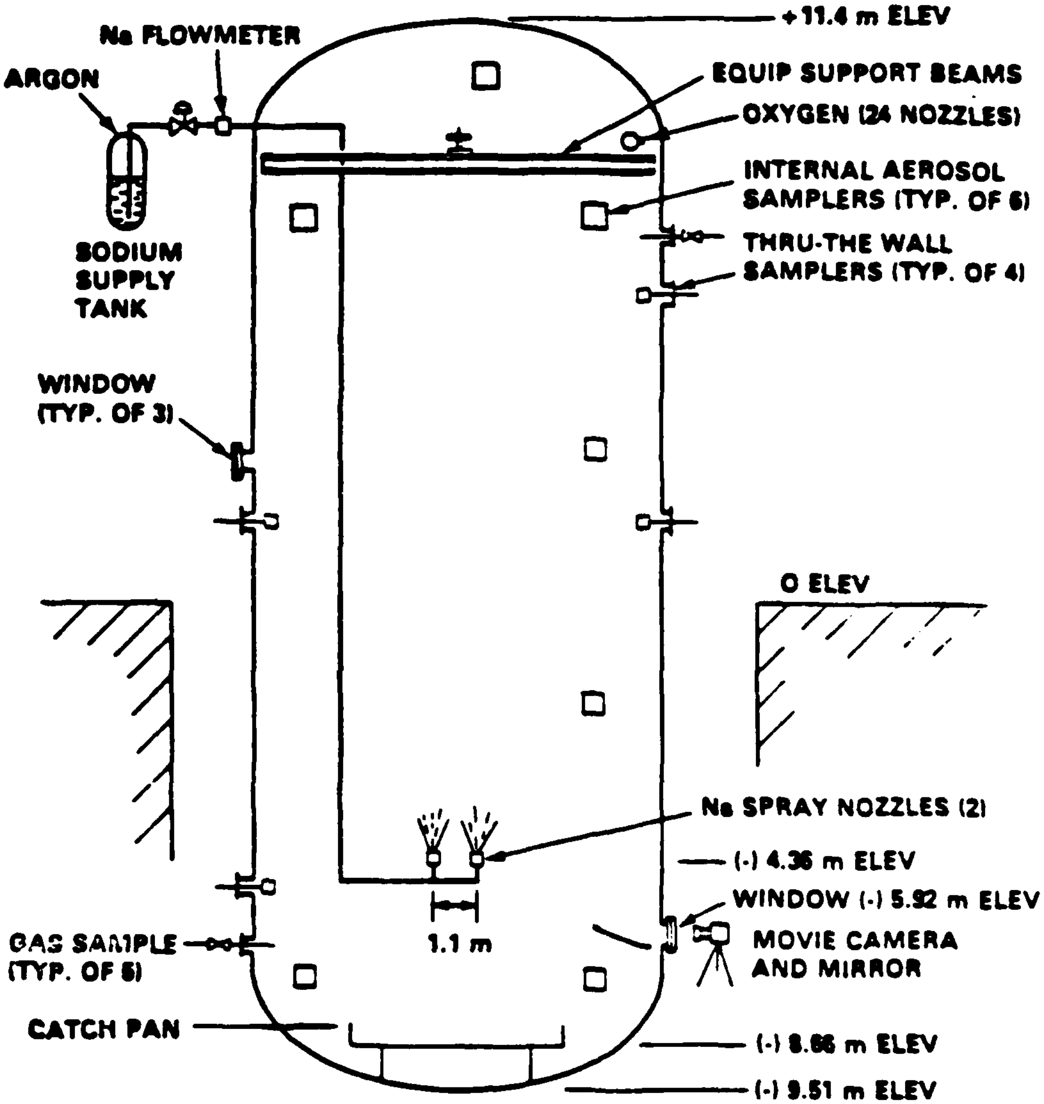

+11.4 m ELEV
Na FLOWMETER
ARGON
EQUIP SUPPORT BEAMS
OXYGEN (24 NOZZLES)
INTERNAL AEROSOL
SAMPLERS (TYP. OF 6)
SODIUM
SUPPLY
TANK
THRU-THE WALL
SAMPLERS (TYP. OF 4)
WINDOW
(TYP. OF 3)
O ELEV
Na SPRAY NOZZLES (2)
(-) 4.36 m ELEV
WINDOW (-) 5.92 m ELEV
GAS SAMPLE
(TYP. OF 5)
1.1 m
MOVIE CAMERA
AND MIRROR
CATCH PAN
(-) 8.66 m ELEV
(-) 9.51 m ELEV

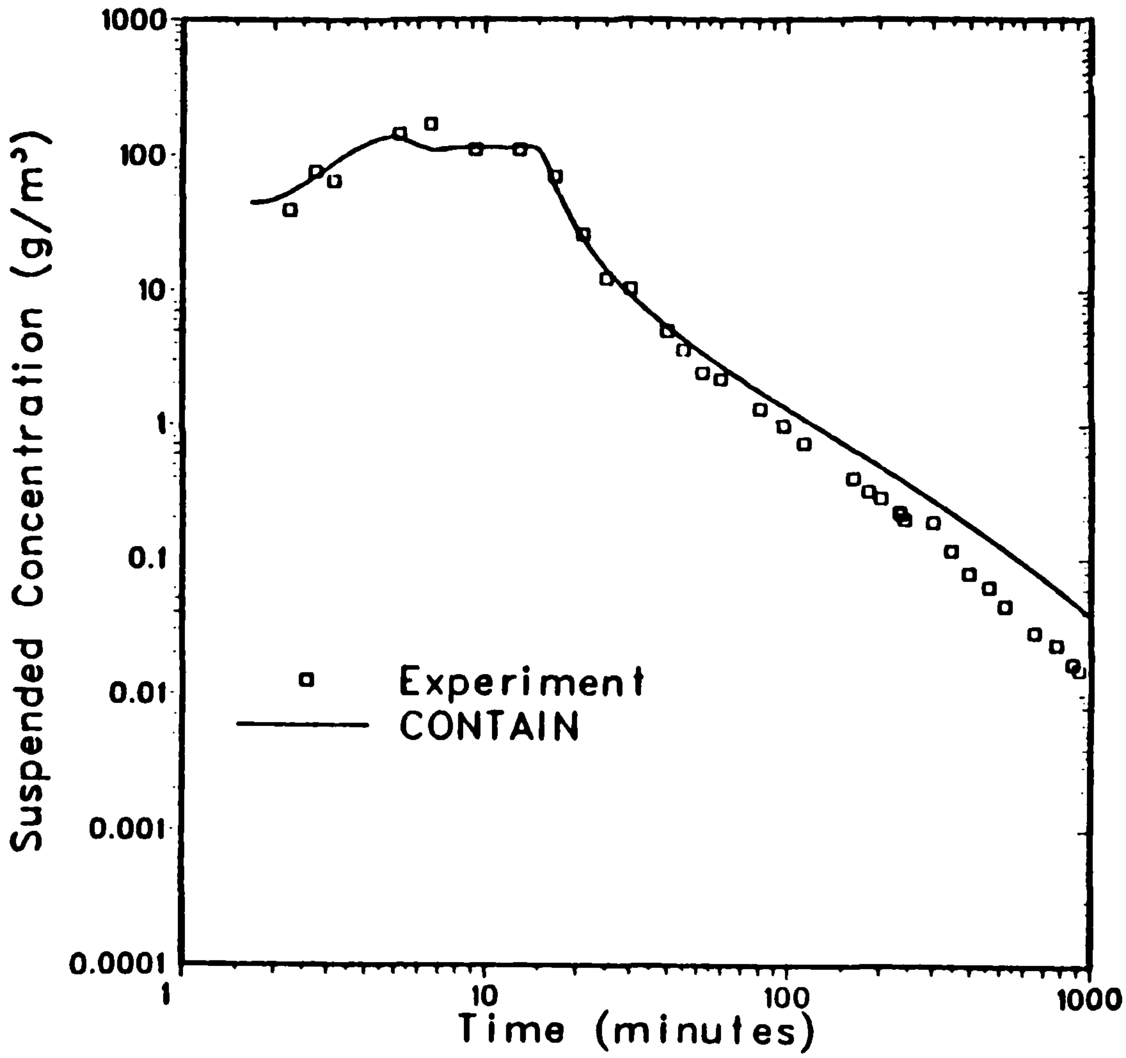

FIGURE 2. THE AEROSOL CONCENTRATION IN AB-5 PREDICTED BY CONTAIN VERSUS THE MEASURED VALUES.

ABCOVE AB–5 Results

* Aerosol behavior measured over 5 days and 6 orders of magnitude in concentration

* Lognormal codes gave poor results after end of source

* Discrete codes did fairly well in general

* CONTAIN and MAEROS outperformed all other codes

ABCOVE Test AB6 Blind Prediction

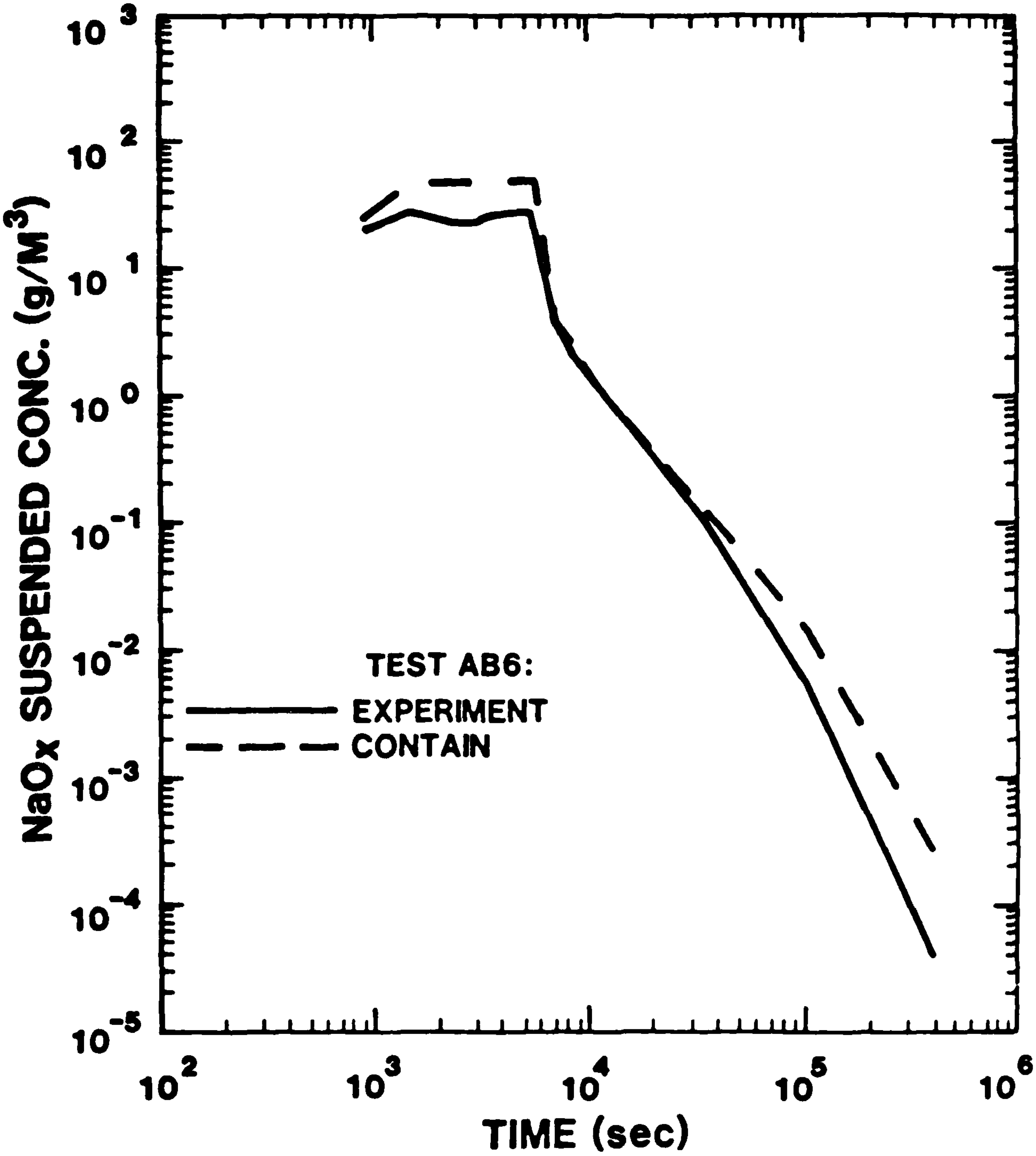

ABCOVE Test AB7 Blind Prediction

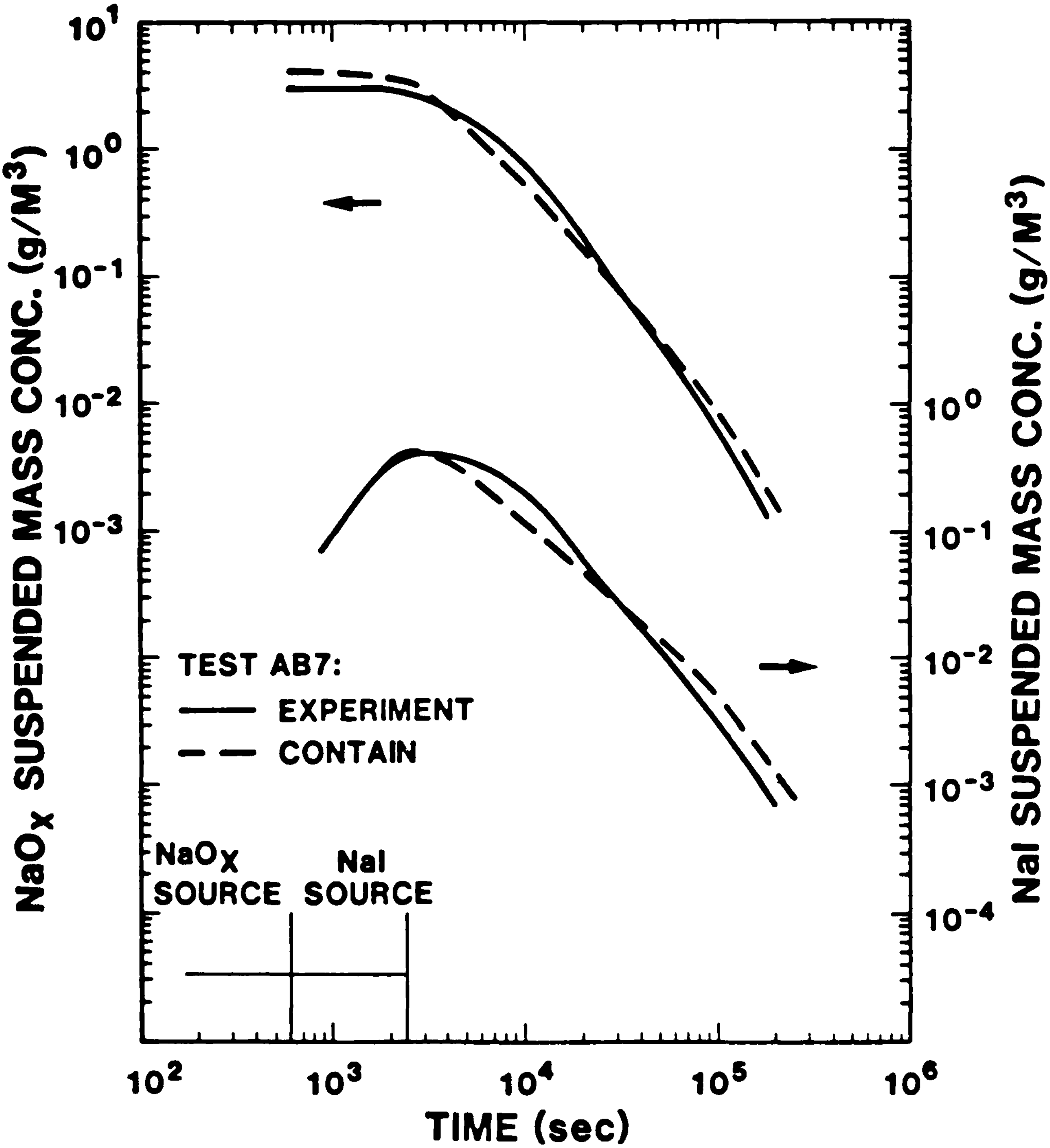

RELATED RESULTS

PRELIMINARY RESULTS OF STACK SAMPLING AT 1/10 SCALE POOL FACILITY

- WITH AIR/FUEL RATIO OF 20/1, RATIO OF PARTICULATE MASS/TOTAL CARBON MASS (GASEOUS AND PARTICULATE) IS ABOUT 3.9%
- THERE IS EVIDENCE OF TIME DEPENDENCE OVER 20 MINUTE TEST

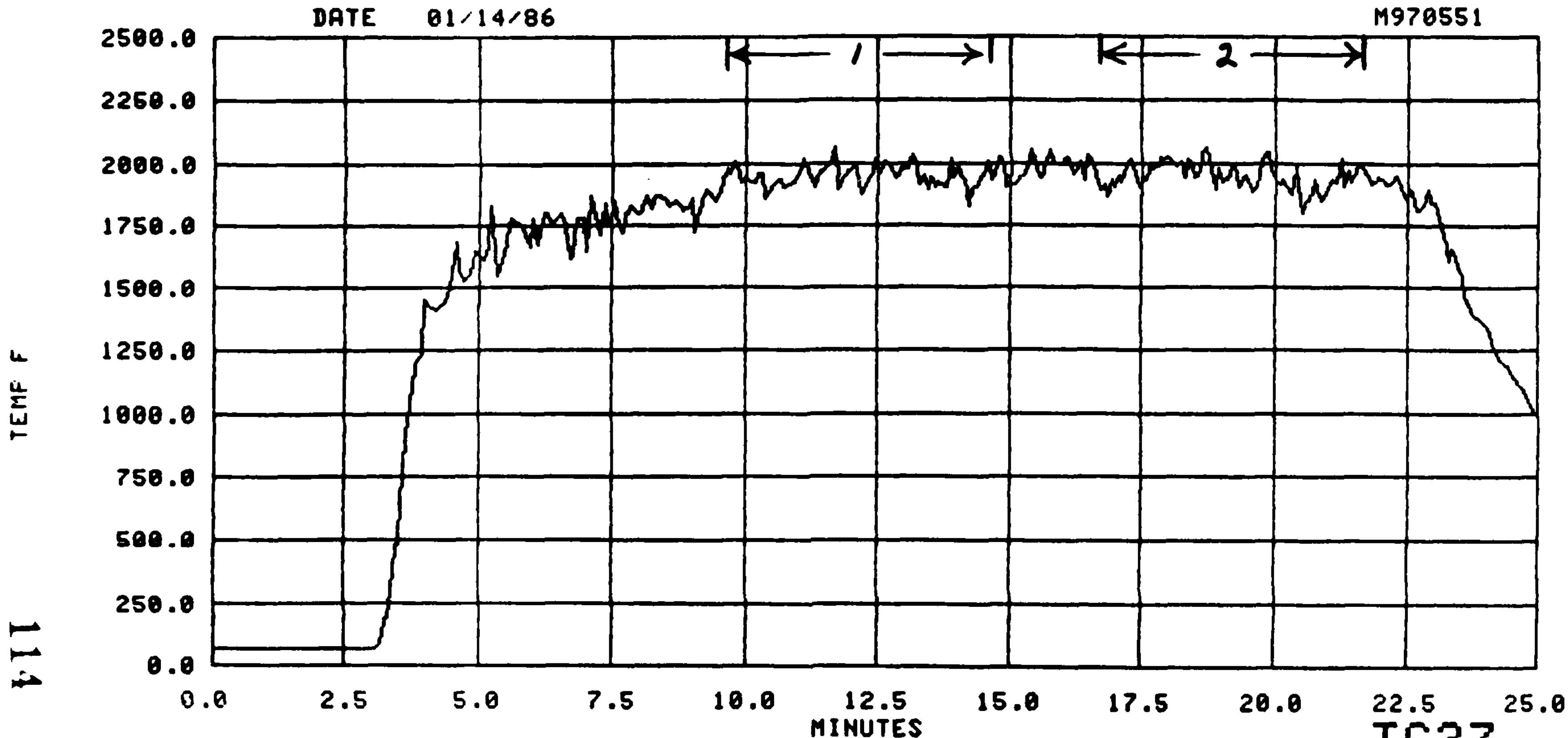

FIGURE 27

1/10 SCALE EMISSONS TEST #4

COLLABORATION WITH OTHER GROUPS

- SNL SOLICITS COOPERATIVE EFFORTS OF OTHER RESEARCHERS ON SANDIA–CONDUCTED EXPERIMENTS, AND SANDIA ELEMENTS OF LARGER FIELD STUDIES

(SS/NW11 7/85)

Measurements of the Radiative Properties
of Smoke Emissions from Vegetative Fuels:
Relationship of this Data to Desired Information
on the Properties of Urban Smoke Emissions

Edward M Patterson
School of Geophysical Sciences
Georgia Institute of Technology
Atlanta, Georgia 30332

ABSTRACT

We have made a series of measurements of the radiative properties of the emissions from burning vegetative materials. These measurements have included measurements of the optical constants of the smoke emissions and the sizes of the smoke particles, as well as the emission factors for the absorbing material. The relation of these properties to the fuel properties and the combustion conditions have been studied in terms of the variation of the absorption with variation in fuel or fire conditions.

The data, although limited, suggest that the absorption of solar radiation by smoke emissions from fires with vegetative fuels will not be of major importance to possible global effects following a nuclear exchange. The burning of such fuels, however, is the most likely possibility for large scale fires that are planned to test our understanding of the effects of urban fires following a nuclear exchange; and so there is a need to understand the differences and the similarities between fires with urban fuels and those with vegetative fuels.

We will review our data on the radiative properties of the emissions from these fuels. We will also discuss some of the relations between the emissions from the different fuels and the applicability of the vegetative fuel data to the understanding of the urban fuel smoke emissions.

Measurements of the Radiative Properties of Smoke Emissions from Vegetative Fuels: Relationship of this Data to Desired Information on the Properties of Urban Smoke Emissions

SUMMARY OF TALK

The purpose of this presentation is a discussion of one of the components of the smoke source term--that of smoke from burning vegetative material. The discussion will include a review of data that serves to characterize the source absorption and size properties of the smoke emissions from vegetative fuels, a reexamination of "blue moon" data to infer size characteristics for a well aged aerosol, a consideration of the efficiency of wet removal mechanisms for graphitic carbon, a report on some measurements of the effects of ultraviolet light on the optical properties of smoke aerosols, and a short discussion on the role of forest fire studies in nuclear winter studies.

Source Characterization

The source characterization work discussed here was done in a cooperative program involving Georgia Tech and the U S Forest Service. This work had as its goals the determination of the absorption characteristics of wildland fires, the determination of the relative importance of absorption in producing radiative effects, and the relating of the radiative characteristics of smoke to fire behavior and fuel composition.

In outline, this study consisted of measurements of optical absorption for the smoke from both field and laboratory fires, together with simultaneous measurements of mass concentration for the aerosol. These experimental data were used to calculate radiative properties of interest (including σ_a, σ_e, and B_a). B_a is defined as the ratio of the absorption coefficient σ_a to the mass concentration of the aerosol and is an important parameter because it is a measure of the relative efficiency of a given mass of aerosol in producing absorption. Graphitic carbon (C_e) concentrations were determined from the absorption data, and emission factors were calculated for both graphitic carbon and total particulate matter. Relationships among the quantities were investigated. A more complete description of these studies is found in Patterson and McMahon(Atm Environ,18, 1984) and in Patterson, McMahon, and Ward (Geophys Res Letters,13, 1986).

Absorption measurements were made using both diffuse transmission and diffuse reflectance methodologies as discussed in the earlier reports. The diffuse transmission data utilized a HeNe laser at 632.8 nm; the diffuse reflectance measurements provided data for a range of wavelengths. These data showed significant differences between flaming and smoldering emissions, with the smoldering emissions having much lower absorption than the flaming emissions. The measured absorption for smoldering emission, however, showed a rather strong wavelength dependence; so that the near ultraviolet absorption was similar for both flaming and smoldering components. In general, the specific absorption, B_a, was approximately 1 for the smoke from flaming combustion at the HeNe laser wavelength. The comparable absorption for smoldering combustion was less than 0.1.

Size distributions were not measured in this series of fires, but previous data from comparable fires showed that the radiative properties of the smoke emissions at solar wavelengths were primarily determined by the submicron mode. The earlier data also showed relatively little variation in sizes between smoldering and flaming combustion. A supermicron mode was present in the field fire emissions, but again these larger particles did not significantly affect the radiative properties of these emissions.

A nominal log normal size distribution with a mean radius of 0.045μm and a σ of 1.75 (values consistent with the earlier data) were used in the radiative calculations. These values showed that the single scattering albedo, ω, the ratio of the scattering to the extinction, is more than 0.6 for flaming combustion and increases to more than 0.95 for purely smoldering combustion. Calculations suggest that the value of the specific absorption is related to the reaction intensity of the fire.

The absorption, mass concentration, and other correlative data were also used to calculate emission factors for the graphitic carbon (C_e) and for the total particulate mass for both field fires and laboratory fires. These data indicate that the specific absorption is inversely related to the total particulate emission factor and that the emission factors for graphitic carbon vary only over a relatively small range. These data indicate that the emission factor for C_e is approximately 1 g/kg, a value significantly lower than earlier estimates for the emissions from these vegetative fuels. The total C_e emissions will also be correspondingly lower than previously estimated.

AGED AEROSOL PROPERTIES INFERRED FROM BLUE MOON OBSERVATIONS

There were extensive wildland fires in western Canada in September, 1950 which produced large amounts of smoke. This smoke produced many atmospheric optics effects including ppearances of blue moons and blue suns that were observed in both North America and Europe. Since such blue moon observations can be produced only by relatively limited size distributions, these observations can be used to infer some characteristic size distributions for these aged smoke aerosols.

Wilson, in Edinburgh, measured atmospheric turbidity at the time of a blue sun occurrence. His turbidity measurements, which showed a turbidity minimum at approximately 440 nm, have been used as the basis for our comparison. Mie calculations of extinction have been made for a series of log normal size distributions in an attempt to match the turbidity measurements of Wilson. Our calculations indicated that the best fit was obtained with a log normal size distribution having a mean radius of 0.6 μm and a standard deviation of 1.3. While no actual inversion has been done, and there is no claim that this is the "best possible" distribution; this is an adequate distribution. It is expected that the distribution determined from the calculations is a good representation of the ambient distribution.

It is apparent that the particle sizes inferred for this aged aerosol are significantly larger than those inferred from the in situ measurements. This larger particle size also suggests that infrared effects may be of greater importance than previously inferred. Additional data will be of obvious value.

ULTRAVIOLET EFFECTS ON SMOKE

A simple laboratory experiment was made in which ultraviolet light was used to illuminate samples of smoke from smoldering combustion and from flaming combustion. This was done in an attempt to determine whether UV illumination over time might have an effect on the optical properties of the smoke, causing an appreciable lightening or darkening of the aerosol, and possibly affecting the radiative properties of the aerosol. When the graphitic carbon conaining smoke from flaming combustion was illuminated with the UV light no changes in sample appearance were observed. When the smoke from smoldering combustion was illuminated, however, the appearance of the sample changed, becoming lighter in appearance.

This test certainly indicates that no additional soot formation would be expected due to the interaction of organic aerosols with UV light. The effect, rather, would be to reduce the absorption at visible wavelengths.

APPLICABILITY OF FOREST FIRE WORK TO NUCLEAR WINTER STUDIES

While it does not appear at the present time that smoke from wildland or forest fuels will be a major contributor to the solar wavelength absorption ofsmoke clouds produced by large scale fires, fires with such fuels are important because these fires are likely to be used as test cases for studies of large scale fires. There is a need to understand the differences and the similarities between fires with wildland fuels and those with more typical urban fuels so that the data gained in the test fires can be transferred to increase the understanding of the properties of other fires of interest.

One particular area of interest is the study of prompt removal mechanisms by cloud processes in the smoke plume. Data from a recent study (Patterson, Castillo, and DeLuisi, submitted to J Geophys Res) suggests that wet removal processes and efficiencies are quite different for graphitic carbon and for hygroscopic material such as sulfates, with the graphitic carbon much less efficiently removed than the hygroscopic material. There are also indications that organic materials are more readily incorporated into cloud droplets than is the graphitic carbon. These differences will presumably affect the prompt removal processes. Since the relative amounts of organic and graphitic materials are expected to quite different for the urban and for the wildland fuels cases, prompt removal mechanisms can also be quite different in the two cases; and measuremnts with one fuel type may not be directly transferrable to other fuel types. Again more work is obviously needed.

Smoke Source Term

1. Source Characterization

2. Size Characterization From "Blue Moon" Data

3 Ambient C_e Removal Efficiencies

4 UV Effects

5 Forest Fires in Nuclear Winter Studies

ABSORPTION CHARACTERIZATION OF SMOKE EMISSIONS FROM WILDLAND FUELS

E. M. PATTERSON GEORGIA TECH

C. K. MCMAHON US FOREST SERVICE -MACON, GEORGIA

D. WARD US FOREST SERVICE--SEATTLE, WASHINGTON

GOALS OF MEASUREMENT PROGRAM:

DETERMINE ABSORPTION CHARACTERISTICS OF WILDLAND FIRES

DETERMINE RELATIVE IMPORTANCE OF ABSORPTION IN PRODUCING RADIATIVE EFFECTS

RELATE OPTICAL AND RADIATIVE CHARACTERISTICS TO FIRE BEHAVIOR

OUTLINE OF WORK:

MEASURE ABSORPTION OF FIELD AND LABORATORY FIRES

CALCULATE RADIATIVE PROPERTIES OF INTEREST (σ_a, σ_e, β_a)

INTERPRET DATA

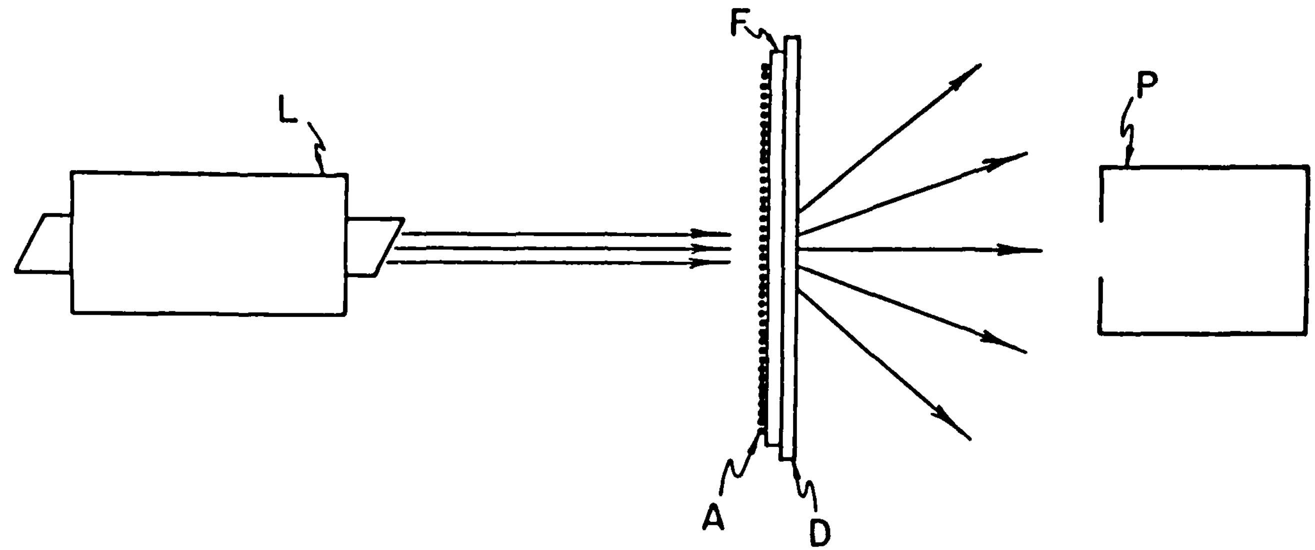

Figure 5. Schematic of Diffuse Transmission System (L Denotes the Laser, A the Aerosol Particles, F the Filter, D the Diffuser, and P the Photomultiplier.

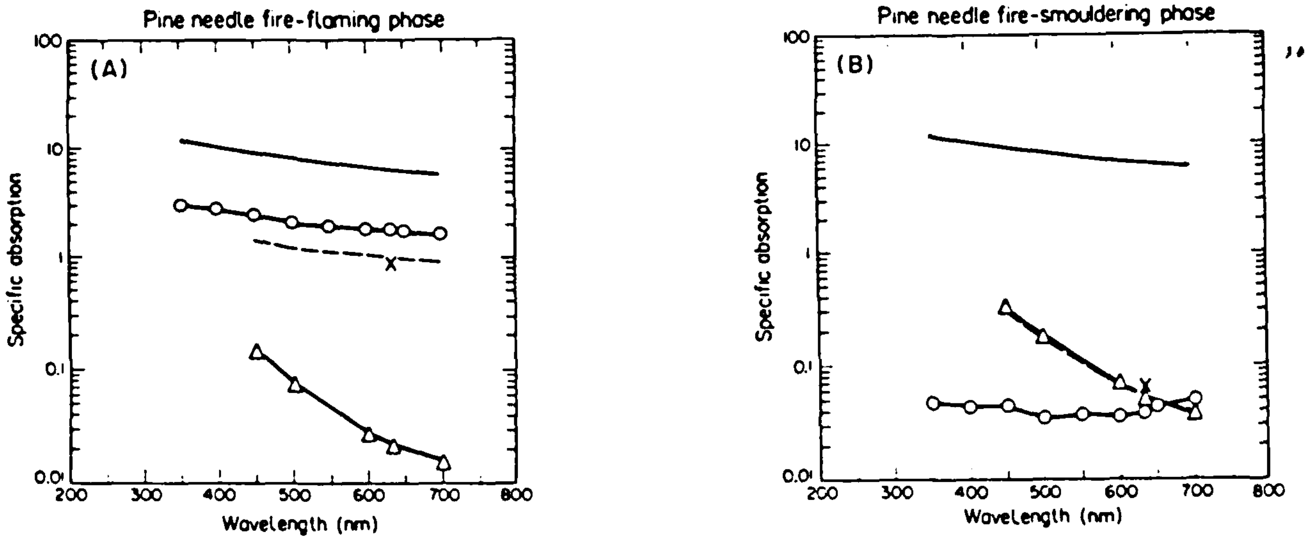

Pine needle fire-flaming phase
(A)
Specific absorption
Wavelength (nm)
Pine needle fire-smouldering phase
(B)
Specific absorption
Wavelength (nm)

Table 3. Simplified pine-needle study results by combustion phase

Combustion Conditions	B_a $m^2\ g^{-1}$	C_e (%)
Flaming Predominates	0.98	15
Smoldering Predominates	0.16	2.5

LOW INTENSITY FIRE

SIZE DISTRIBUTION DATA

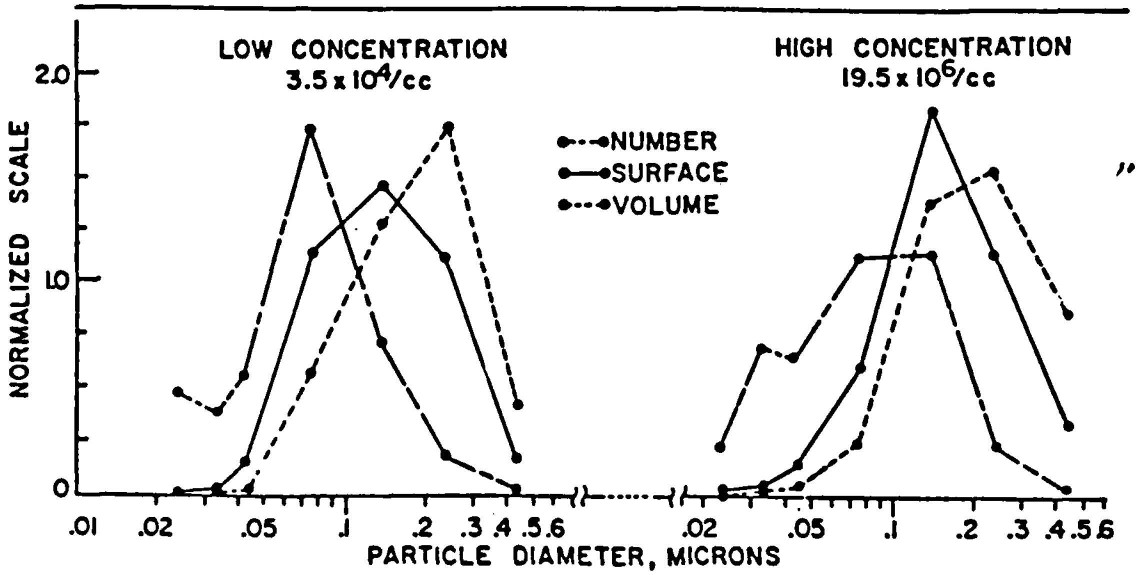

Fig. 4 - Normalized number, surface, and volume size distributions for high and low concentration smoke(from Ryan and McMahon, 1976)

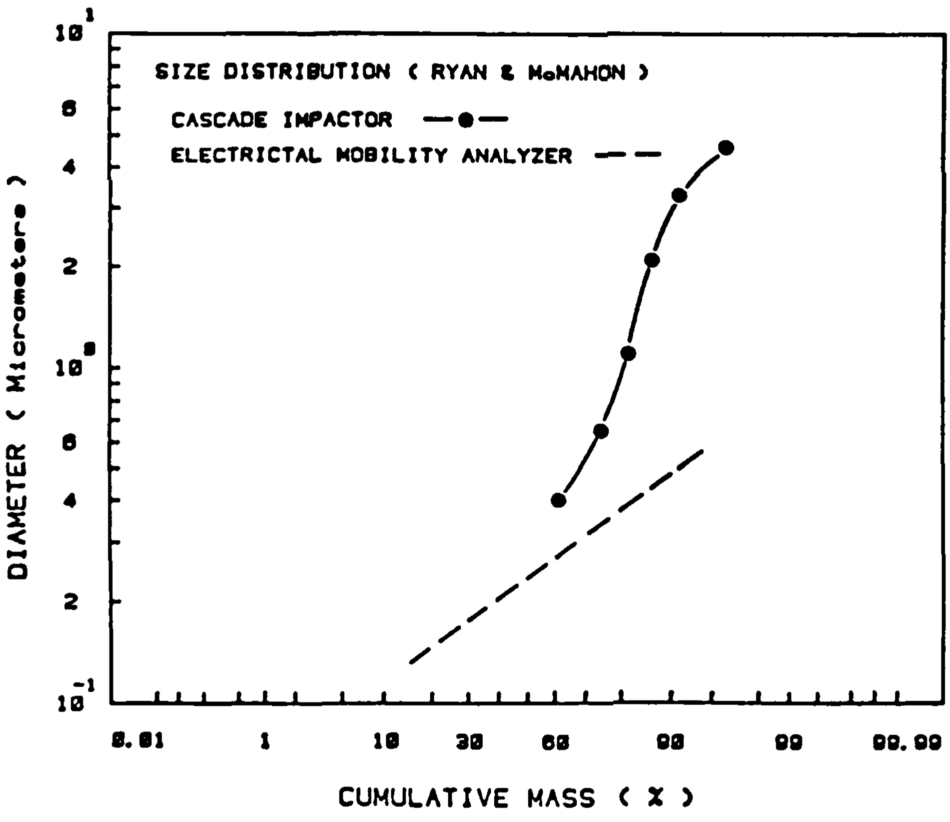

Fig. 5 - Size distributions, plotted as cumulative mass distributions, for Ryan and McMahon (1976) data. The solid line (•-•-•) represents cascade impactor data, and the dashed line (— — —) represents an approximate log-normal fit to the electrical mobility analyzer data.

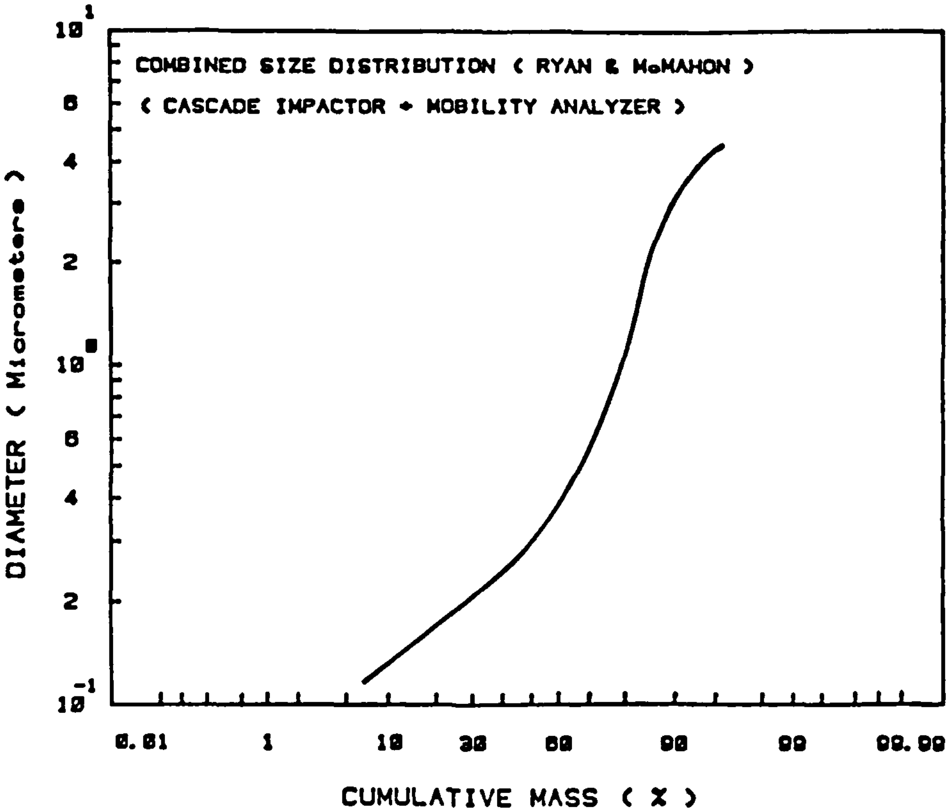

Fig. 6 - Cumulative mass distribution determined by combining the Ryan and McMahon(1976) cascade impactor and electrical mobility analyzer data. See text for details.

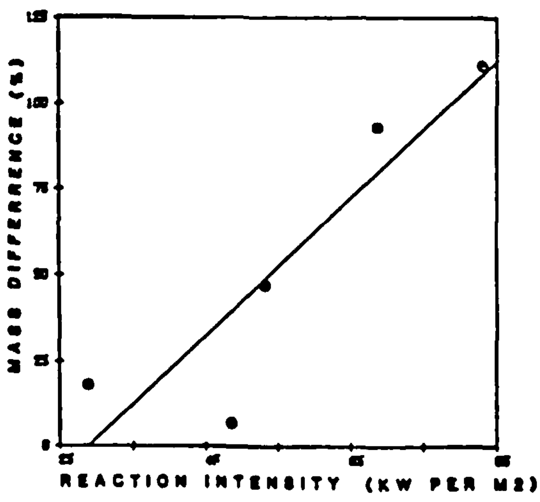

Fig. 7 - Percent difference between emission factors determined from gravimetric samples of particulate mass collected on open-faced 47 mm and 37 mm filters (with 2.5 μm cutpoint presampler) as a function of reaction intensity (from Ward and Hardy, 1984)

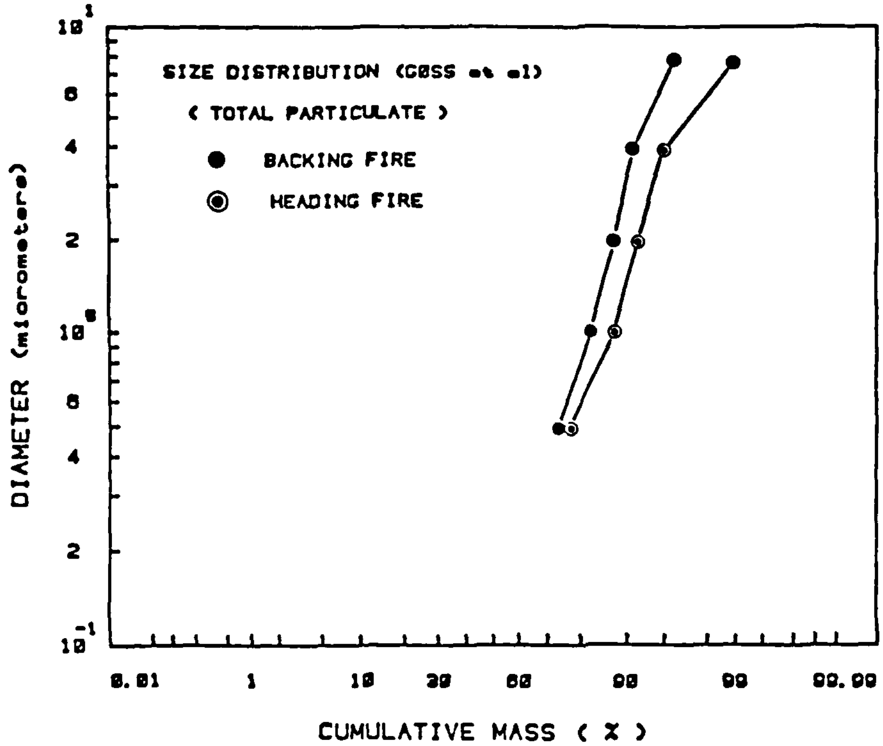

Fig. 8 - Cumulative mass distributions for the total particulate mass measured by Goss et. al. (1973) for backing(●-●) and heading(◉-◉)fires.

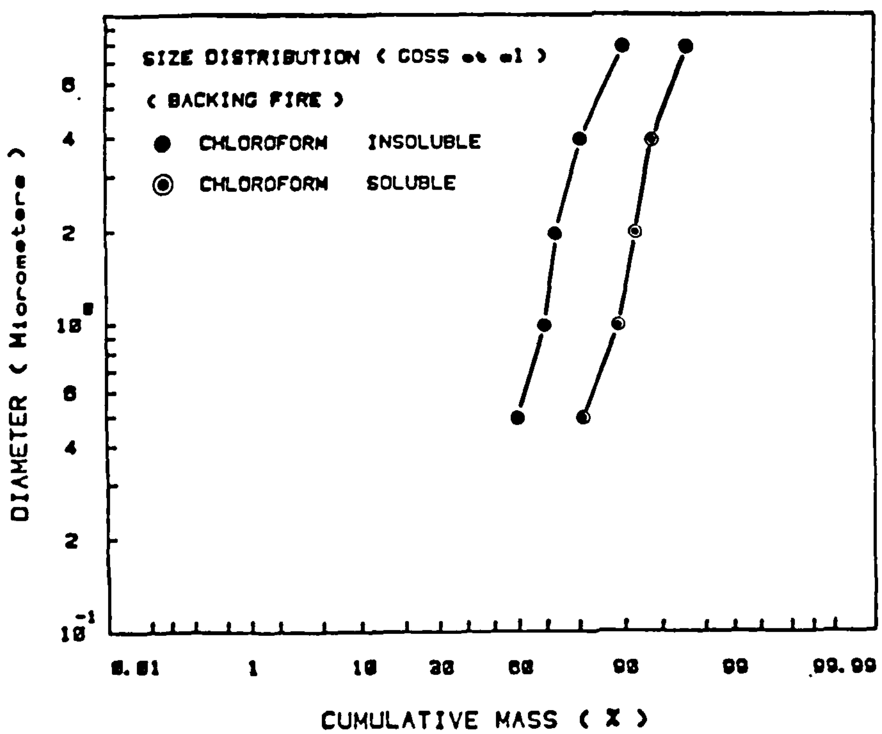

Fig. 9 - Cumulative mass distributions for particulate emissions in a backing fire measured by Goss et. al.(1973) for the chloroform insoluble component(●-●) and the chloroform soluble component(◉-◉).

Table 5. Calculated radiative properties for particulate emissions at $\lambda = 550$ nm

Combustion Phase	n_{IM}	$\sigma_E(m^{-1})$	$\sigma_S(m^{-1})$	ω
Flaming	0.07	2.46×10^{-3}	1.62×10^{-3}	0.66
Transition	0.011	2.01×10^{-3}	1.86×10^{-3}	0.93
Smoldering	0.004	1.95×10^{-3}	1.90×10^{-3}	0.97
"General" Case	0.03	2.16×10^{-3}	1.77×10^{-3}	0.82

Properties are calculated assuming a log normal size distribution with mean radius, $r_g = 0.045$ μm, standard deviation, $\sigma = 1.75$, and total particle number $N_p = 3.21 \times 10^5$ cm^{-1}, normalized to a total particulate volume of 500 μm^3 cm^{-3}. An n_{RE} value of 1.53 is assumed.

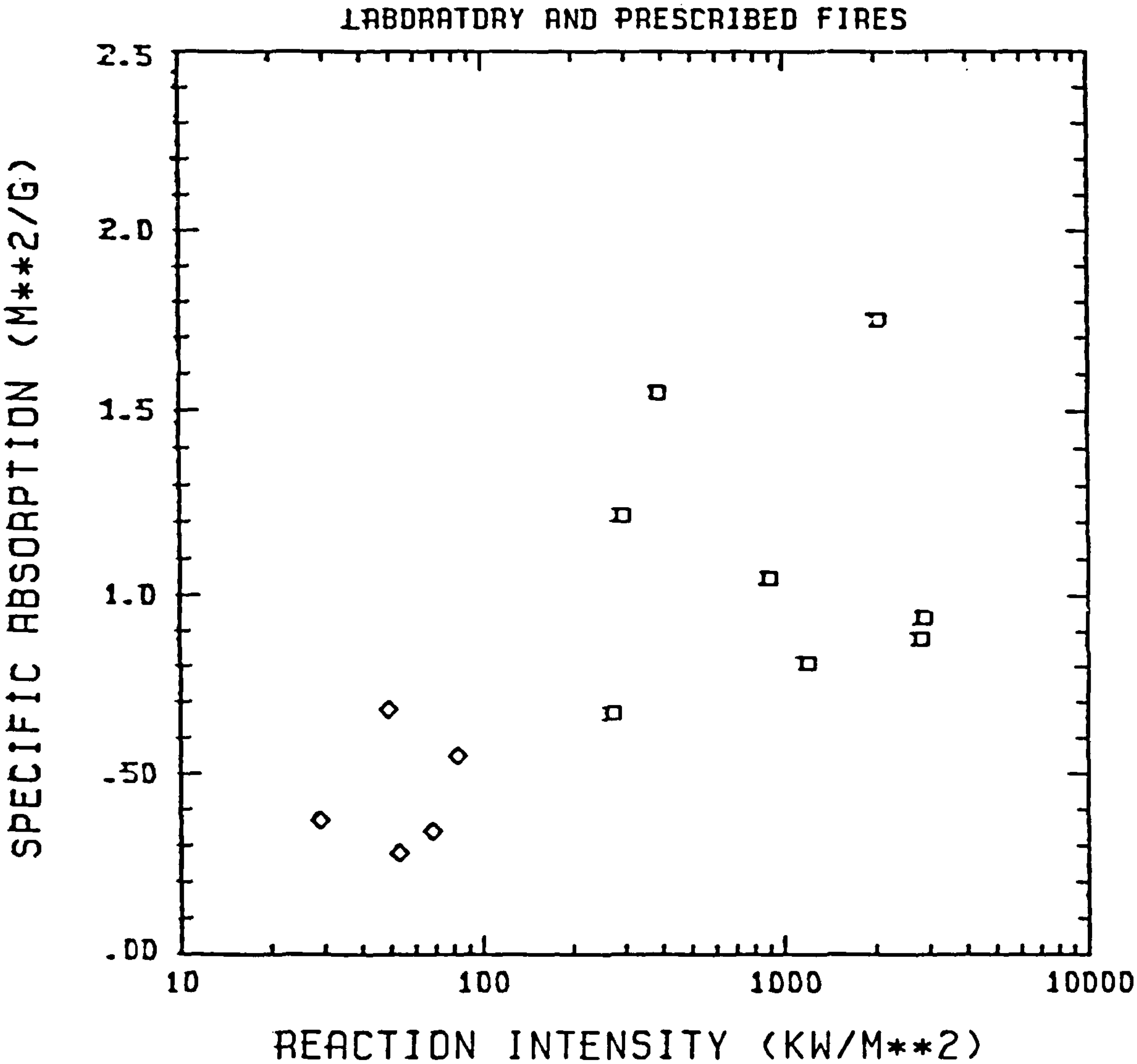

Fig. 1. Specific Absorption, B_a, values for samples collected during flaming combustion plotted as a function of reaction intensity. The ◊'s represent slash burn samples of Ward and Hardy, the □'s represent data from the laboratory pine needle study of Patterson and McMahon.

TABLE 2. B_a and Emission Factor Data for a Series of Experimental Pine Needle Burns Conducted at the Southern Forest Fire Laboratory

FIRE SERIES	FIRE PHASE	B_a (m^2/g)	EF(PM) (g/kg)	EF(C_e) (g/kg)
01	F1	.81	19.0	2.30
	F2	1.35	27.0	5.40
		<.93>	<21.0>	<2.90>
02	F1	2.27	7.6	2.60
	F2	1.28	9.6	1.80
		<1.60>	<8.2>	<2.00>
03	F1	.94	5.9	.82
	F2	.80	10.5	2.31
		<.88>	<8.3>	<1.10>
04	F1	1.75	3.0	.78
	F2	.45	13.8	.92
		<.65>	<8.8>	<.85>
05	F1	2.36	3.6	1.26
	F2	.95	72.5	10.20
	T	.58	---	---
		<1.26>	<15.3>	<2.90>
06	F1	1.55	7.0	1.61
	T	.62	52.4	4.81
		<.98>	<13.6>	<2.00>
07	F1	.67	10.0	.99
	T	.17	70.0	1.76
	S1	.04	87.0	.52
	S2	.04	67.0	.40
		<.16>	<45.5>	<1.10>
08	F1	1.22	6.7	1.21
	T	.20	53.0	1.57
	S1	.05	102.0	.76
	S2	.07	114.0	1.18
		<.15>	<60.9>	<1.30>
09	F1	.88	9.1	1.19
	T	.61	40.0	3.61
		<.73>	<14.5>	<1.60>

TABLE 1. B_a and Emission Factor Data for a Series of Prescribed Burns of Broadcast Logging Slash in the Pacific Northwest (Ward and Hardy, 1984).

TEST FIRE*	FIRE** PHASE	B_a (m^2/g)	EF(PM) (g/kg)	EF(C_e)+ (g/kg)
CAT	F1	.37	15.6	.85
	S1	.24	13.8	.50
	S2	.26	11.7	.46++
				<.63>
HEBO	F	.28	23.4	.96
	S1	---	12.2	---
				<.96>
MARIA 1	F	.34	23.5	1.18
	S1	.18	20.4	.55
	S2	.20	20.3	.61
				<.78>
DLAKE 1	F	.68	10.2	1.03
	S1	.40	14.1	.83
	S2	.36	13.4	.71
				<.86>
DLAKE 2	F	.55	11.6	.94
	S1	.25	14.1	.52
	S2	---	12.4	---
				<.65>

* Fire designation follows Ward and Hardy (1984)

** F = Flaming; S = Smoldering

\+ EF(C_e) determined using B_a data

++ < > emission weighted fire averages

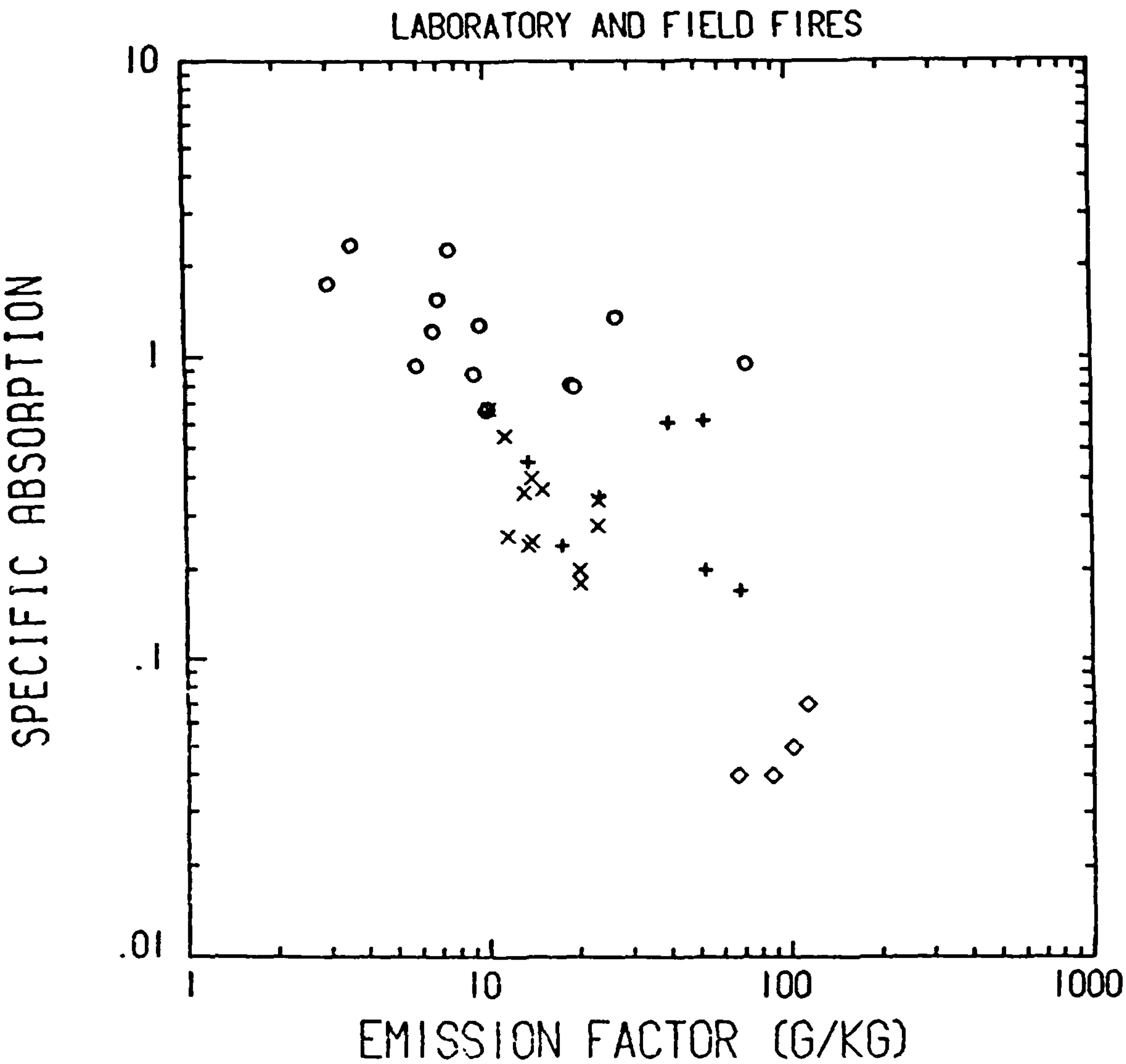
LABORATORY AND FIELD FIRES
SPECIFIC ABSORPTION
EMISSION FACTOR (G/KG)
10
1
.1
.01
1
10
100
1000

EMISSION FACTOR DATA – TOTAL PARTICULATE (PM)
– GRAPHITIC CARBON (Cc)

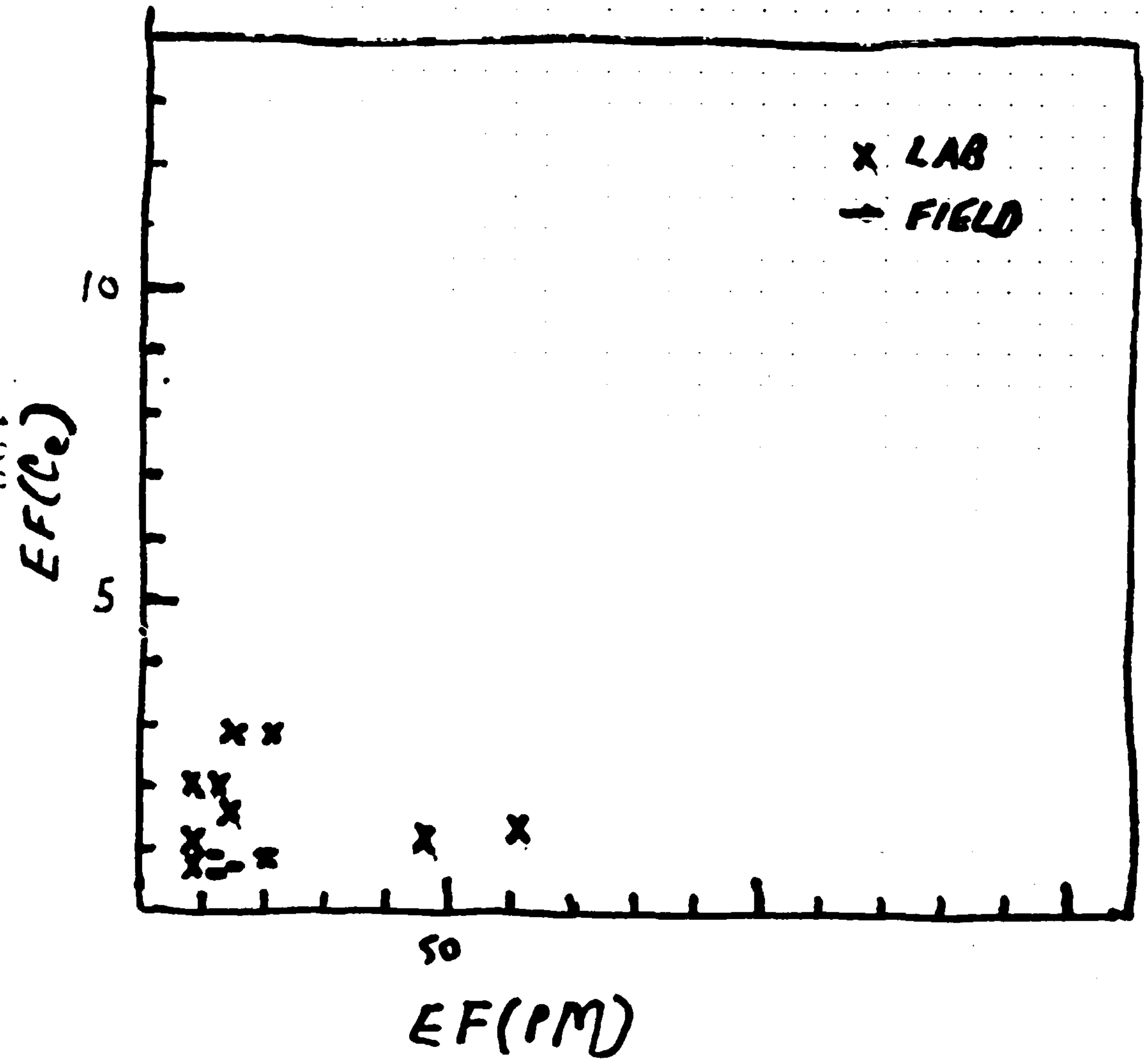

SMOKE EMISSION FACTORS -- WILDLAND FUELS

CRUTZEN ET AL(1984)	6 G/KG
NAS (1985)	3 G/KG
PATTERSON ET AL(1985)	~1 G/KG

TABLE 5.7 Fire and Smoke Parameters in the Present Nuclear War Analysis

	Baseline	Excursions[a]
Urban fire smoke emission, Tg	150	20-450
Forest fire smoke emission, Tg	30	0-200
Total smoke emission, Tg	180	20-650
Tropospheric injection, Tg/km	20 (0-9 km)	1.5-53 (0-12 km)
Stratospheric injection, Tg/km	0	1 (12-20 km)
Urban fire area, km^2	250,000	125,-375,000
Urban fuel consumption, g/cm^2	3.0	1.5-3.0
Urban smoke emission factor,[b] g/g	0.02	0.01-0.04
Urban fire duration, days	$\lesssim 1$	--
Forest fire area, km^2	250,000	0-1,000,000
Forest fuel consumption, g/cm^2	0.4	0.4
Forest smoke emission factor, g/g	0.03	0.02-0.05
Forest fire duration, weeks	$\lesssim 1$	--
Smoke composition (by mass)	20% graphitic carbon, 80% oils	5-50% graphitic carbon
Smoke refractive index (visible)[c]	1.55-0.10 i	1.5-0.02 i to 1.7-0.30 i
Smoke particle number median size, μm	0.10	0.05-0.5
Smoke particle log normal width, γ	2.0	2.0
Smoke specific extinction (visible),[c] m^2/g	5.5	2.0-9.0
Smoke specific absorption (visible),[c] m^2/g	2.0	1.0-6.0
Smoke specific absorption (infrared), m^2/g	0.5	0.2-5.0

[a]Some values are given only to illustrate the range that is plausible, and are not discussed specifically in the text.
[b]Average value after 50 percent prompt scavenging in the convective fire columns.
[c]At a nominal wavelength of 550 nm.

SMOKE EMISSIONS (TG)

	PM	C_E	C_E (PMW)
URBAN			
CRUTZEN	80	45	
NAS	150	33	
WILDLAND			
TTAPS	80	~30	3
CRUTZEN	60-240	6-24	1-4
NAS	30	3	1
S&B	.3-3	----	<.4

BLUE MOON DISCUSSION

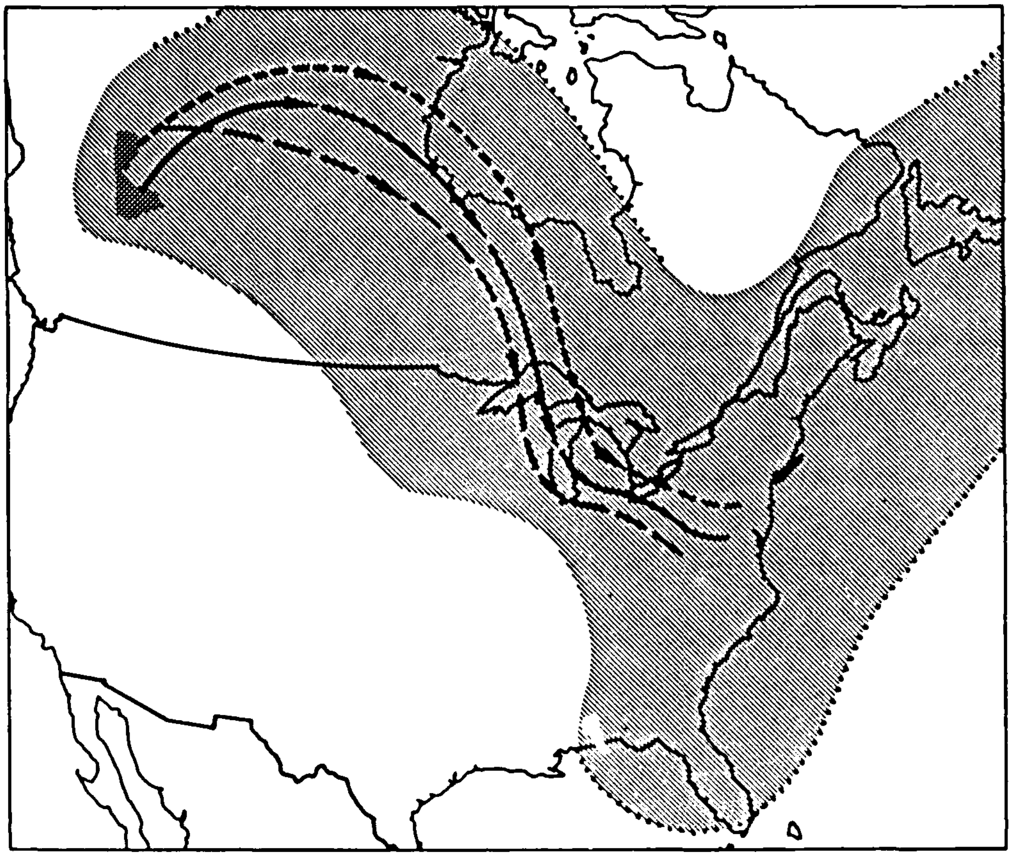

FIGURE 7.12 The hatched area represents the region over which smoke was observed from the western Canada forest fires of September 1950 (exclusive of observations from Western Europe). The boundary of this area is dotted where it is tentative. The darkened areas in western Canada are the areas in which the fires occurred, and the curves mark calculated trajectories for smoke reaching the vicinity of Washington, D.C., by September 24, two days after the most intense burning episode. (From Smith, 1950.)

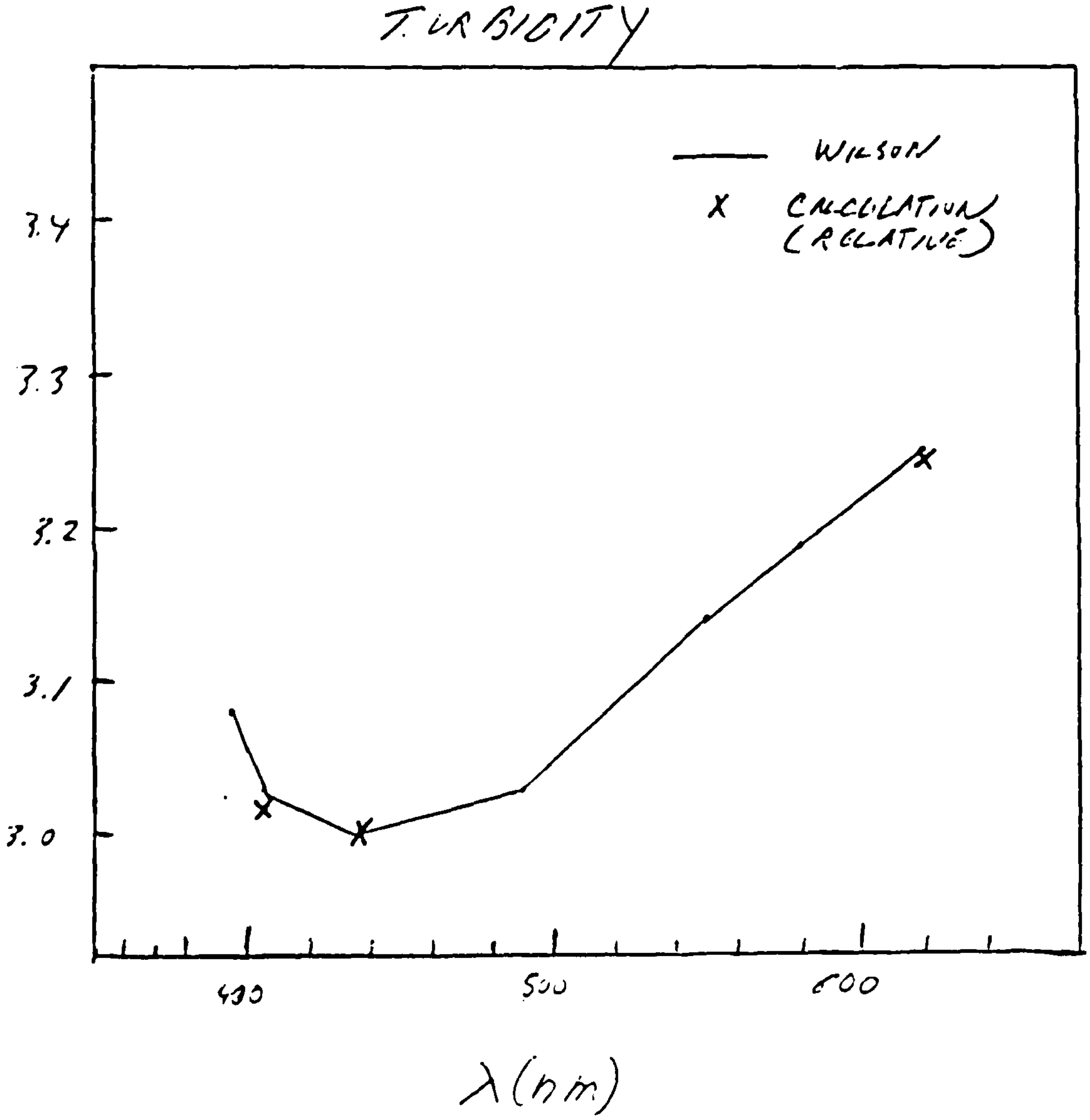
TURBIDITY
WILSON
X CALCULATION (RELATIVE)
3.4
3.3
3.2
3.1
3.0
400
500
600
λ(nm)

FIG 1

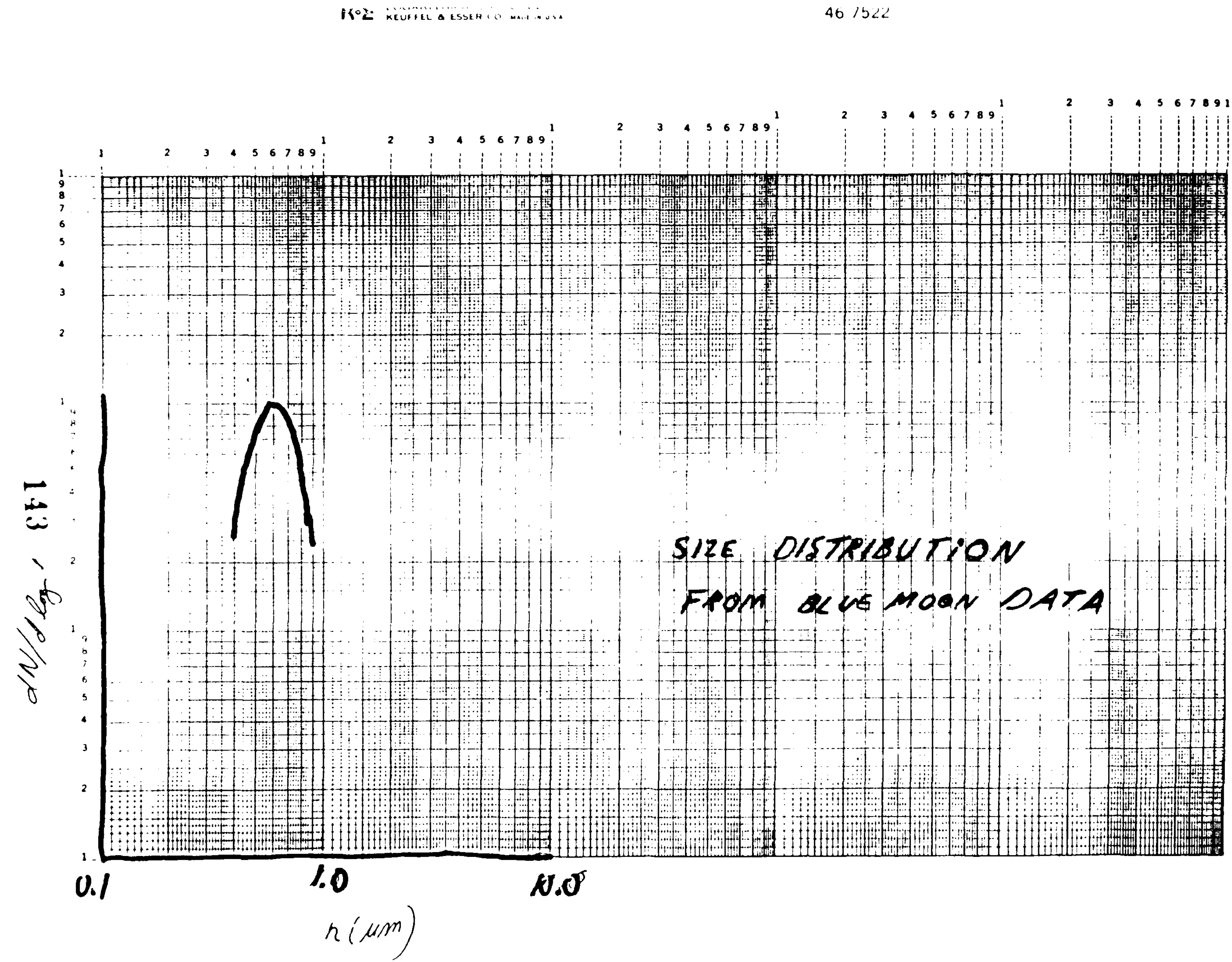
K&E KEUFFEL & ESSER CO. MADE IN U.S.A.
46 7522
SIZE DISTRIBUTION
FROM BLUE MOON DATA
0.1
1.0
10.0
r (μm)
dN/d log r

UV effects on Smoke

soot — no effect

organic - bleach

UV WILL PROBABLY NOT CAUSE IN SITU SOOT FORMATION IN THE ATMOSPHERE AT HIGH ALTITUDES

Applicability of Forest Fire Work to Nuclear Winter Studies

- Parameterization of Scaling effects
- Determination of properties of large scale fires
- Transfer of data to urban fuel loadings
- Plume dynamics
- Prompt removal mechanism determinations
- Post attack burn assessment

"Wildland Fires and Nuclear Winters: Selected Reconstructions of Historic Large Fires"

Stephen J. Pyne
History Department
University of Iowa

Philip N. Omi
Department of Forest and Wood Sciences
Colorado State University

Under the nuclear winter scenario large wildland fires are expected to contribute to a general smoke plume and are considered potential analogues for the behavior of gigantic palls. As a means of testing the reasonableness of current estimates of a wildland fire contribution, we reconstructed from the historic record two major events: the Tillamook Burn (Oregon) of August 1933 and the 1910 fire complex (Northern Rocky Mountains). Both events are near the upper limit for wildland fires--the 108,000 ha Tillamook Burn for a single fire, and the 1.3 million ha 1910 burn for a regional fire complex. To assist in analyzing the 1910 fires, for which environmental data are feeble, we relied on a modern analogue, the Sundance fire (1967), for certain extrapolations.

Total particulates emitted during the Tillamook Burn's three major runs (August 14-16, 20-22, 24-26) ranged from 4.5 x 10^8 kg to 1.0 x 10^9 kg. An average 1% of the total emissions during the major runs originated within the flaming front, and 75% of total area involved was burned during the 20- to 30-hr period that constituted the third run. The third run progressed in four phases, only one of which (during a decrease in ambient winds) showed significant convective development. Over the life of the 1910 fires, we estimate that total emissions ranged from 8.0 x 10^7 to 9.0 x 10^8 kg. The ratio of forest to grassland burned was 3:1. Based on the example of the Sundance fire, an average 16% of the total emissions from forest areas was associated with frontal flaming zones. Probably 85-90% of the total area involved burned during a 36-hr period on August 20-21. The smoke plumes from both events were immense but apparently ephemeral. Unfortunately, neither direct sampling of particulates nor lapse rates for the upper atmosphere are available.

Both fires were dependent on powerful near-surface winds. Although convective clouds did evolve, strong wind shear probably blocked the ascent of most combustion products, including soot and particulates. The dominance of the lower-atmosphere winds was interrupted only ephemerally from time to time, but it was enough to send the convective clouds from the Tillamook Burn to 12,200 m above MSL and the clouds from the 1910 fires, based on the Sundance analogue, to a probable height of 10,675 m.

Both events were typical of large wildland fires, too, in that they attained their dimensions by means of staged increments or runs. This demanded recurring weather patterns (east wind outbreaks, cold fronts) such that the process of scaling up required a period of several weeks. Since urban fires are expected to evolve rapidly following a nuclear exchange, there is some question whether urban and wildland fires will be synchronized. They may even be competitive.

It is doubtful that further reconstructions of historic fires can substitute for laboratory and field experimentation. On the contrary, better models for large wildland fire behavior and for smoke production are needed to bridge gaps in the historic record. If additional historic studies are desired, the chaparral brushlands of Southern California and the boreal forest of Alaska are the best candidates. Probably the critical fire environment, however, will be the boreal forests of Siberia and Canada.

UCRL- 94226
PREPRINT

Progress in Developing the Smoke Source Term for "Nuclear Winter" Studies: Major Uncertainties

Joyce E. Penner

THIS PAPER WAS PREPARED FOR THE
DEFENSE NUCLEAR AGENCY PROGRAM TECHNICAL REVIEW
HELD AT
NASA AMES RESEARCH CENTER
MOFFETT FIELD, CALIF
FEB 25-27, 1986

March 1986

Lawrence Livermore National Laboratory

DISCLAIMER

Progress in Developing the Smoke Source Term for "Nuclear Winter" Studies: Major Uncertainties

Joyce E. Penner

Lawrence Livermore National Laboratory, University of California
Livermore, California 94550

February 1986

Abstract.

The potential effects on climate of large amounts of smoke injected into the atmosphere following a major nuclear exchange have been widely analyzed (Crutzen and Birks, 1982; Turco et al., 1983, NRC, 1985; Pittock et al., 1986). Although simplifications and uncertainties still exist in the application of climate models to calculate the effects of smoke, many of the simplications that were necessarily made in the first studies have now been corrected. These improved climate models have shown that the effects of smoke on climate depend on the quantity and optical properties of the smoke that is generated and dispersed into the global atmosphere. The smoke amount and its optical properties can be summarized by the average optical depth that would result if the smoke were dispersed throughout half the northern hemisphere. In this paper a range of values for this average optical depth is determined, consistent with recent analyses. Different estimates for each of a variety of contributing factors give rise to a wide range of average optical depths, encompassing values that imply comparatively minor effects on climate to values that imply massive effects. Suggestions for further research that might narrow the range of possibilities are made.

*This work was performed under the auspices of the U.S. Department of Energy by Lawrence Livermore National Laboratory under contract No. W-7405-Eng-48.

1. Introduction.

The climate effects of smoke are often parameterized in terms of the average extinction or absorption optical depth which might occur after a major nuclear war. This quantity can be calculated from

$$\overline{\tau} = k \times S / A$$

where k is the extinction or absorption cross section of the smoke (m^2/g), S is the amount of smoke (g), and A is the area blocked by the smoke cloud (taken as half the area of the northern hemisphere or 1.28×10^{14} m^2). The quantity of smoke may be calculated from

$$S = \epsilon \times F \times (1 - f_r)$$

where ϵ is the emission rate of smoke (g smoke/ g of fuel burned), F is the amount of fuel burned, and f_r is the fraction of smoke removed by precipitation in the convection column above the fires and in the first few days after the war during which the smoke is presumed to spread out to global scales. The original "baseline" analysis of Turco et al. (1983) resulted in an estimate for $\overline{\tau}$ that was close to 6 for smoke produced in urban fires. Consideration of the additional smoke from wildlands fires, long term fires, and dust from surface bursts increased this estimate to about 8.[1] All subsequent analyses have similarly implied "best estimates" for $\overline{\tau}$ that were substantially larger than 1. This apparent consensus has led to the claim that large climate impacts are not only possible, but

1. Turco et al. (1983) spread their smoke over the entire northern hemisphere, so that their published optical depths differ from these by a factor of 2.

probable (Sagan, 1985). In this paper, we review the estimates for the various factors which contribute to $\overline{\tau}$ in order to obtain reasonable bounds on the possible range of magnitudes consistent with current knowledge. This range encompasses values for $\overline{\tau}$ that may indeed be associated with major climate impacts if a large fraction of the available urban combustible load is burned. On the other hand, within the bounds set by current analysis, comparatively minor impacts are also possible, especially if the targeting avoids refineries and other large storage facilities which contain petroleum or other fossil fuels. We recommend several areas for research that could lead to more certain estimates of the effects of such a war.

2. Estimates for the amount of fuel burned in urban fires.

As pointed out by Bing (1985), several methods have been adopted for estimating the amount of fuel that might burn in urban fires. These methods are not mutually consistent. The first method, that adopted by Turco et al. (1983), yields the highest fuel estimate. In this method of analysis, the amount of fuel burned in urban fires is determined from the product

$$F = FL \times f_b \times A \times SF$$

where FL is the average areal fuel load within the burned-out region (g/m^2), f_b is the fraction of fuel that is consumed by fire within the area that burns over the first 24 hours, A is the area that is initially ignited by the fireball (m^2), and SF is the average areal spread factor for the fires.

An overestimate by this method may be caused by at least two factors. First, generally no account is taken of the overlap of burned areas when detonations take place within close proximity. Second, the entire ignited area and its radially expanded spread is assumed to coincide exactly with the urban fuel bed and with the average fuel load FL. This assumption may be seriously in error, for example, for targets such as airports that generally reside on the outer edges of cities. It is often argued that these effects are mitigated by the choice of a "conservative" value for A, i.e. one that corresponds to the area that would be ignited by a thermal fluence of 20 cal/cm^2 rather than the area associated with a thermal fluence of 7-10 cal/cm^2, considered sufficient to ignite at least the lighter fuel elements such as paper and twigs. Broyles (1985), however, argues that the ignited area determined by taking an ignition fluence of 20 cal/cm^2 is too low, because window glass and screens would reduce the fluence available inside rooms by 20 to 60 percent. In Nagasaki, the actual area burned (A x SF) corresponded to the area which would have received a thermal fluence of 20 cal/cm^2, while in Hiroshima, the area burned corresponded to the area which received only 7 cal/cm^2. It would therefore seem that the area corresponding to 20 cal/cm^2 is indeed "conservative", if SF is taken as equal to 1.

However, it is not known at this time whether the two effects mentioned above (i.e. overlap and improper average values for FL) would indeed be balanced by an underestimate for A x SF. Several lines of inquiry suggest that the overestimate is significantly larger than the factor of two underestimate made by using a fluence area corresponding to 20 cal/cm^2 rather than 7-10 cal/cm^2. For example, the analysis of Levi and Rothman (1985) suggests that consideration of overlap may reduce the value of A by as much as a factor of 4.

The value used for the average fuel load can also be checked by analysis of some of the fire spread modeling results carried out by Reitter et al. (1985). All previous studies of the amount of fuel that might burn have assumed average values for FL of about 40 kg/m^2 (see Table 1), although ranges from 10 to 400 kg/m^2 are quoted as possible (NRC, 1985). Table 1 also shows the average areal fuel loads within the burned areas corresponding to a 1 Mt nuclear explosion over the center of Detroit and several 1 and 0.5 Mt bursts over detonation points above Detroit and San

Jose, as taken from the work of Reitter et al. (1985). The average fuel loads from the work of Reitter et al. only consider areas which were occupied by buildings, so that these average values do not account for any decrease in FL due to targeting on the fringes of cities or near lakes or parks which would have lower average fuel loads. The fuel loads in the study of Reitter et al. were developed from surveys taken in the late 1960's, but recent analyses of fuel loads in San Jose (D. S. Simonett, 1986) have confirmed the average fuel load for areas occupied by buildings used in Reitter et al.'s study. From Reitter et al.'s study, it seems probable that values closer to 10 kg/m^2 should be used for most urban/suburban areas. Values for FL of close to 40 kg/m^2 are only appropriate for weapons directed on the city centers of large cities. Furthermore, the number of large cities is quite limited. Detroit's population is over 4 million. There are only 39 urban centers with a population of over 3 million people in the entire world and only 80 cities in the NATO and Warsaw pact with populations over 1 million. The oft-quoted "100 Mt central city" scenario of Turco et al. (1983), assumed values for FL equal to 200 kg/m^2 occurring in 100 cities. These loads appear to be overestimated by a factor of 5. Of course, there is a need to check whether European cities or cities in the Eastern portion of the United States contain much higher fuel loads than those represented by Detroit. But it seems highly probable that the estimates for FL used previously are too large, especially in view of the analysis of total combustible load outlined below. Furthermore, the above analysis for FL assumed targets which were entirely contained within the urbanized areas occupied by buildings. Consideration of actual target locations, some of which will occur on the fringes of cities and some of which will fall near lakes or other low fuel density areas, will reduce the estimate for FL even more.

Significant further reduction of the uncertainties using this approach requires a detailed analysis on a city-by-city basis with consideration of specific target locations, fuel loads, and overlap of fire areas. For the moment, we shall instead consider an alternative approach, wherein total combustibles are estimated directly and then a fraction is assumed to be ignited and burned.

This approach has been followed by Crutzen, Galbally, and Brühl (1984) and by Bing (1985) using different methodologies. Crutzen, et al. work from production figures for various raw materials and estimates of their lifetimes to obtain estimates for the total abundance of cellulosic materials, polymeric materials, and asphalt. Bing, on the other hand, gathered data from surveys on fuel loads in various types of structures and their contents for the United States and extrapolated these data to Europe and the Soviet Union. The two sets of published figures are not directly comparable, since Crutzen et al. estimate the amount of cellulosic and polymeric materials in the developed world whereas Bing's estimates refer to only the NATO and Warsaw Pact countries. Crutzen et al. and Bing also separately estimate the amount of petroleum available to burn, including petroleum stored as primary stocks and petroleum stored as secondary stocks. However, Crutzen et al.'s figures refer to the amount of petroleum stored globally, whereas, Bing's numbers again refer only to that fraction contained within the NATO and Warsaw Pact countries. In order to consider similar scenarios, we have reduced the inventories published by Crutzen et al. (1984) for the developed world by the ratio of population for NATO and Warsaw Pact countries to that of the developed world. We also reduced their estimates for petroleum by the ratio of consumption rates in NATO and Warsaw Pact countries to that of the world. As shown in Table 2, Crutzen et al.'s inventory implies a factor of 2.5 more cellulosic material than Bing's. The estimates for primary stocks of petroleum and for petroleum-derived materials are comparable, and the estimates for secondary stocks of petroleum differ by a factor of 2 to 4.

Both methodologies have obvious difficulties, and it is not clear to this author which method is more appropriate. We note, however, that the totals for cellulosic and polymeric materials assumed by Crutzen et al. (1984) are not entirely consistent with the fuel load estimates derived from the work of Reitter et al. (1985). For example, we may use the average areal fuel load for urban/suburban areas from the work of Reitter et al. (1985) together with the total urban area in cities with population greater than 2500 in the United States, 135,000 km^2, to arrive at a combustible load for the U. S. of 1350 Tg. Consideration of 50 city centers with fuel loads similar to Detroit might increase this total to 2000 Tg. This number is close to the value derived by Bing (1985) for the United States (i. e. 2119 Tg), and thus lends confidence to his estimates. On the other hand, when we scale Crutzen's numbers for the developed world by the ratio of population in the United States to that in the developed world (0.225) we arrive at 4400 Tg, which is at least a factor of 2 larger than the estimate above. However, in the analysis that follows, both numbers will be used to estimate the range of optical depths that are possible, given current uncertainties.

Table 2 summarizes the inventory of combustibles in NATO and Warsaw Pact countries developed using these two methodologies. In order to consider the range of smoke absorption properties from various fuel types, Table 2 divides the inventories into cellulosic fuels, petroleum-derived fuels, and liquid fossil fuels. This last category has been subdivided into primary and secondary stocks of petroleum. Secondary stocks are considered to be distributed with other fuels, while primary stocks of petroleum are considered separately in order to calculate the effect of a concerted effort to avoid or include these targets (see section 6).

Typically, only some fraction of the total available combustible material might actually burn in flaming combustion. Here, we assume 25% of the distributed fuels (cellulosic, polymeric, and secondary stocks of petroleum) for both our high and low estimates. In this way the range that we consider can be considered independent of any particular scenario, although more (or less) fuel might burn if the warring nations made a concerted effort to try to ignite (or avoid burning) the available fuel. A 25 percent fraction might come about, for example, by associating approximately 65 percent of the total fuel with people who live in cities (the average proportion of city dwellers for Europe, the USSR and the United States), and then burning 80 percent of the total fuel in cities, half in flaming combustion and half in longer term, smoldering combustion. Alternatively, most city fuels might burn in flaming combustion but, because of clustering of targets and overlap of ignition areas only 40 percent of the fuel in cities actually ignites and burns.

3. Estimates of the emission rate for smoke.

The appropriate smoke emission rate in a large area urban fire depends on a number of poorly estimated and poorly known factors. Various studies (e.g. Bankston et al., 1978; Tewarson, 1984) have shown that emission rates can vary depending on the type of fuel, the ambient air temperature, the availability of oxygen, the radiant intensity (as determined by the proximity of nearby fires), the geometric arrangement of fuel, etc. Only very limited data from large fires are available. Thus, most studies have used values consistent with the range of emission rates measured in laboratory scale fires (see Table 3). These might be under-estimates, if oxygen availability is truly limited in a large-area fire. On the other hand, Carrier et al. (1984) have argued that oxygen availability should not be an issue, given the turbulent motions above the fire. In view of the lack of credible data for smoke emission factors from large scale intense fires, we too adopt values estimated from the limited available data. But we emphasize that the values used here are highly uncertain. Table 3 also includes a range of estimates for emission factor as compiled by Crutzen et al. (1984) from (primarily) laboratory data. In the analysis below, we shall adopt a range of values for the emission factor, consistent with the values chosen by Crutzen et al. (1984) and NRC (1985). We caution, however, that larger uncertainties apply because of the possible inapplicability of these emission rates to actual large-area fires.

4. Optical properties of smoke.

Just as the emission rate for smoke depends on the burning conditions and type of fuel, so does the chemical, morphological and optical character of the smoke. Nevertheless, various authors have estimated the absorption and extinction coefficients for smoke, based on a variety of measurements that have tended to emphasize the data available from smoke emitted under flaming conditions. The evaluations are summarized in Table 4. In most recent evaluations, the optical properties of wood smoke are distinguished from those of fuels such as oil, plastics, and other polymers whose chemical structure has little available oxygen. These latter fuels tend to produce much blacker smoke. The table shows wide variations in the estimates of the absorption and extinction coefficients for fresh smoke.

In addition to variations in average optical absorption and extinction from different evaluations in these properties for fresh smoke, two mechanisms may act to make aged smoke less absorbing. The first mechanism is coagulation. This process may act on short time scales (in very dense smoke plumes) or on longer time scales (i.e. from days to a week in the spreading global plume) to create larger particles. These larger particles would be less absorbing and scattering of radiation if they are spherical. Because some smoke particles are quite oily (and therefore spherical), while others appear as fluffy or chained agglomerates, it is not possible at this time to predict the effects of coagulation on optical properties. Chained agglomerate particles might become spherical if they coagulated with oily smoke particles or by passing through condensation and reevaporation stages in a cloud, for example, which might allow the chains to collapse (Goldsmith et al., 1966). To the extent that the agglomerates remain in a chained formation, their absorption properties are not expected to change significantly. Thus, in the following, we shall adopt two extremes. In the first case, we assume coagulation has no effect on optical properties. In the second case, we assume coagulation does act to reduce extinction and absorption and adopt the estimate of Penner and Porch (1986) for these effects after 10 days of coagulation. This additional consideration widens the discrepancy between the lowest and highest estimates of absorption coefficient by an additional factor of about 3 for the highly carbonaceous, absorbing smokes. The extinction coefficients differ by a factor of more than 2. The absorption coefficient for less absorbing smoke is not significantly changed by coagulation.

5. Fraction of smoke rained out in early scale plume.

The last factor which contributes to estimates of the average optical depth is the amount of smoke which is removed by precipitation occurring in the smoke plume over and just downwind of the fire. Several authors have estimated that, especially for large, intense fires, large quantities of water will condense (Penner et al., 1986; Cotton, 1985). Cotton (1985) attempted to calculate the amount of smoke scavenged above a large fire, but neglected the effects of nucleation scavenging. Pruppacher (1985) included the effects of nucleation scavenging and suggests that rainout would be unlikely because of overseeding effects. On the other hand, in both Hiroshima and Nagasaki, a "black rain" fell coincident with the fires which followed the nuclear blasts of August 1945. The black rain is presumably smoke that has been scavenged by rain.

The amount of smoke scavenged by rain depends, once again, on properties of the smoke which are poorly known. For example, the number of smoke particles which act as condensation nuclei for cloud drops depends on the highest level of supersaturation attained above the fire as well as on the size distribution of the smoke and debris and their affinity for water. The highest level of supersaturation depends on the updraft velocity within the plume as well as the growth rate of the drops which form. The growth rate of drops depends on their size, which depends, initially at least, on the size of smoke and debris particles that act as nuclei. Other mechanisms may also act to attach smoke particles to cloud drops. These include electrical capture, phoretic forces, and turbulent motions. Once cloud drops are formed, they may or may not form precipitation-sized rain drops. The probability of this occurring depends on the initial size of debris and smoke particles and on the number that become nucleated to form drops. Once the drops become large enough to obtain a significant fall velocity, they may capture more smoke particles by impaction scavenging. The probability of this occurring again depends on the size of smoke particle (with larger particles being more likely to be scavenged).

The capture mechanisms described above apply to warm-rain precipitation only. Additional mechanisms and pathways for capture must also be considered in the case of ice formation.

Clearly, the theoretical analysis of scavenging is complex and difficult. For this reason, many authors have simply guessed a fraction for smoke that might be removed by rainout. These guesses range from close to 0 percent to 50 percent (see Table 5), although the real range of possibilities might include values up to 100 percent in some cases (Hobbs et al., 1984). For lack of a more definitive answer, in this paper, we consider the range from 50 percent to zero. Obviously, the range of average optical depths that we calculate could be larger, if rainout removed 90 percent of the smoke, for example.

6. Range of values for average optical depth and the resulting climate variations.

If we combine all the choices described above, emphasizing the smallest factors in one case, and the largest factors in the second, we obtain the range in absorption and extinction optical depths shown in Table 6. Table 6 considers separately the optical depths from cellulosic fuels, from distributed fuels producing highly carbonaceous smoke (i.e. polymeric materials and secondary stocks of petroleum), and from primary stocks of petroleum. In the case of distributed fuels, one quarter of the total abundance in the NATO and Warsaw Pact countries is assumed to burn. As shown in Table 6, the burning of polymers and petroleum contributes significantly to the total optical depth. For this reason, we consider two separate scenarios. In the first, the contribution of primary stocks of petroleum to the total optical depth is not included. This scenario might result if the warring nations specifically tried to avoid targets such as refineries that would add disproportionately to the optical depth. In the second scenario, these targets are all included, so that 100 percent of the primary stocks of petroleum are burned. Table 7 summarizes the high and low estimates of optical depth for these two cases. If the primary stocks of petroleum are not included, the absorption optical depth varies from 0.19 to 4.23. Including these stocks increases the range of absorption optical depths to from 0.38 to 6.07. In the first case, the low estimate is equivalent to 12 Tg of smoke with the optical properties assumed by NRC (1985). This increases to 24 Tg of smoke if primary stocks of petroleum are included. This case is close to the lowest smoke amount (i.e. 20 Tg) considered by Malone et al. (1986) in an advanced three dimensional climate simulation. Their results are consistent with widespread temperature changes over continents in summer of from -4 to -6 degrees C. The largest average optical depth which we calculate is equivalent to almost 400 Tg of smoke (assuming the absorption coefficient from NRC (1985)). This is somewhat less than the largest amount of smoke assumed by Malone et al. (i.e. 500 Tg) and would, according to their results, lead to profound climate changes, particularly as its removal would be inhibited by changes to atmospheric stability.

The range of values calculated here is disquieting, because we attempted to choose values for each of the various factors that were thought to be a "best estimate" by at least one of the authors whose works we are quoting here. In addition to the possible ranges considered here, there are added uncertainties caused by the lack of good data on the properties of smoke (e.g. emission rate, optical properties, and interaction with and effect of clouds) from large fires. Furthermore, little is known about the scavenging and rainout of smoke in fire plumes. Good data on the properties of smoke from large fires will only be developed via large fire experiments; but great care is needed in the design and interpretation of the large-scale fires which will be used in the reanalysis of these data. The planned experimental programs sponsored by the DNA must not stop after only the first few experiments, since we must try to understand the more complex situations that will exist in a real nuclear fire. In addition, more and g eater emphasis must be placed on understanding scavenging and rainout. Here, some progress seems possible by the development of advanced modeling capabilities, coupled with verification by large-scale fire experiments.

7. Final comments.

While our lowest estimate for $\overline{\tau}_a$ may produce only minor climate effects, scenarios can easily be constructed in which more fuel is burned, so that even in the low case, the estimate for $\overline{\tau}$ would correspond to a major climate impact if the war takes place in the spring or summer. On the other hand, it is entirely possible that such impacts could be avoided if the low estimates are correct and if targets such as refineries, oil and gas production fields, and coal storage areas are avoided. Impacts could also be lessened if the war occurred during the winter. It seems clear, therefore, that "nuclear winter" is not necessarily a probable outcome of nuclear war, although it is certainly possible. The full range of possible impacts can never be completely narrowed because we can never have access to the war plans of the nations of the world, nor predict the course of any given war once it began. This paper has shown, however, that for the scenario considered here, i.e. one in which 25 percent of the total distributed fuels are burned, further research is needed in order to be able to predict the effects on climate.

Some will fear that the recognition of a range of possibilities that includes only minor impacts might make nuclear war seem acceptable. I believe and hope, however, that even in the event of no climate effect from nuclear war, the immediate effects and destruction that would be caused by the massive use of nuclear weapons would continue to deter their use.

8. References.

Bankston C. P., Cassanova R. A., Powell E. A., and Zinn B. T. (1978) Review of smoke particulate properties data for burning natural and synthetic materials. National Bureau of Standards report NBS-GCR-78-147.

Bing G. (1985) Estimates of total combustible material in NATO and Warsaw Pact countries. Lawrence Livermore National Laboratory Report UCRL-93192 (draft).

Bing, G. (1986) Private communication.

Broyles A. A. (1985) Smoke generation in a nuclear war. Am. J. Phys. 53, 323-332.

Brunswig H. (1985) Private communication.

Carrier G., Fendell F. F., and Feldman P. (1984) Big fires. Combustion and Science Technology,

Cotton W. R. (1985) Atmospheric convection and nuclear winter. American Scientist 73, 275-280.

Crutzen P. J. and Birks J. W. (1982) The atmosphere after nuclear war: twilight at noon. Ambio 11, 114-125.

Crutzen P. J., Galbally I. E., and Brühl C. (1984) Atmospheric effects from post-nuclear fires. Climatic Change 6, 323-364.

Goldsmith P., May F. G., and Wiffen R. D. (1966) Chromium trioxide aerosol from heated 80:20 nickel-chromium wire. Nature 210, 475-477.

Hobbs P. V., Radke L. F., and Hegg D. A. (1984) Some aerosol and cloud physics aspects of the "nuclear-winter" scenario. In the proceedings of the ICSU-SCOPE Workshop on "Nuclear Winter Scenario: Current Studies of Scavenging Models," Supplemental Vol. to the Proceedings 9th Int'l. Cloud Physics Conference, Tallinn, Estonia, USSR, 21-28 August, 1984.

Levi B. G. and Rothman T. (1985) Nuclear winter: A matter of degrees. Physics Today 38, 58-65.

Malone R. L., Aver L. H., Glatzmaier G. A., Wood M. C., and Toon O. B. (1986) Nuclear winter: Three-dimensional simulations including interactive transport, scavenging, and solar heating of smoke. J. Geophys. Res. 91, 1039-1053.

National Research Council (NRC) (1985) The effects on the atmosphere of a major nuclear exchange. National Academy Press, Washington, DC.

Penner J. E., Haselman L. C. Jr., Edwards L. L. (1986) Smoke plume distribution above large scale fires: Implications for simulations of "nuclear winter". Submitted to the J. Climate and Applied Meteorology.

Penner J. E. and Porch W. M. (1986) Coagulation in smoke plumes after a nuclear war. Manuscript in preparation.

Pittock A. B., Ackerman T. P., Crutzen P. J., MacCracken M. C., Shapiro C. S., and Turco R. P. (1986) Environmental Consequences of Nuclear War, Vol. 1, Physical and Atmospheric Effects, John Wiley & Sons, New York.

Pruppacher H. R. (1985) On the scavenging of aerosol particles by atmospheric clouds and precipitation. Proceedings of the International Seminars on Nuclear War, SDI, Computer Simulations, New Proposals to stop the Arms Race," Erice, Italy, August 19-24, 1985.

Reitter T. A., Kang S. -W., and Takata A. N. (1985) Toward quantifying the source term for predicting global climatic effects of nuclear war: Applications of urban fire codes. Lawrence Livermore National Laboratory report UCRL-53647.

Simonett D. S. (1986) Private communication.

Sagan C. (1985) On minimizing the consequences of nuclear war. Nature 317, 485-488.

Tewarson A. (1984) Particulate formation in fires. Proceedings of the Conference on Large Scale Fire Phenomenology, 10-13 September, 1984.

Turco R. P., Toon O. B., Ackerman T. P., Pollack J. B., and Sagan C. (1983a) Nuclear winter: global consequences of multiple nuclear explosions. Science 222, 1283-1292.

Table 1. Average Combustible Fuel Load in Cities

Author	Fuel load (kg/m^2)
Turco et al. (1983)	
baseline case	33.5[1]
100-Mt city-center	200.0
Crutzen et al. (1984)	40.0
NRC (1985)	40.0
Reitter et al (1985)	
Detroit, center	34.5
Detroit/San Jose, suburbs	10.2

Footnote:

[1]Average of 100 kg/m^2 in "city centers" and 30 kg/m^2 in suburbs.

Table 2. Inventory of Total Available Combustibles in NATO and Warsaw Pact Countries (Tg)

Author	Cellulosic Materials	Primary Petroleum Stocks	Secondary Petroleum Stocks	Polymeric Materials
Crutzen et al. (1984)	16,500[1]	462[2]	198–462[2]	574[1]
Bing (1985)	6,444	480[3]	100[3]	753

Footnote:

[1]Reduced from the estimate for the "developed world" as developed by Crutzen et al. (1984) by the ratio of populations or 0.87 (Bing, 1986)

[2]Reduced from the estimate for the whole world as developed by Crutzen et al. (1984) and Pittock et al. (1986) by the ratio of consumption rates in NATO and Warsaw pact countries to that of the world or 0.66 (Bing, 1986)

[3]From Bing (1986). Bing (1985) suggests there are 548 Tg of primary and secondary stocks of petroleum.

Table 3. Emission Rates For Smoke

Author	Percent of fuel
Turco et al. (1983)	2.7[1]
Crutzen et al. (1984)	
wood	1.5
oil, polymers, etc.	7.0
NRC (1985)	
wood	3.0
oil, polymers, etc.	6.0
Range of values in flaming combustion: (from Crutzen et al., 1984)	
wood	0.085 2.5
oil	2 10
plastics	1.2–50

Footnote

[1]This is a weighted average of the "net emission rates" of 1.1% for urban centers and 3.3% for suburbs. These values may include some allowance for scavenging by rain. Emission rates in an earlier version of this paper were 2.5% for city centers and 5% for suburbs.

Table 4. Absorption and Extinction Coefficients for Smoke from Urban Fires

Author	k_a (m^2/g)	k_e (m^2/g)
Turco et al. (1983)	2.9	5.8
Crutzen et al. (1984)		
wood	3.3	6.8
oil, etc.	7.0	10.5
NRC (1985)	2.0	5.5
Penner and Porch (1986)		
wood, no coagulation	1.5	6.6
oil, etc., no coagulation	5.6	9.5
wood, after coagulation	1.3	4.0
oil, etc., after coagulation	1.8	4.0

Table 5. Fraction of Smoke Removed by Rain

Author	Fraction Removed
Turco et al. (1983)	
suburban fires	0.25
firestorms	0.50
Crutzen et al. (1984)	0.30
NRC (1985)	0.50
Cotton (1985)	< 0.02

Table 6. Calculated Range of Average Optical Depth from Urban Fires

Category	k_a (m^2/g)	k_e (m^2/g)	ϵ (g/g)	F (Tg)	$(1-f_r)$	$\bar{\tau}_a$	$\bar{\tau}_e$
Wood							
high	3.3[1]	6.8[1]	0.03[2]	16500[1]/4	1.0[3]	3.19	6.57
low	1.3(1.5)[4]	4.0(6.6)[4]	0.015[1]	6444[5]/4	0.5[2]	0.12(0.14)	0.38(0.62)
Polymers, plastics etc., and secondary stocks of petroleum							
high	7.0[1]	10.5[1]	0.07[1]	1083[6]/4	1.0[3]	1.04	1.55
low	1.8(5.6)[4]	4.0(9.5)[4]	0.06[2]	674[7]/4	0.5[2]	0.07(0.22)	0.16(0.38)
Primary stocks of petroleum							
high	7.0[1]	10.5[1]	0.07[1]	480[5]	1.0[3]	1.84	2.76
low	1.8(5.6)[4]	4.0(9.5)[4]	0.06[2]	462[1]	0.5[2]	0.19(0.61)	0.43(1.03)

Footnotes:

[1]Crutzen et al. (1984) and Pittock et al. (1986).

[2]NRC (1985).

[3]Based on Cotton (1985).

[4]Penner and Porch (1986). Numbers in parenthesis refer to case with no coagulation.

[5]Bing (1985) and Bing (1986).

[6]This number is the sum of the average of high and low estimates for secondary stocks of petroleum from Crutzen et al. (1984) and Bing's (1985) estimate for polymeric materials (see Table 2).

[7]This number is the sum of Bing's (1985) estimate for secondary stocks of petroleum and Crutzen et al.'s (1984) estimate for polymeric materials (see Table 2).

Table 7. Average Optical Depth

Scenario	$\bar{\tau}_a$	$\bar{\tau}_e$
Distributed fuels only		
high	4.23[1]	8.12
low	0.19[2](0.36)[3]	0.54(1.00)
With primary stocks of petroleum		
high	6.07[4]	10.88
low	0.38[5](0.97)	0.97(2.03)

Footnotes:
[1]Equivalent to 270 Tg of smoke with $k_a = 2\ m^2/g$.
[2]Equivalent to 12 Tg of smoke with $k_a = 2\ m^2/g$.
[3]Optical depths in parentheses refer to case that assumes no coagulation.
[4]Equivalent to 388 Tg of smoke with $k_a = 2\ m^2/g$.
[5]Equivalent to 24 Tg of smoke with $k_a = 2\ m^2/g$.

... Department, Lawrence Livermore National Laboratory
... Livermore, California 94550

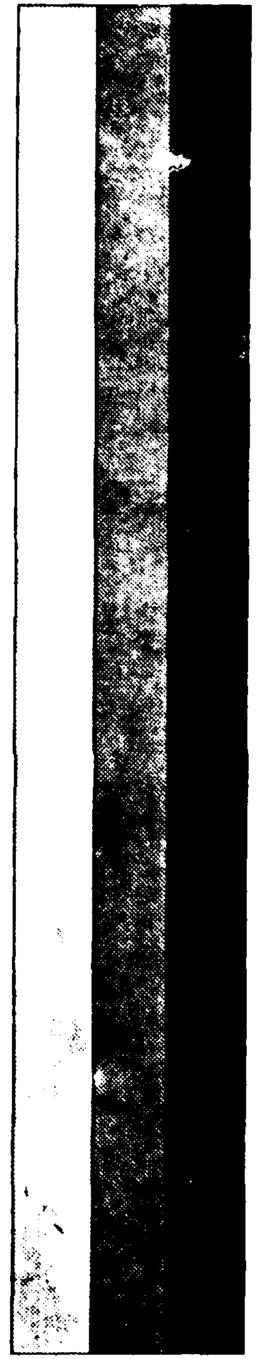

Supermicron Wind Suspended Particles and Firestorm Plume Coagulation

William M. Porch

Joyce E. Penner

Lawrence Livermore National Laboratory
Livermore, CA 94550

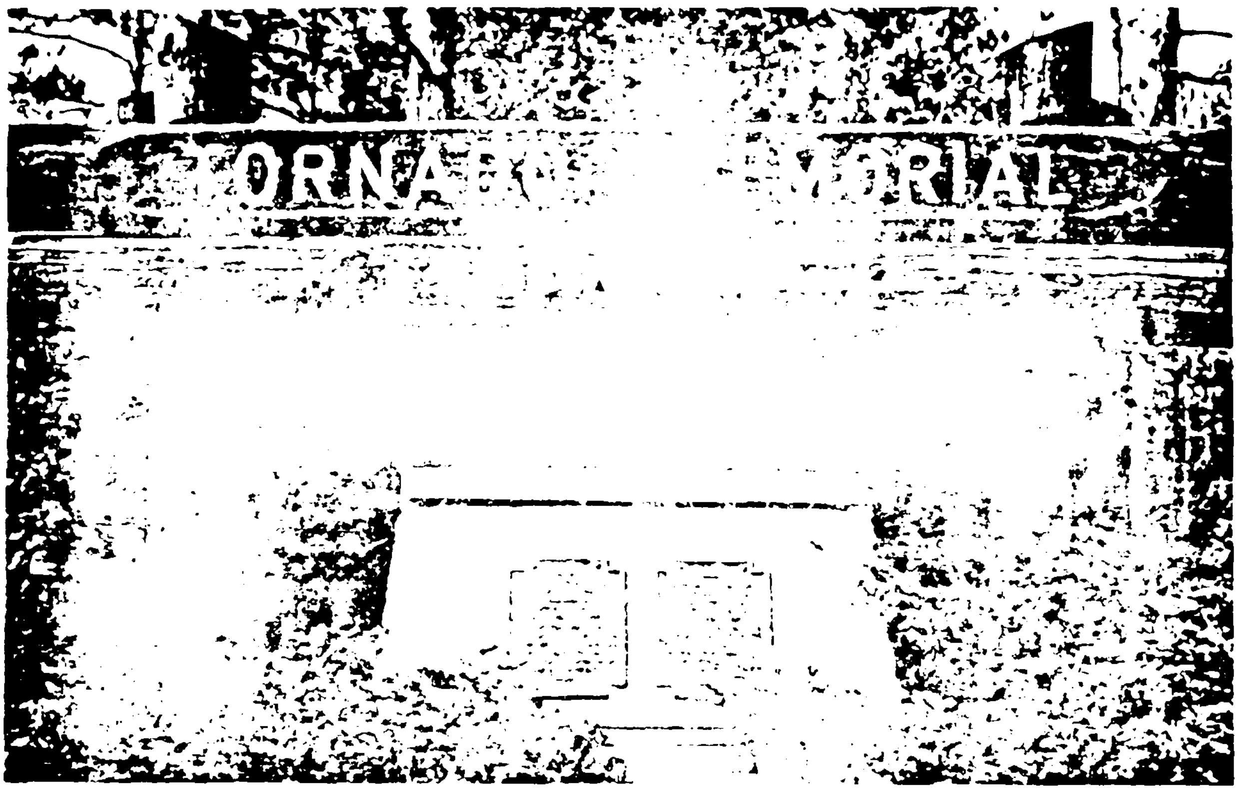

Tornadoes of Fire

The Tragic Story of Williamsonville, Wisconsin

October 8, 1871

By Joseph M. Moran and
Ronald D. Stieglitz

Tornado Memorial Park, located 4.1 miles north of Brussels, Wisconsin, on State Highway 57, commemorates the leveling of the tiny village of Williamsonville on the night of October 8, 1871. All but 17 of the settlement's 77 inhabitants were killed not by the ravages of a tornado in the usual sense, but rather by what was described by eyewitnesses as a "tornado of fire."

The burning of Williamsonville was one of many similar tragedies that struck October 8, 1871, [illegible] into remote lumber [illegible] towns situated [illegible] of Green Bay [illegible] sin. In all, perhaps [illegible] perished. A key source [illegible] the events of the [illegible] is [illegible] Tilton's *The Great Fire in Wi[illegible]*, a pamphlet published [illegible]. A local newspaper [illegible] portrays events leading up to and following the conflagration [illegible] words of eyewitnesses. These accounts also provide some [illegible] the meteorological aspects of the fires.

In 1871 the [illegible] weather station was in Milwaukee, more than 125 miles to the south. The station [illegible]

[illegible] keeping [illegible] with no [illegible] of the [illegible] forest fires had [illegible] these fires were the [illegible] material [illegible] Winds were [illegible] the most part [illegible] were able to con-

[illegible] same characteristics with dust devils for which vertical flux increases at least as [illegible] of speed

Kinetic Coagulation Equation

Change in Particle Density at Volume v_j

$$\frac{dn(v_j)}{dt} = \int_{v_{min}}^{v_j/2} K_{i,j-1}\, n(v_i)\, n(v_j - v_i)\, dv_i \qquad \text{(production)}$$

$$-\, n(v_j) \int_{v_{min}}^{\infty} K_{i,j}\, n(v_i)\, dv_i \qquad \text{(loss)}$$

- Equation assumes no bounce off but
Also no shape fluffy particles can coagulate much faster than spheres

Coagulation Coefficients

$$K_{i,j} = K^B_{i,j} + K^T_{i,j} + K^S_{i,j}$$

B-Brownian; T-Turbulent; S-Sedimentation

$$K^B_{i,j} = 4\pi\beta_{i,j}(r_i + r_j)(D_i + D_j)$$

$$K^T_{i,j} = 1.3\,(r_i + r_j)^3\,(\epsilon/\nu)^{1/2}$$

$$K^S_{i,j} = (\pi\rho g/9\mu)\,r_j^2\,(r_i^2 - r_j^2) \quad \text{for } r_i \geq r_j$$

Coagulation coefficients (cm^3/s)
Comparing Thermal and Turbulent Coagulation

r_2 (cm)	1.0×10^{-4}	1.0×10^{-3}	1.0×10^{-2}
r_1 (cm)	thermal coagulation only		
1.0×10^{-4}	6.4×10^{-10}		
1.0×10^{-3}	2.0×10^{-9}	6.1×10^{-10}	
1.0×10^{-2}	1.7×10^{-8}	1.8×10^{-9}	**6.0×10^{-10}**
	thermal and turbulent coagulation ($\epsilon=8000 cm^2s^{-3}$)		
1.0×10^{-4}	3.1×10^{-9}		
1.0×10^{-3}	4.1×10^{-7}	2.4×10^{-6}	
1.0×10^{-2}	3.2×10^{-4}	4.0×10^{-4}	2.4×10^{-3}

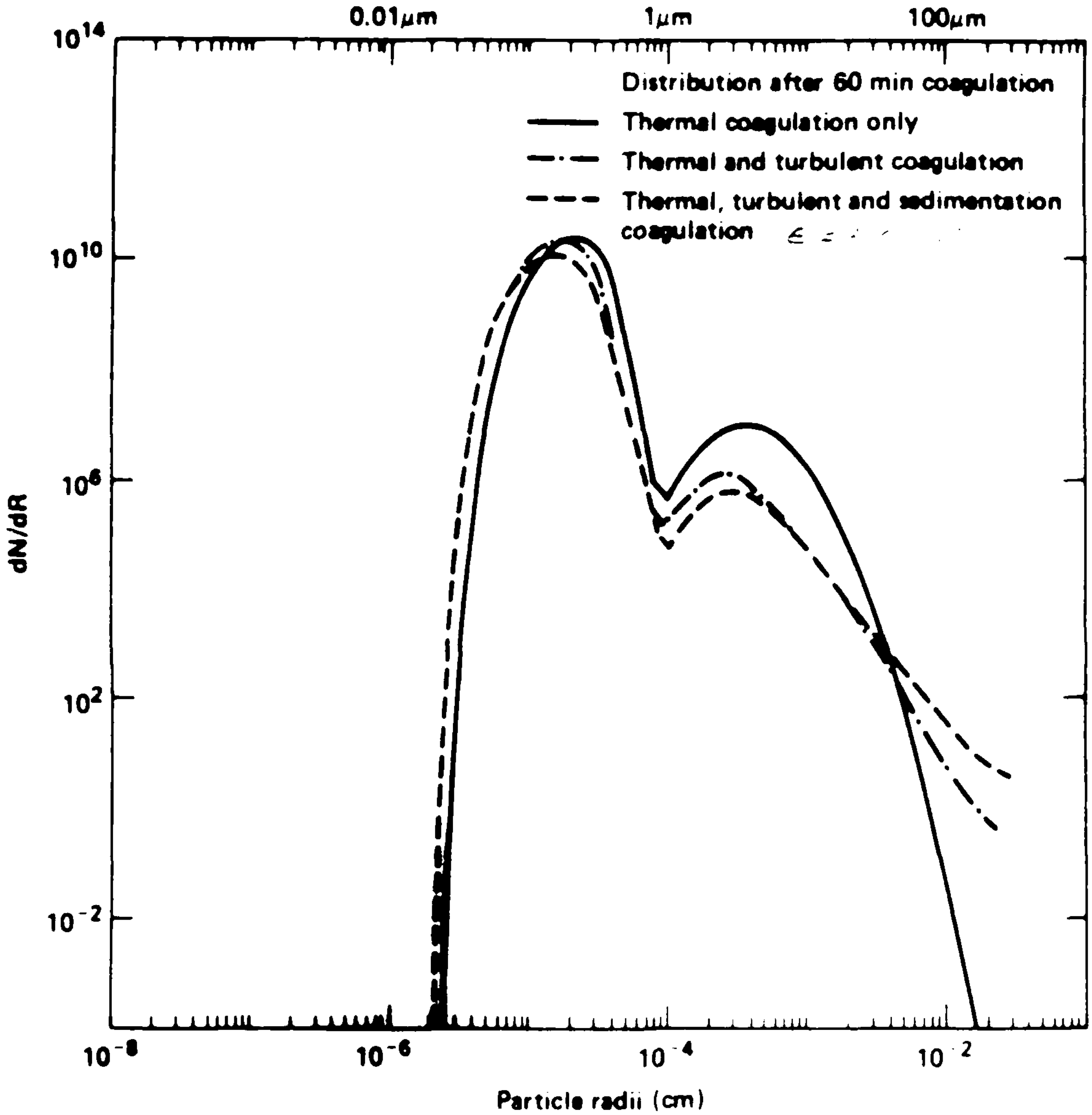

Figure 1

assuming size
[illegible]
[illegible]
arge particles and
5 g/m³ air density
shows evolution after hr

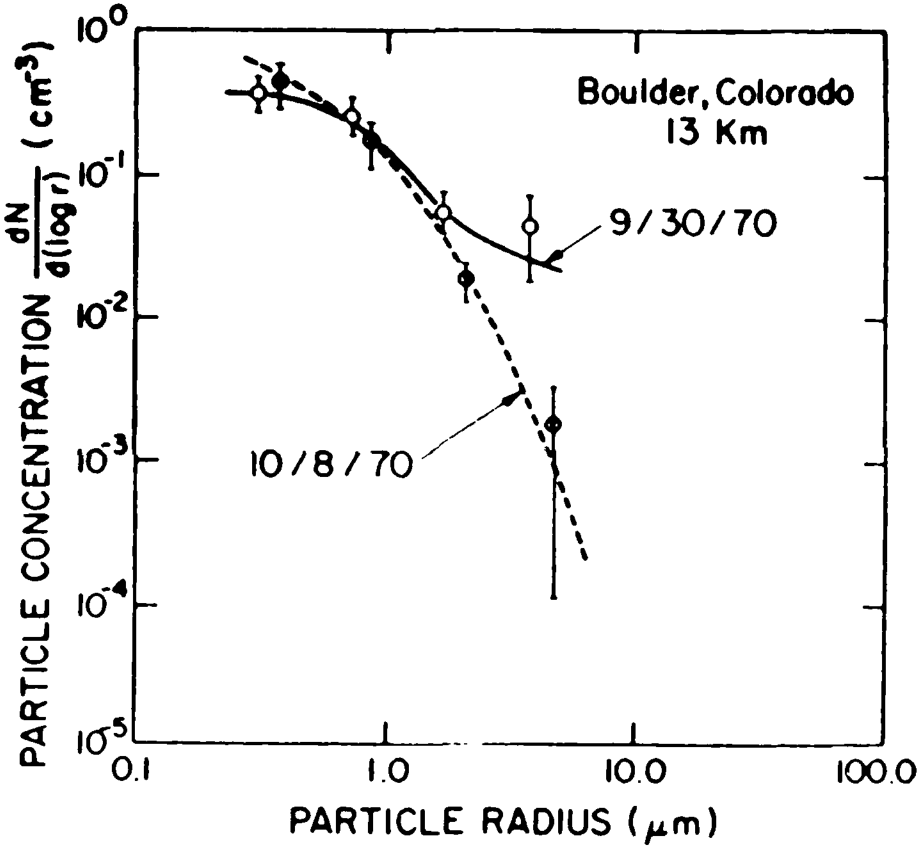

FIG. 3. Size distribution of particles collected at 13 km altitude at Boulder, Colo., on 30 September and 8 October 1970.

associated with
large fire ash
from Calif to Boulder

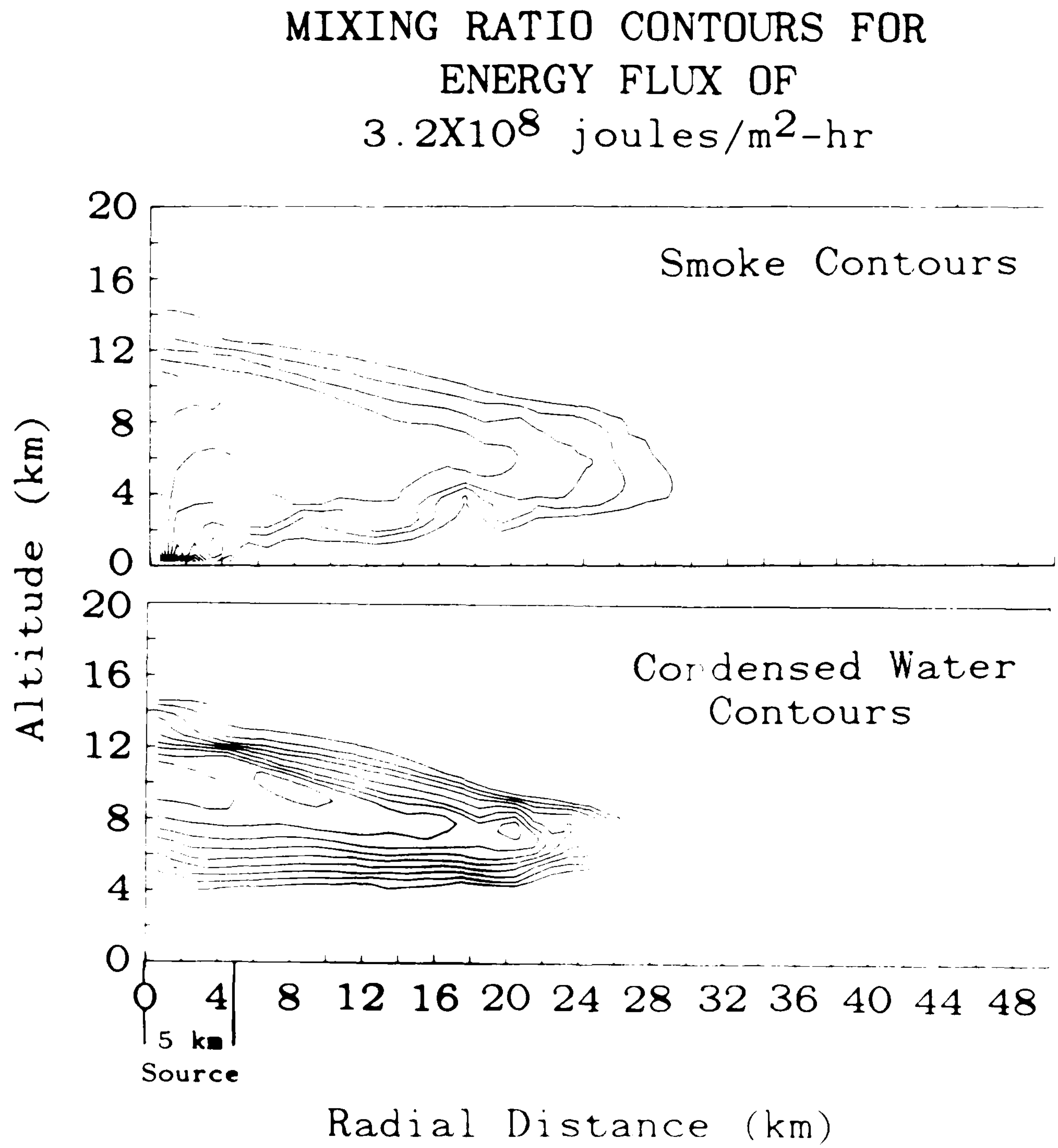

Numerical model used to simulate ... concentration variations for coagulation calculations

Figure 9. Smoke and condensed water mass mixing ratio contours after 1 hour for an energy flux of 3.2×10^8 J/m^2-hr. In contrast to the calculation shown in Fig. 8, water vapor was allowed to condense for this calculation.

Influence of Supermicron Aerosols on Submicron Optical Parameters (λ=0.55μm n=1.53-0.05i)

Case 1: No supermicron aerosols

Time	Submicron Mass Concentration	τ_a	τ_s
0(min.)	5.2×10^{-8} (g/cm^3)	69	196
10	1.3×10^{-8}	20	77
30	1.2×10^{-8}	19	79

Case 2: Including supermicron aerosols*

0	5.2×10^{-8}	69	196
10	4.6×10^{-9}	14	52
30	3.1×10^{-9}	10	39

A factor of 2 decrease in 10-30 min in submicron extinction due to supermicron turbulent coagulation

* ϵ=4000cm^2/s^3, rm=5μm, initial concentration=15 g/m^3

STAN MARTIN & ASSOCIATES

Consultants in Fire and Explosion Safety

ABSTRACT

HIGH RELIABILITY FIRE-START MECHANISM

The urban fire-starting ability of nuclear explosions may be more reliable--less subject to the caprice of target variables--than has heretofore been commonly recognized; this could be particularly true in multiburst attacks.

In a 1953 atmospheric test of nuclear explosive (ENCORE event), a furnished room, directly exposed to the thermal pulse of the fireball, flashed over in a fraction of a minute, exhibiting unusually intense dynamics, and the fire survived an incident airblast of about 5 psi. This behavior was dismissed as anomalous, and forgotten for nearly 30 years.

At the DIRECT COURSE "1-KT" HE event in 1983, blockhouse-fire experiments patterned on the 1953 model were exposed to airblast loadings in the range of 3 to 9 psi peak overpressures. All fires survived the airblast insult, and dramatic (virtually explosive) flashover dynamics were observed, being remarkably similar to the ENCORE experience. The Harvard Fire Code has since been used to lend analytical support to the ENCORE response.

This presentation will illustrate these combined thermal/airblast effects, and interpret their significance in practical situations, with special note of their potential impact in multiburst scenarios.

860 Vista Drive Redwood City, California 94062 (415) 365-4969

STAN MARTIN & ASSOCIATES

Consultants in Fire and Explosion Safety

NARRATIVE

It is difficult to reconcile the fire-starting experience of the nuclear attacks on Japan, in 1945, with mechanistic fire-start models in current use to predict incendiary consequences of nuclear explosions. This may be due to a special vulnerability of urban Japan, as it was four decades ago, or it may be symptomatic of inadequacies of the models or of the concepts on which they are based. This paper examines these prospects, and introduces new findings that bear on the inconsistencies.

The current models of primary-fire starting by the thermal pulse from a nuclear fireball are basically kindling/tinder-fuel ignition algorithms in which the enclosure's only role, at first, is to limit exposure of room contents to the initiating thermal radiation. Only much later, following a growth process that may take from many minutes to an appreciable fraction of an hour, does the enclosure's heat-conserving character manifest itself in a flashover response.

Intrusion of the air blast of the explosion into this process, usually occuring within seconds of initiation while the fires are still incipient, can profoundly alter its course and outcome. Flames of such incipient fires are known to be easily extinguished by the rapidly rising air flows accompanying a shock wave (typically, only 2-to-3-psi peak overpressures). Loss of confining walls and ceilings and outright collapse of structural enclosure, due to blast damage, alter the configurational requirement for flashover development. And clearly, incipient fires in kindling/tinder materials are readily snuffed out when buried in debris.

All of this seems inconsistent with the two experiences of nuclear attack on urban targets at the end of World War II. Hiroshima was totally burned out to about 6000 feet from ground zero, and despite collapse of the majority of structures in that same area, a mass fire developed within 20 minutes of the explosion. Ground surveys, conducted by fire specialists in the occupying forces, positively identified primary fires in uncollapsed buildings of Hiroshima in the annulus between 5 and 20 psi overpressure contours, and at overpressures of at least 17 psi at

Nagasaki. In both cities, most building fires inside the 4000-ft radius were of unknown origin, but it can be argued that they, too, were primary fires that not only survived severe blast effects, but developed quickly -- in Hiroshima's case, into a mass fire often since described as a "firestorm."

Postwar atmospheric testing of nuclear explosives provided almost no comparable situations. An exception, in the ENCORE test of 1953, when a furnished room flashed over immediately and the fire survived at least 5 psi, was dismissed as anomalous. A similar experiment was conducted for the Federal Emergency Management Agency in 1983 as a part of the high-explosive, "1-KT" DIRECT COURSE Event at White Sands, NM. Furnished rooms, patterned after the ENCORE blockhouses, were set alight by comparably high rates of energy deposition. Airblast loadings in the range of 3 to 9 psi failed to extinguish any of the enclosure fires--although some fires in the open were blown out--and dramatic (virtually explosive) flashover dynamics were observed, remarkably similar to the photographic record at ENCORE.

The design of the DIRECT COURSE enclosure-fire experiment, the observed results, and conclusions derived from them are described. It is shown how they are supported by independent experiments in model-scale enclosure fires and by recent analytical results provided by the Harvard Fire Code. Far from being an anomaly, the ENCORE Effect is now seen to be an important fire-start mechanism in conditions of high rates of energy deposition, a mechanism that accounts, in large measure, for the experiences of 1945.

authors: Stanley B. Martin
Stan Martin & Associates

Robert G. McKee, Jr.
Los Alamos Technical
Associates

March 1986

STAN MARTIN & ASSOCIATES

Consultants in Fire and Explosion Safety

HIGH RELIABILITY FIRE-START MECHANISM

Global Effects Program

Technical Meeting

25-27 February 1986

Ames Research Center

Moffett Field, California 94035

860 Vista Drive Redwood City

AD-A185 149 TECHNICAL PAPERS PRESENTED AT THE DEFENSE NUCLEAR AGENCY GLOBAL EFFECTS R..(U) DOD NUCLEAR INFORMATION AND ANALYSIS CENTER SANTA BARBARA CA.. 15 MAY 86 3/3

UNCLASSIFIED DASIAC-TN-86-29-VOL-1 DNA001-82-C-0274 F/G 15/6.4 NL

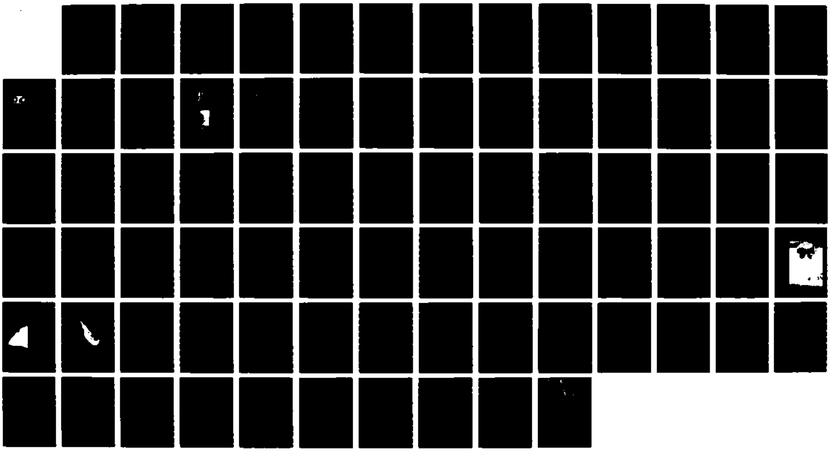

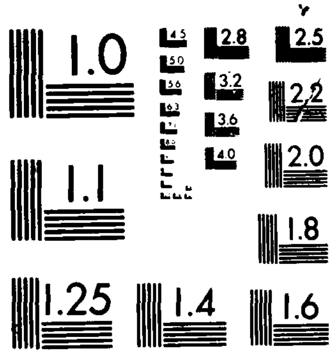

MICROCOPY RESOLUTION TEST CHART
NATIONAL BUREAU OF STANDARDS-1963-A

JAPAN 1945

Hiroshima

* totally burned-out to 6000 ft from GZ
* mass fire developed within 20 minutes
* building fires directly set alight by thermal radiation to at least 5000 ft
* positive identification of primary building fires between 1000 and 5000 ft; corresponds to 20 psi (reg. reflection) to 5 psi (Mach reflection)
* inside 4000 ft most fires were of unknown origin

Nagasaki

* positively identified primary building fires inside 3000-ft radius; corresponds to > 8 psi
* most fires inside 4000-ft radius were of unknown origin

* *

Contrast this with the experimental evidence of incipient fires being blown out by 2 to 3 psi airblasts:

* UCLA thermal-source/shocktube experiments (1950s)
* Nevada Test Site, fires in the open (1950s)
* URS Tunnel, incipient room fires (1970-1975)
* SRI Fire/Airblast Facility (1980-1982)
* LATA debris-fire experiments at DIRECT COURSE (1983)

FIRE BLOWOUT - - Two Issues

1. Fires in the Open

   - liquid-fueled (volatility)

   - solid-fueled (preburn time)

2. Fires in Rooms

   - heat-feedback reinforcement

   - stagnation of blast-induced flow (e.g., ENCORE)

ENCORE Effect

- 27-KT nuclear airburst
- Upshot/Knothole Series (1953)
- Residential mock-ups
  (2 furnished "blockhouses")
- $\sim$1 mile from GZ
- $\sim$25 cal cm^{-2}
- One flashed over immediately
  (fire not blownout by 5 to 7 psi)

TEST CONDITIONS

ENCORE

* 10' x 12' floor, 8' ceiling, 4' x 6' unglazed window
* 1.7 MJ thermal radiation (from fireball) deposited in about 2 seconds
* ~2 to 7 MJ of sensible heat gain (including combustion)
* airblast arrival in 4 seconds

DIRECT COURSE (7-psi station)

* 12' x 12' floor, 8' ceiling, 4' x 6' unglazed window
* 20 g/s propane flow for 10 s (shut off at either -10 or -20 seconds)
* corresponding heat deposition on order of < 1 MW
* sensible heat gain <u>perhaps</u> 5 to 15 MJ
* airblast arrival, 0.65 s (~11 to 21 s after propane shutoff)

DIRECT COURSE Results

1. The ENCORE response is not anomalous.

Room Fires

2. Well established fires do not blow out at OPs → 10 psi.
3. The 1950 UCLA empirics seem OK.
4. Confirms SRI shocktube data.

Debris Fires <u>in</u> <u>the</u> <u>open</u>

FURTHER CONFIRMING EVIDENCE FOR ENCORE EFFECT

* State-Transition Concept (P. H. Thomas et al.)

* Full-Scale Room Tests

  - IITRI and Swedish criteria for flashover

  - high heat-release-rate fires (e.g., NBS/CFR)

* Model-Scale Room Fires

  - heat-deposition criterion, based on SRI's study for Product Research Committee, used to design DIRECT COURSE; roughly confirmed at DIRECT COURSE

* SRI's use of Harvard Fire Model roughly "predicts" the ENCORE <u>and</u> DIRECT COURSE observations

ENCORE

AS A

MULTIBURST EFFECT

FIRST BURST:

Overpressures of ~1/2 psi and less can remove glass and other window coverings.

SUBSEQUENT BURSTS:

The overlap region -- order of 20-mile radius around first burst and ~20 cal cm^{-2} from any subsequent burst -- could exhibit ENCORE-type response in many buildings still standing after first burst.

Collision Formation Kinetics and Optical Properties of Submicrometer, Post Detonation Aerosols.

William H. Marlow
Civil Engineering Department
Texas A & M University

W. MARLON
TEXAS A&M UNIVERSITY

I. INTRODUCTION

A. AEROSOL COLLISION KINETICS

1. soot precursor growth and effects of ventilation

2. internal vs. external mixing in atmosphere

B. OPTICAL PROPERTIES

1. chains of soot precursors - exact

2. multi-ball linear chains - exact
   - branched chains, perhaps

3. hydrocarbons condensed on irregular particles

TERMINOLOGY

TRANSPORT

ℓ = GAS MOLECULAR MEAN FREE PATH (~0.06 μm AT SEA LEVEL

a = PARTICLE RADIUS

$\ell/a \gtrsim 10$ FREE MOLECULE REGIME OF TRANSPORT

$0.25 \lesssim \ell/a < 10$ TRANSITION " " "

$0.25 > \ell/a$ CONTINUUM " " "

LONG-RANGE "VAN DER WAALS" INTERACTIONS

ANALOGY WITH MOLECULAR CASE

MOLECULAR INTERACTIONS, V ←— d —→

$$V \sim \int_0^\infty d\omega\, \alpha_1(\omega)\, \alpha_2(\omega)\, e^{-\hbar d/\omega}$$

α = MOLECULAR POLARIZABILITY AT FREQUENCY ω

FOR $d \ll$ WAVELENGTH OF ACTIVE BANDS $\equiv \lambda$

$V \sim 1/d^6$ "LONDON - VAN DER WAALS", NON-RETARDED INTERACTION

FOR $d > \lambda$

$V \sim 1/d^7$ "RETARDED" VAN DER WAALS OR CASIMIR-POLDER

NOTE: FOR SIMILAR PARTICLE COLLISIONS, WHEN $\ell/a \sim 10$, $d \sim \lambda_{optical}$

β = MULTIPLICATIVE COLLISION RATE ENHANCEMENT FACTOR USED IN FITTING DATA

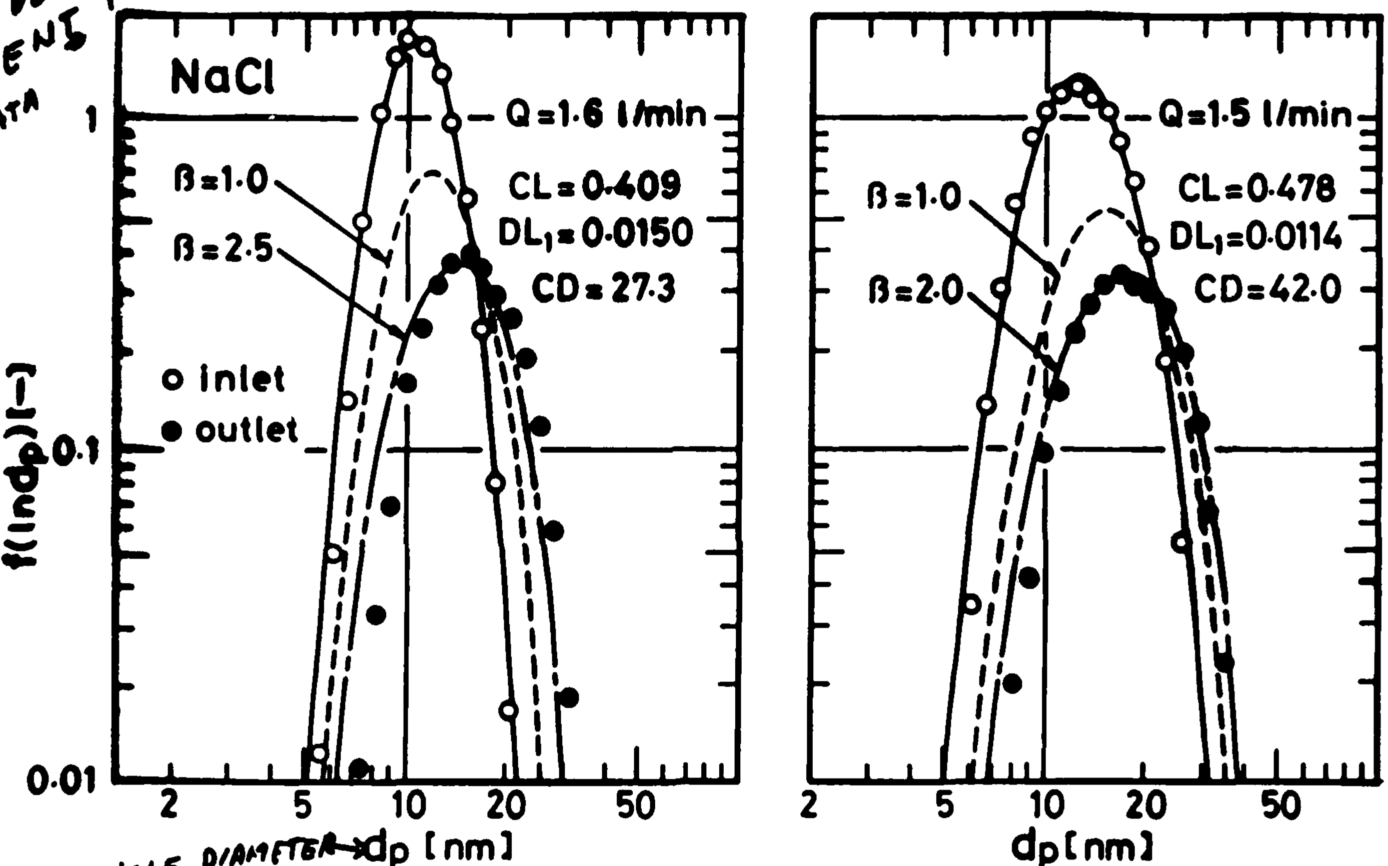

Okuyama, Kousaka, Hayashi
J. COLLOID INTERFACE SCI. 101, 98 (1984)

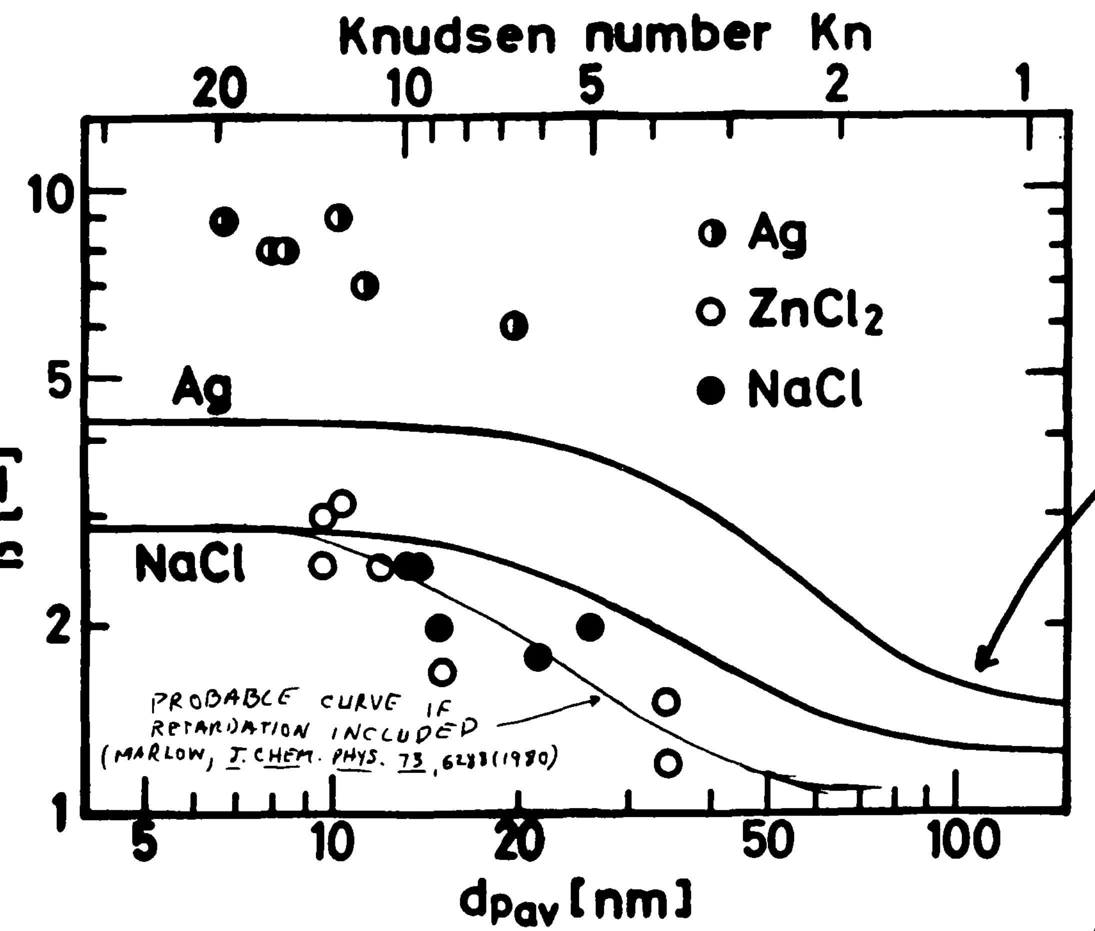

Figure 9; Coagulation enhancement factor

CURVES FOR β ~~CALCU~~ CALCU-LATED USING FORMULA DERIVED IN MARLOW, J. CHEM. PHYS. 73 6283 (1980)

RETARDATION NEGLECTED IN THIS FIT

FROM OKUYAMA, ET AL

WORK IN PROGRESS ON SUBMICROMETER COLLISION RATE DENSITIES OF SPHERES

VISCOUS DAMPING – K. ALAM (TO APPEAR)

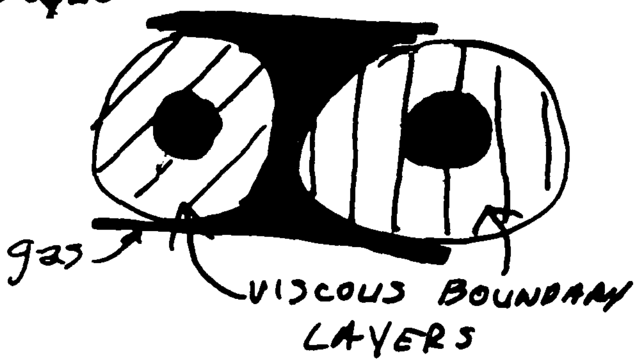

SLIP-FLOW AND CONTINUUM REGIME

$\ell/a \lesssim 0.25$

VISCOUS DAMPING + IMPROVED TREATMENT OF RETARDATION – ALAM AND MARLOW (IN PROGRESS)

EXTERNAL VS. INTERNAL MIXING

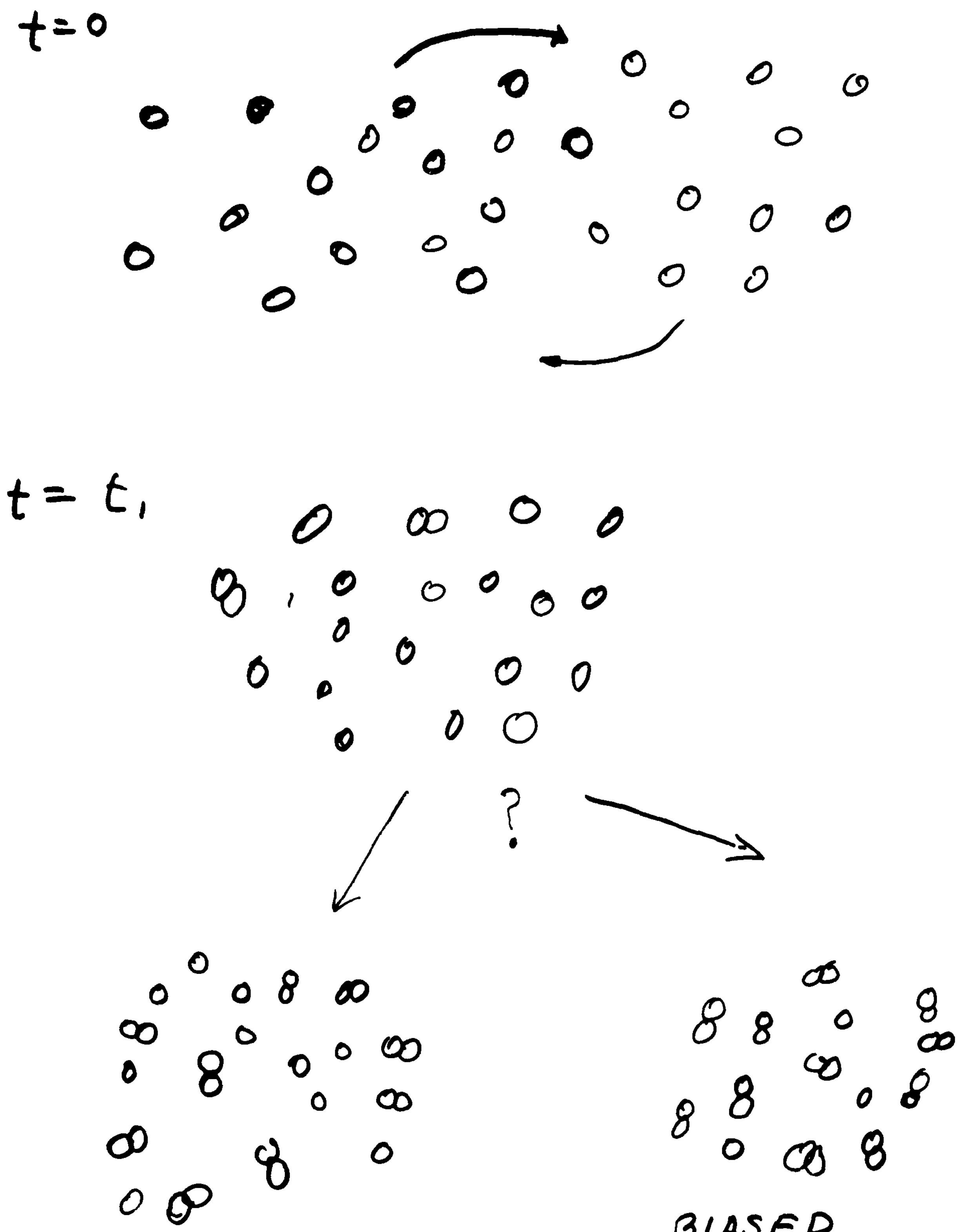

JONKMAN, EVEN, KOMMANDEUR

J. PHYS. CHEM. 1985, 89

4240-4243

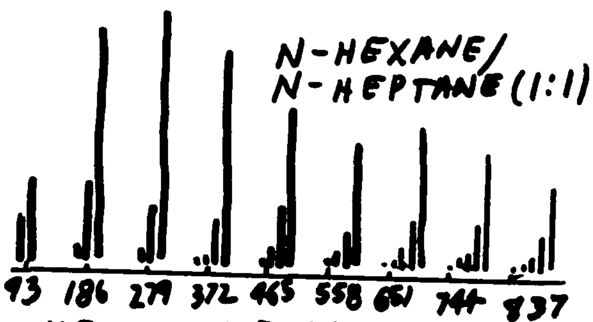

MOLECULAR MASS DISTRIBUTION FROM NOZZLE BEAM EXPANSION OF 1:1 GAS MIXTURE

THE LITTLE PEAKS TO THE LEFT OF THE MAIN ONES ARE DUE TO THE HEXANE-CONTAINING CLUSTERS, OF WHICH THERE ARE ONLY VERY FEW

SOOT PRODUCTION FROM FLAMES
WITH NO TRANSVERSE ADVECTION

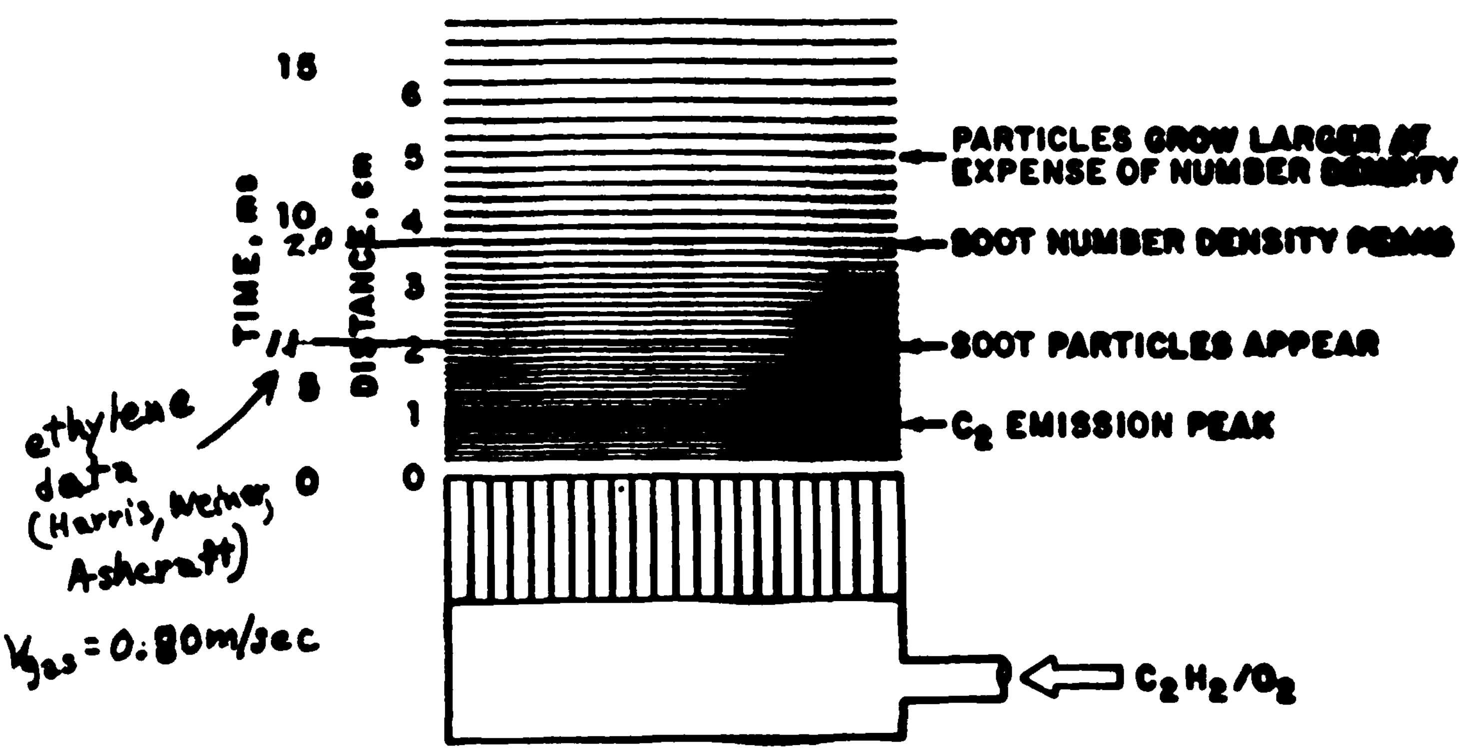

Fig. 2. Typical sooting flame on a flat flame burner.

QUESTION: HOW DOES ADVECTION, AS IN FIRESTORM AFFECT SOOT FORMATION?

- DETAILS OF COAGULATION AT EARLIEST STAGE IMPORTANT

PARTICLE OPTICAL PROPERTIES

SOOT PRECURSOR CHAINS — COUPLED POLARIZABILITIES, EXACT

2-SPHERE SOLUTION IN LITERATURE (KATTAWAR, DEAN, OPTICS LETTERS 8, 48(1983))

SOOT CHAIN — EXACT WORK IN PROGRESS

ALSO MIXED CHAIN

HYDROCARBONS CONDENSED UPON IRREGULAR PARTICLES — EXACT

PROPOSED WORK

COLLISION KERNAL: $1\,NM \leq r \leq 1000\,NM$

1. BICUBIC SPLINE FITTING TABLE
   a. SOOT MODELS
   b. MINERAL MATTER
   c. MIXED COMPOSITIONS

2. EXTEND METHODS USED FOR SPHERICAL COLLISIONS TO SPHERE + CHAIN AND INCLUDE COMPOSITION

SINGLE PARTICLE LIGHT SCATTERING AND ABSORPTION

1. CHAINS OF MIE SPHERES

2. LIQUID SPHERES WITH CHAIN-LIKE INCLUSIONS

SECTION 3

DUST SOURCE TERM

RADIATIVE PROPERTIES OF DUST FOR INPUT TO DUST SOURCE TERMS FOR MODELS OF THE GLOBAL EFFECTS OF A NUCLEAR EXCHANGE

E M Patterson

School of Geophysical Sciences

Georgia Institute of Technology

Atlanta, Georgia 30332

ABSTRACT

A limited set of measurements of the radiative properties of dusts that are possible sources for the injection of material into the atmosphere following a nuclear exchange have been made. These measurements show that the visible wavelength absorption of bulk dusts is somewhat less than the estimates that have been used in previous models. The absorption appears to increase, however, with decreasing size fraction; and so the resulting absorption of the dust will depend on the details of the generation processes and on any fractionation that occurs during the generation processes.

The results of these preliminary measurements suggest that the earlier estimates of dust absorption are reasonable, although more experimental data are needed to adequately bound the range of absorption to be expected for this dust at solar wavelengths. other data suggest a relatively strong infrared absorption for the dust.

INTRODUCTION

The amount of dust injected into the atmosphere by nuclear explosions is strongly dependent on the magnitude and height of the blasts. Dust lofted into the stratosphere can have global climatic effects. On a smaller scale, massive amounts of dust injected into the lower atmosphere by surface and penetrating bursts can have regional and local effects, such as producing a dust laden thermal layer producing the non-ideal blast behavior of the shock wave.

The global effects of dust lofted into the stratosphere by a possible large scale nuclear exchange were considered by a recent National Academy of Sciences report. The committee's analysis showed that for their baseline case, the dust injected into the stratosphere was less important than the smoke emissions; but that much larger counterforce exchanges could lead to significant effects.

In all cases of global or regional optical radiative effects, the effects are dependent on the assumed optical properties, including size distributions and optical constants. When aerosols are generated by wind erosion processes, there is a fractionation in particle size that takes place, with the aerosols generated from the soil having smaller characteristic sizes than the parent soil. This fractionation is shown in Fig. 1. As the particles age there will be a further fractionation leading to the differences in the size distributions shown in Fig. 2. For soil aerosols produced as a result of nuclear explosions the likelihood of fractionation in the generation process is not as clear cut.

The optical constants of soil aerosols (or other aerosols) can be expressed in terms of the quantities shown in Fig. 3. The absorption parameters n_2 and B_a are of particular interest.

The NAS committee assumed that most of the long-lived stratospheric dust would be composed of melted or vaporized material for which the characteristics of volcanic ejecta would be appropriate. Their assumed optical properties expressed in terms of a complex refractive index were $1.5 - .001\ i$ at solar wavelengths, which is based on measurements of volcanic materials by Patterson and by Pollack. Significantly higher or lower values could alter the conclusions of the effects of the dust; and the range of visible wavelength absorption in volcanic ejecta can be rather large. The range can extend by an order of magnitude or more in either direction, depending of the properties of the material. Flyash, which can also be considered as an analog of the dust produced by these nuclear explosions since it consists of vaporized and recondensed silicate material, can also have a fairly wide range of absorption values.

Soil materials can have a wide range of values of absorption, with values that vary with particle size, as shown in Fig. 4, in which the larger size fraction value is given by the solid line and the smaller size values by the dashed and the dotted lines. The range of values is decreased considerably when measurements are made of the smaller size fraction only, as shown in Fig 5, in which measurements from various remote areas are compared.

Since possible targets can be identified, we have the ability to reduce the possible range of uncertainty by determining the absorption of material that is characteristic of that which could actually be injected by such explosions. Some preliminary measurements that address this question have been made for soils of interest.

PRELIMINARY MEASUREMENTS OF DUST OPTICAL PROPERTIES AT SOLAR WAVELENGTHS

A small number of soil samples were obtained from the area near Whiteman Minuteman Wing IV in western Missouri. These samples were collected by Glen Rawson and sent to Ga Tech for the optical analysis. The samples ranged in appearance from light tan in color to a dark brown. Each consisted of uniformly mixed material from the sampling site, and each had been sieved to remove clumps larger than about 250 μm diameter. Three representative samples were chosen for a preliminary analysis, one representative of the light tan samples and two that were typical of the dark brown samples.

Each of these soil samples contained an appreciable amount of organic material, which could have the effect of modifying the optical properties of the mineral constitutents of the soil. In order to look at the optical properties of the mineral component alone, these soil samples were treated with a concentrated hydrogen peroxide solution to oxidize the organic material. There was a lightening or bleaching of each of the samples--a slight bleaching for the already tan sample and a significant bleaching for the dark brown samples. The samples were allowed to stand with an excess of the hydrogen peroxide and so we assume that the organic material was essentially completely oxidized.

In addition, for two of the samples, a crude separation by size was made by sedimentation. Although size separation by sedimentation is, in principle, possible of quite detailed size analysis, we were concerned with only a crude separation to determine whether there was a difference in the n_2 values with particle size. For our separation, particles smaller than about 20 μm diameter were classified as small particles and the particles larger than about 20 μm were classified as large particles. It is emphasized, of course, that such a separation is only a first cut at determining whether there are size effects, since the long lived aerosol particles will have sizes that are less than 5 μm--a size significantly smaller than our cut size.

The absorption was then determined for these samples, with the absorption expressed in terms of the absorption index n_2. The techniques used were the same as those used in determining n_2 for the volcanic materials that have been previously reported. Specifically, absorption measurements were made on portions of the original untreated dark samples, and each of the treated samples from which the organics had been removed. For one of the samples (Sample 18) absorption measurements were made of both the large and the small fraction. For another sample (Sample 17), although a separation was made, there was no significant difference in the appearance of the two fractions and results are reported for the total sample only.

The measured data are shown in Fig. 6 and in Table I. Samples 17 and 18 were the original dark samples and their n_2 values are approximately 1.8 and 2.2×10^{-3} at 500 nm with an appreciable wavelength dependence. These measurements showed that the removal of the organic material resulted in a reduction of the n_2 value for Sample 17 from 1.8×10^{-3} to 4×10^{-4}. For Sample 18, absorption values were measured for the two size fractions separately, the values at 500 nm were 1.0×10^{-3} for the small size fraction and 3×10^{-4} for the larger fraction. The third sample (Sample 22) showed a value of 3.1×10^{-3} at 500 nm for the original sample and 4×10^{-4} for the minerological component.

These results may be summarized in relation to the previous estimates of the NAS report as follows:

1. n_2 of the dark (untreated) soil samples is approximately 2×10^{-3}, a value that is higher by a factor of 2 than the NAS estimate of 10^{-3} at 500 nm for an average soil.

2. The absorption of the mineral component of the soils is approximately 4×10^{-4}, a value that is lower by a factor of 2 than the previous estimates.

3. The absorption of these samples has an appreciable wavelength dependence with significantly more absorption at near ultraviolet and blue wavelengths (350-450 nm) than at red wavelengths.

4. There can be a dependence of n_2 on particle size. For our treated bleached samples, our measurements show that the

smaller particles have significantly higher absorption than the larger particles in at least one of the samples. Although our measurements are sufficient to indicate that there are some size effects, they are not sufficient to determine the magnitude of the effect for the smallest long-lived particles.

QUESTIONS TO BE ANSWERED WITH REGARD TO VISIBLE WAVELENGTH ABSORPTION

The data discussed in the preceeding section represent a first cut at determining the absorption of soil material that could be injected into the atmosphere by a possible nuclear exchange. They suggest that for this small set of samples, the earlier estimates are reasonable.

There are still significant unknowns, and we still have the question "What are the best estimates of soil aerosol absorption to use in determining the radiative effects of dust produced by the nuclear explosions?" In order to answer this basic question there are some specific questions that need to be answered. Some of these are:

1. Are these few samples representative of the range of soil absorption in possible target areas?

2. Since soils can contain an appreciable organic component, are the values of soil absorption that include the organic component most appropriate or should the absorption values of the minerological component only be used? Presumably there would be considerable heating and vaporization of the soil material which would remove the organic component and so the minerological component only is most appropriate; but we don't really know. (As another question, could combustion of the organic material in the soil produce soot?)

3. Is an increase of absorption with decreasing size common? The soil aerosol data of Patterson suggest that it is; but then we have the question of whether a fractionation of the soil material occurs, and whether the smaller glass particles formed are also more highly absorbing than the average soil mineralogical material. For large optical depths, the observed differences could be significant.

INFRARED DATA

No infrared measurements have been made of the soil samples of interest, other soil and soil aerosol samples shown in Figs. 7 and 8 show a broad absorption peak in the 8 to 12 μm band. On the basis of these data it is estimated that the average specific absorption coefficient at these infrared wavelengts is roughly 0.3 m^2/g.

TABLE I

SAMPLE ID	APPEARANCE	n_2 VALUES at 500 nm ($\times 10^3$) untreated (w/ organics)	mineral only small*	large	total
17	Dark Brown	1.8			.4
18	Dark Brown	2.2	1.0	.3	
22	Light Tan	1.3			.4

* the small fraction consists of particles of approximately 20 μm and smaller. The large fraction contains particles from about 20 μm to 250 μm

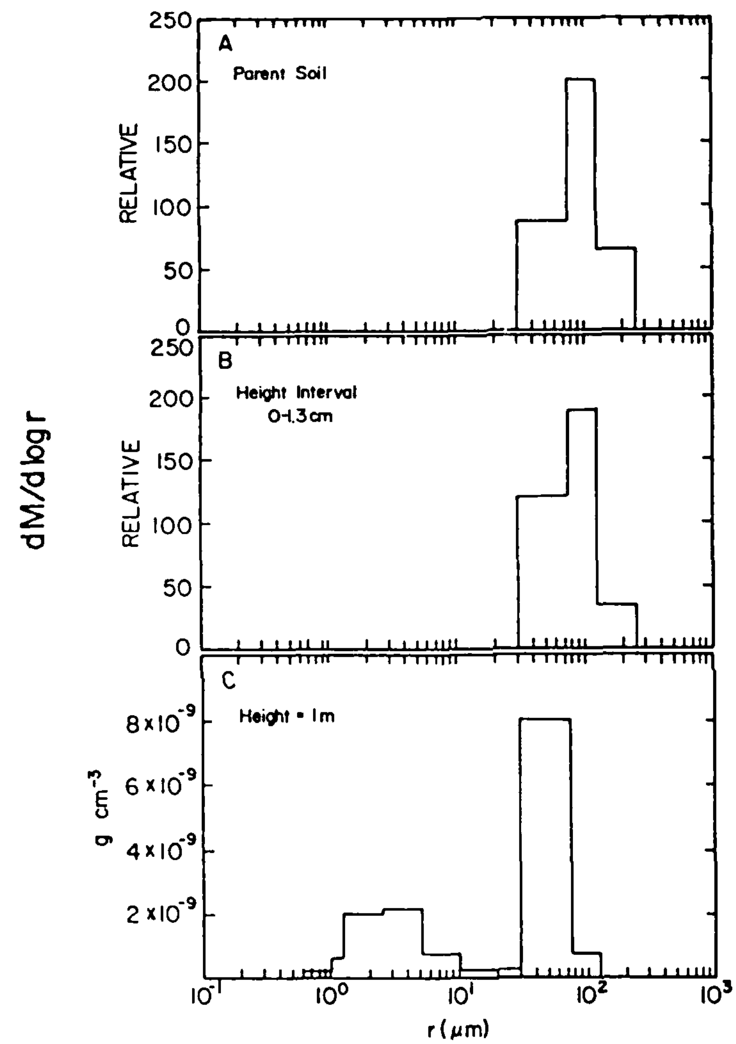

Fig. 1. Size distributions of soil particles eroded from a sandy soil. (*a*) The relative size distributions of dry parent soil determined by sieving. (*b*) The relative size distribution of particles moving at heights of 0–1.3 cm above the ground for different wind speeds. (*c*) The mass size distributions for airborne particles at 1 m above the ground [after *Gillette and Walker,* 1977].

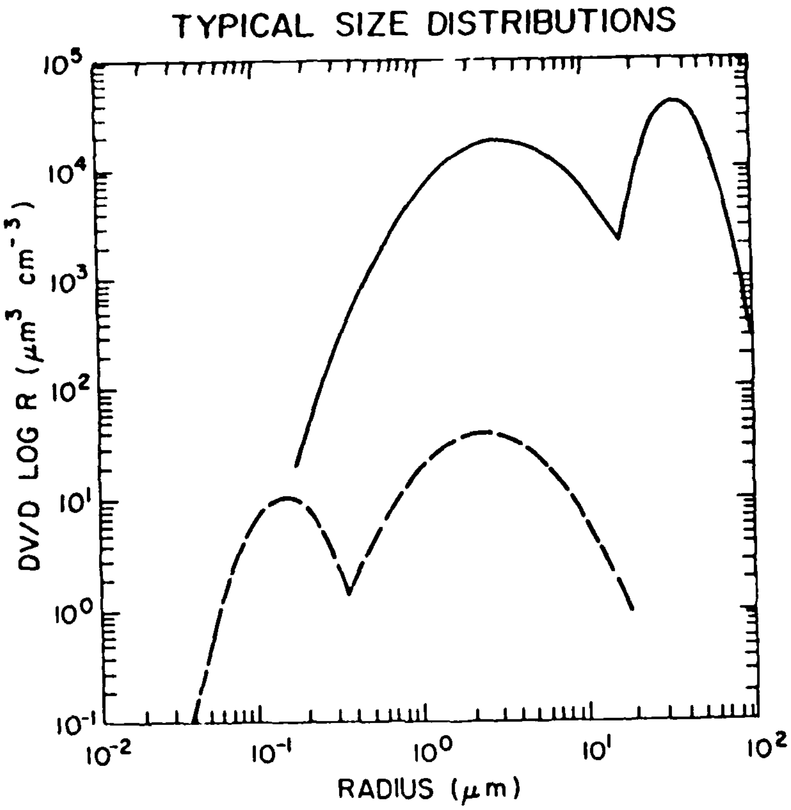

Two size distributions measured in the southwestern United States under conditions of greatly reduced visibility due to locally generated crustal aerosols (——) and under normal conditions with high visibility (---). Two modes are seen in each case: the low visibility case shows a clay particle mode centered around 3 μm and a soil particle mode near 40 μm, the high visibility case shows the clay particle mode with a slightly smaller mean radius and an additional mode centered near 0.1 μm composed of secondary and combustion aerosols. Although the possible presence of a secondary particle mode in the low visibility case is not ruled out, both the total mass and optical effects will be dominated by the crustal aerosol modes.

FIG 2

POSSIBLE QUANTITIES OF INTEREST

σ_A, σ_S, σ_E - ABSORPTION, SCATTERING, EXTINCTION COEFFICIENT

$\tilde{\omega}$ - SINGLE SCATTER ALBEDO

B_A - MASS ABSORPTION COEFFICIENT

N_2 - IMAGINARY COMPONENT OF REFRACTIVE INDEX

RELATIONS

$\omega = \sigma_S/\sigma_E$

$B_A = K/\rho$ - BULK MATERIAL

$B_A = \sigma_A/M_V$ - AEROSOL M_V = MASS CONCENTRATION

$N_2 = \frac{B_A \rho \lambda}{4\pi}$ - BULK MATERIAL

$= \frac{B_A \rho \lambda}{4\pi} \left[\frac{(N_1{}^2 + 2)^2}{9\ N_1} \right]$ - AEROSOL (SMALL PARTICLE LIMIT)

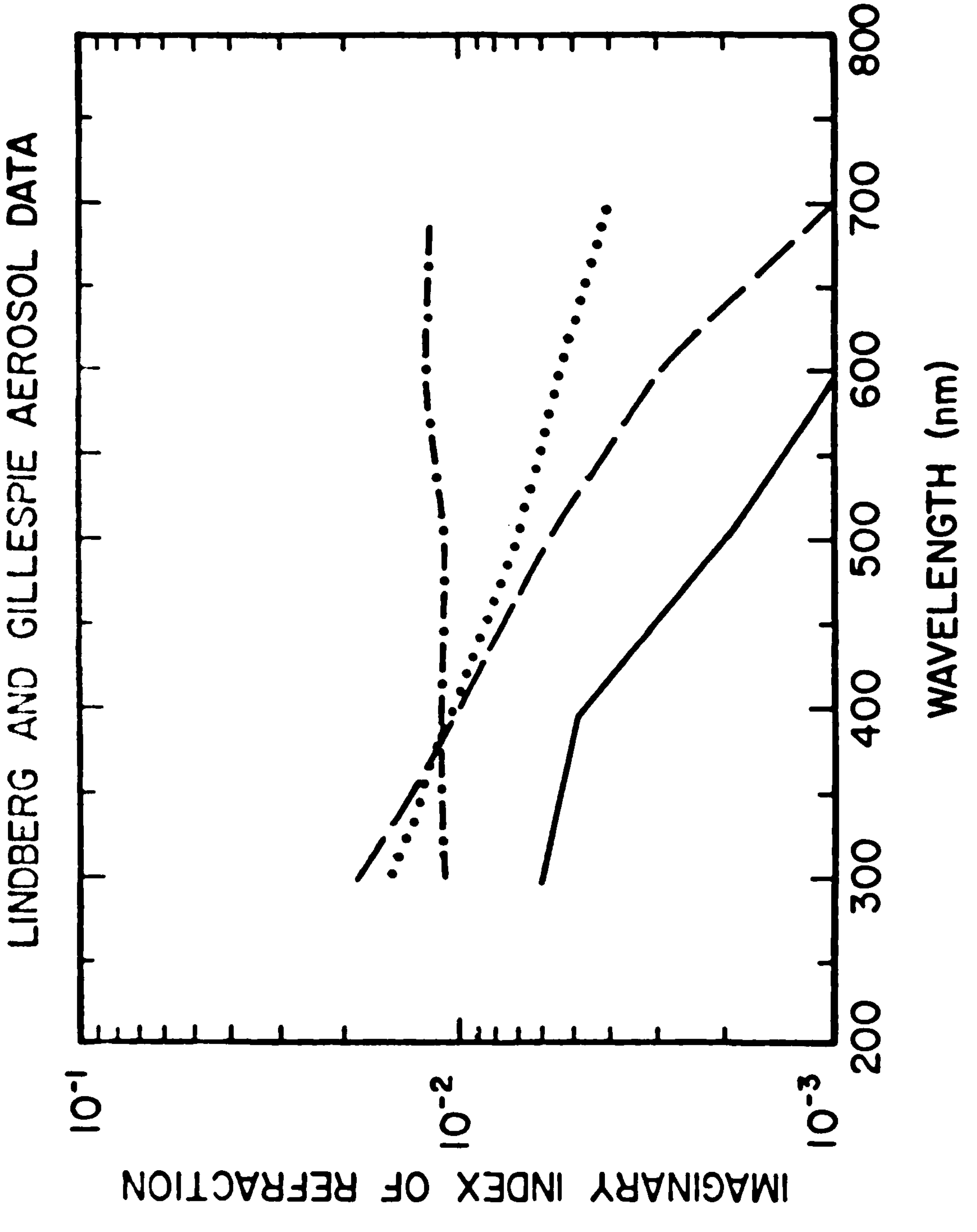

LINDBERG AND GILLESPIE AEROSOL DATA
IMAGINARY INDEX OF REFRACTION
10^-1
10^-2
10^-3
200
300
400
500
600
700
800
WAVELENGTH (nm)

Fig. 4

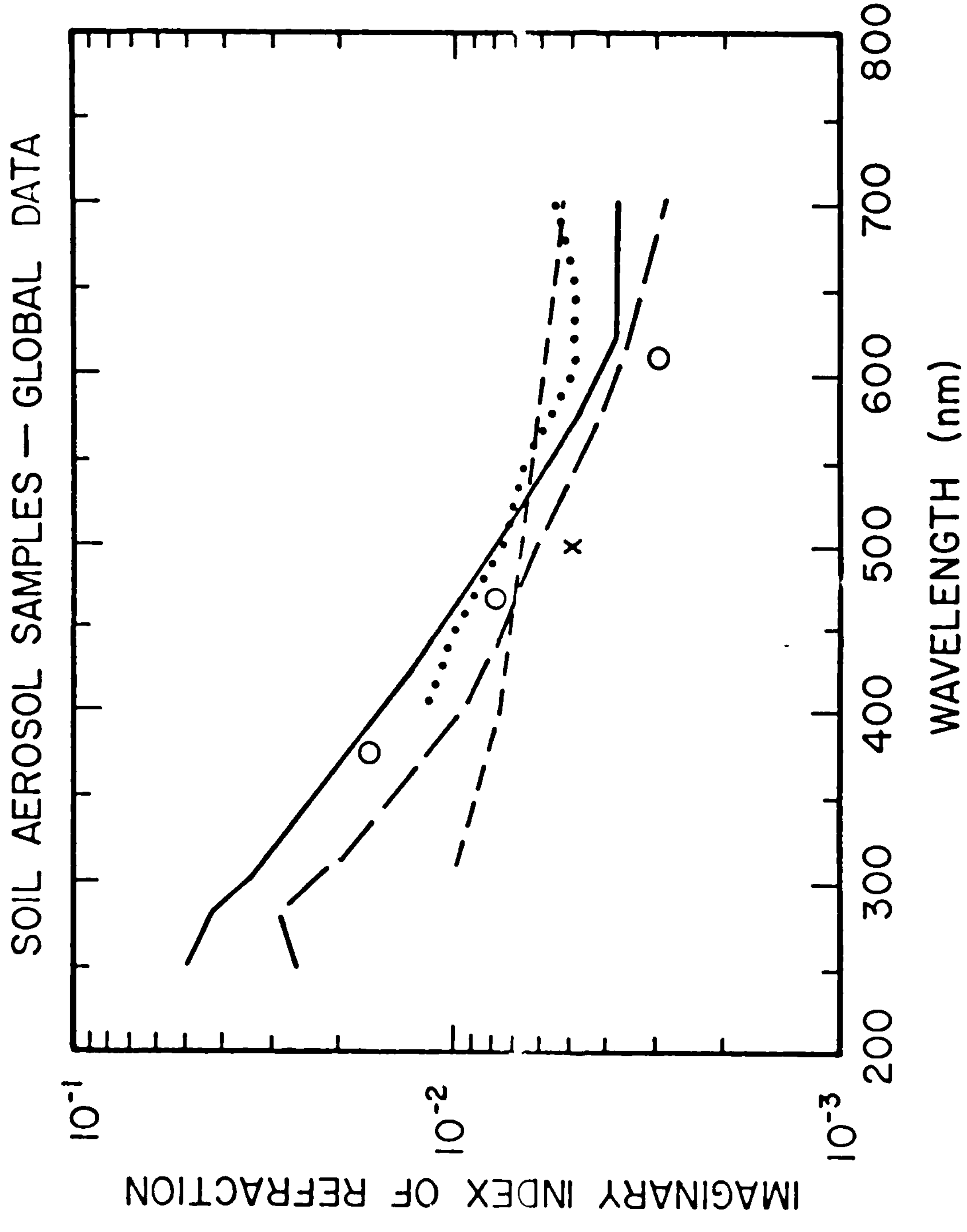

SOIL AEROSOL SAMPLES — GLOBAL DATA
IMAGINARY INDEX OF REFRACTION
10^{-1}
10^{-2}
10^{-3}
200
300
400
500
600
700
800
WAVELENGTH (nm)

Fig. 5

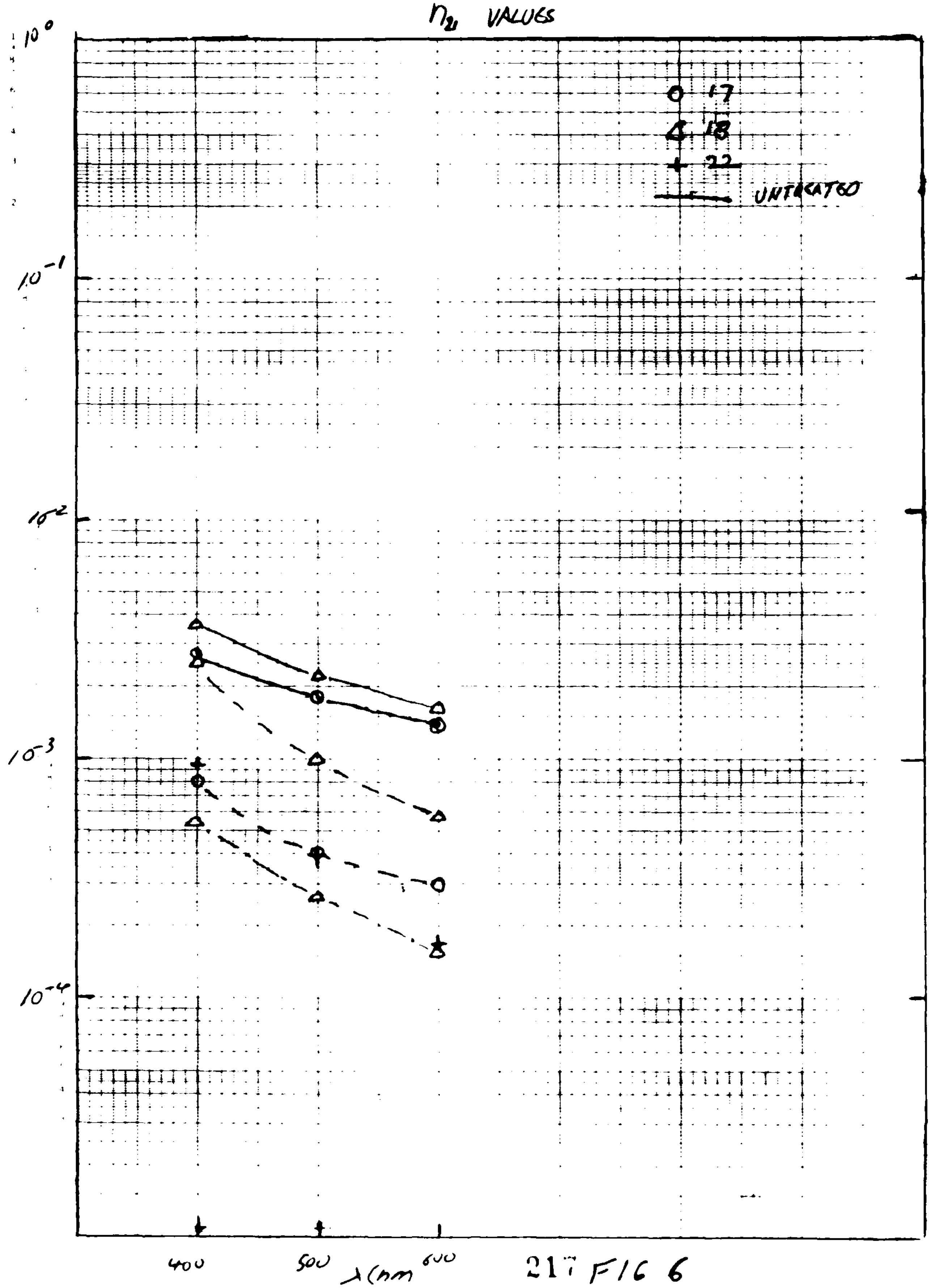

n_{2i} VALUES
10^{0}
10^{-1}
10^{-2}
10^{-3}
10^{-4}
○ 17
△ 18
+ 22
UNTREATED
400
500
600
λ (nm

217 FIG 6

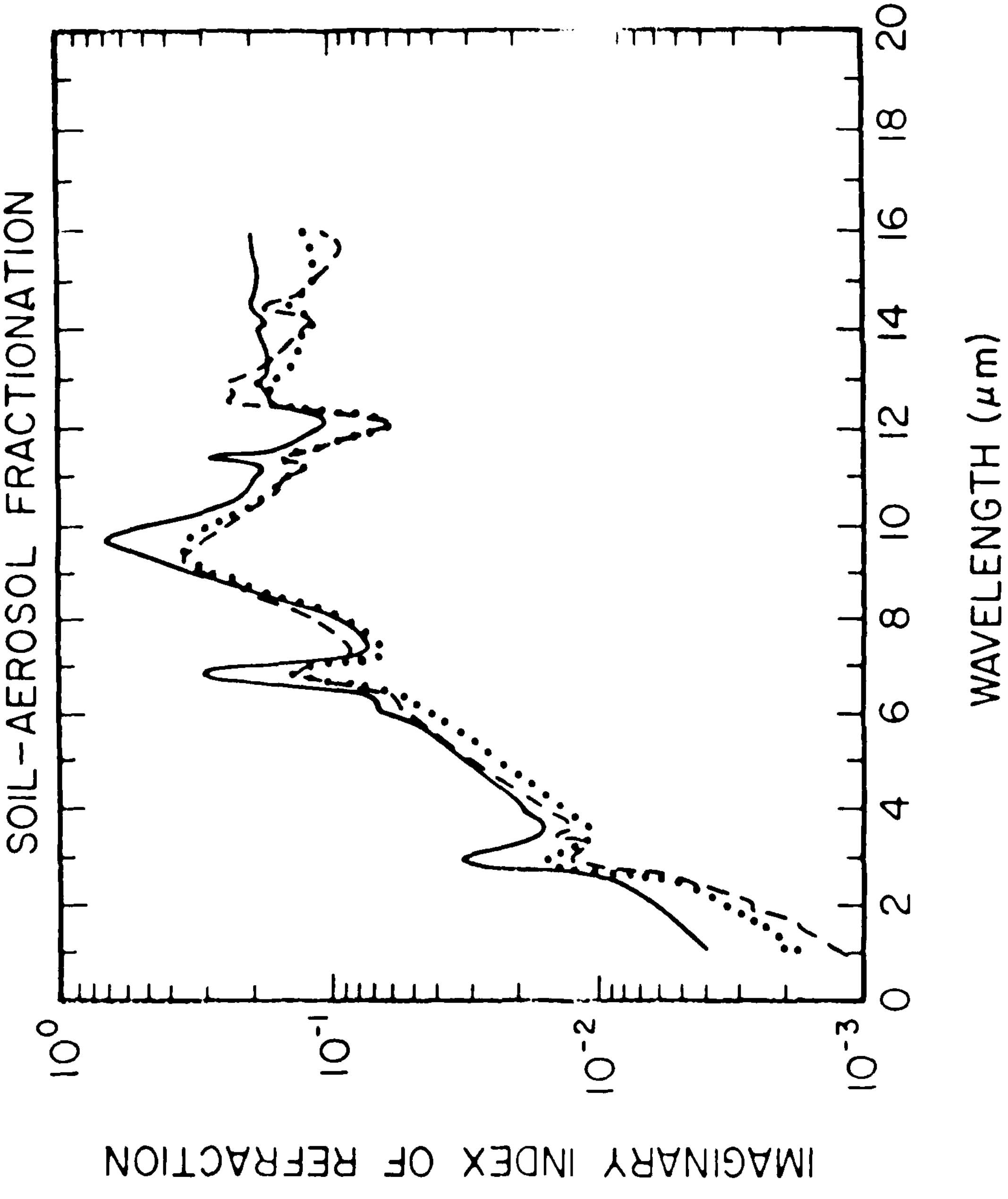
SOIL-AEROSOL FRACTIONATION
IMAGINARY INDEX OF REFRACTION
10^{0}
10^{-1}
10^{-2}
10^{-3}
0
2
4
6
8
10
12
14
16
18
20
WAVELENGTH (μm)

Fig. 7

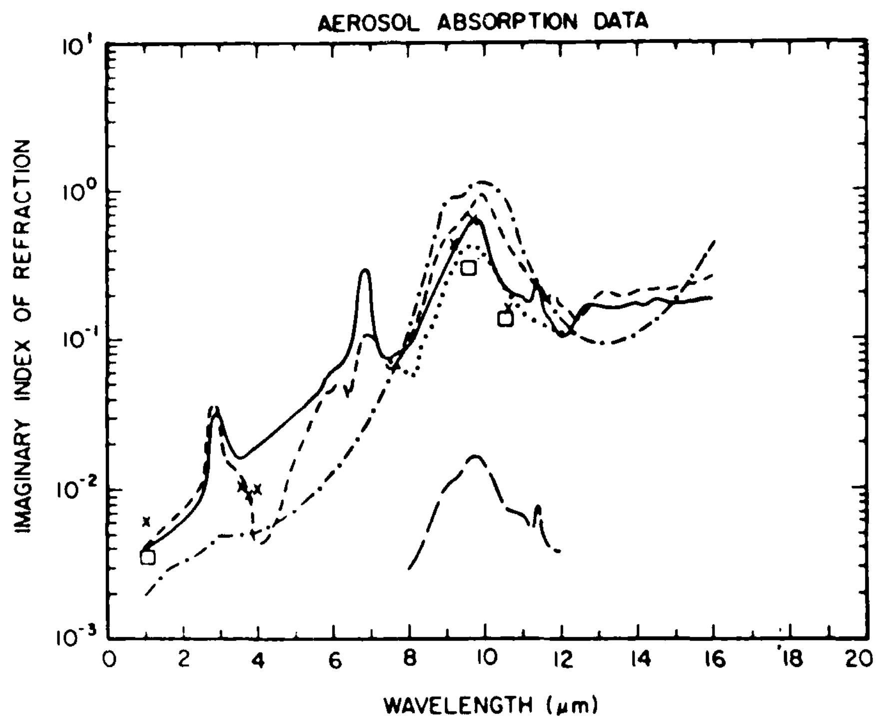

Fig. 9. Infrared $n_{i\lambda}$ measurements for crustal aerosols whose absorption is dominated by clay mineral absorption: data of Patterson (solid line), Lentz and Hoidale (long dashed line), Lindberg (cross), and Schleusner (square) for North American aerosols; data of Fischer (dotted line) for Negev aerosols; data of Volz for Saharan aerosols measured at Barbados (short dashed line); also shown is the basalt data of Pollack from Figure 8. The Lentz and Hoidale data are qualitative; the other data are quantitative

MICRO-ANALYTICAL TECHNIQUES FOR CHARACTERIZING THE OPTICAL PROPERTIES OF SOIL AEROSOLS

John S. Kinsey and Gregory E. Muleski
Midwest Research Institute
and
Raymond M. Coveney
University of Missouri-Kansas City

STUDY OBJECTIVE

To assist in determining the complex refractive indices of soil particles existing as an aerosol by the characterization of mineral composition on a size-specific basis.

EXPERIMENTAL PROCEDURE

- Size - Classification
  - Mechanical Sieving
  - Sonic Sieving
  - Fluidization/Inertial Impaction
  - Optical Microscopy
- Mineral Determination
  - Optical Microscopy
  - X-Ray Diffraction
  - X-Fluorescence (Iron Minerals)
  - Debye-Scherrer Photography

SIZE CLASSIFICATION PROCESS

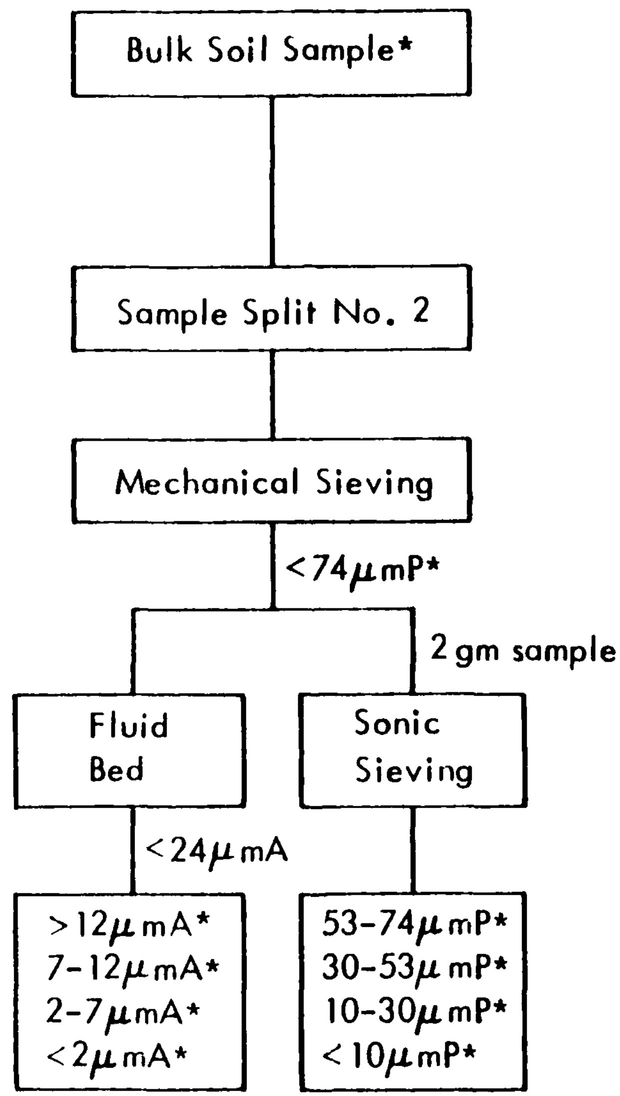

* Analyzed for mineral composition

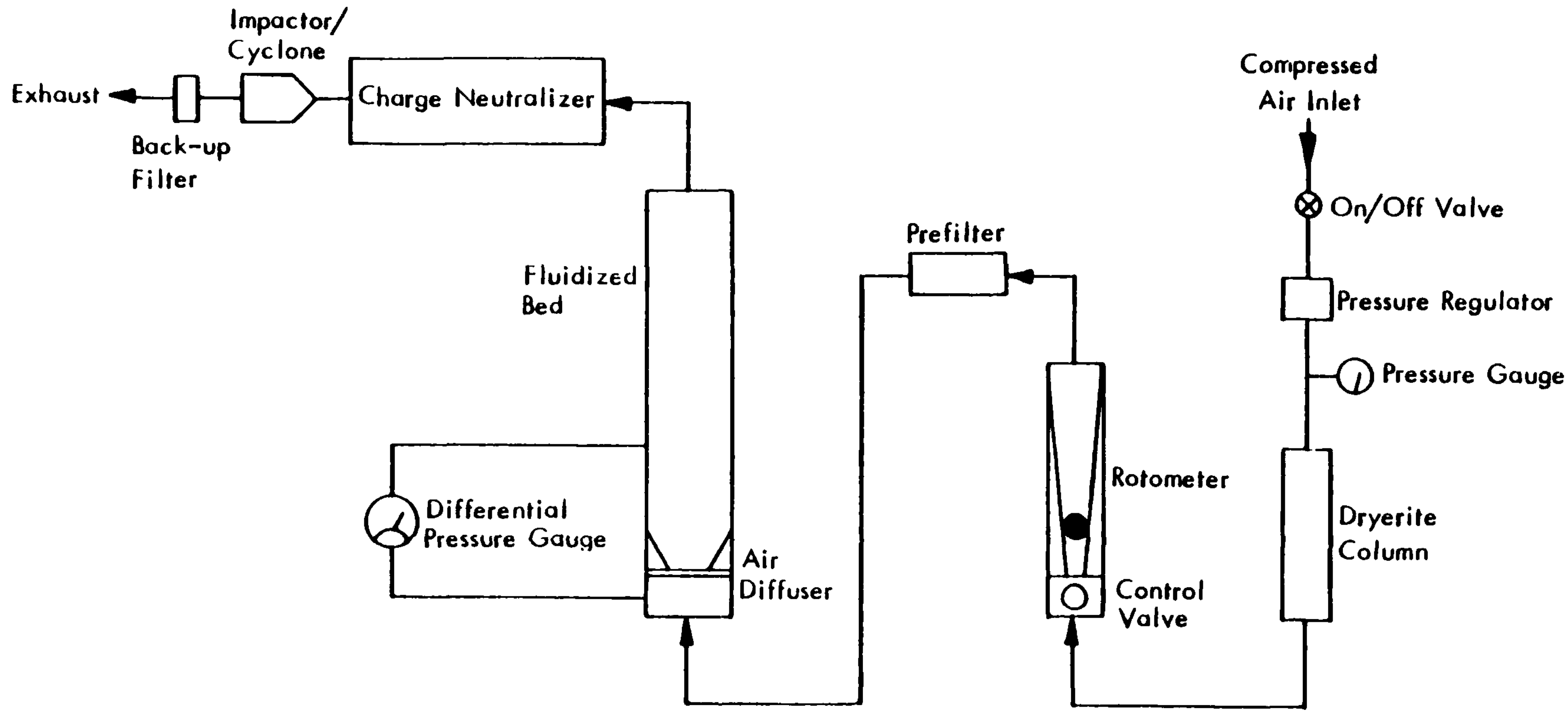

Figure 2 - Flow Diagram for Fluidized Bed Apparatus

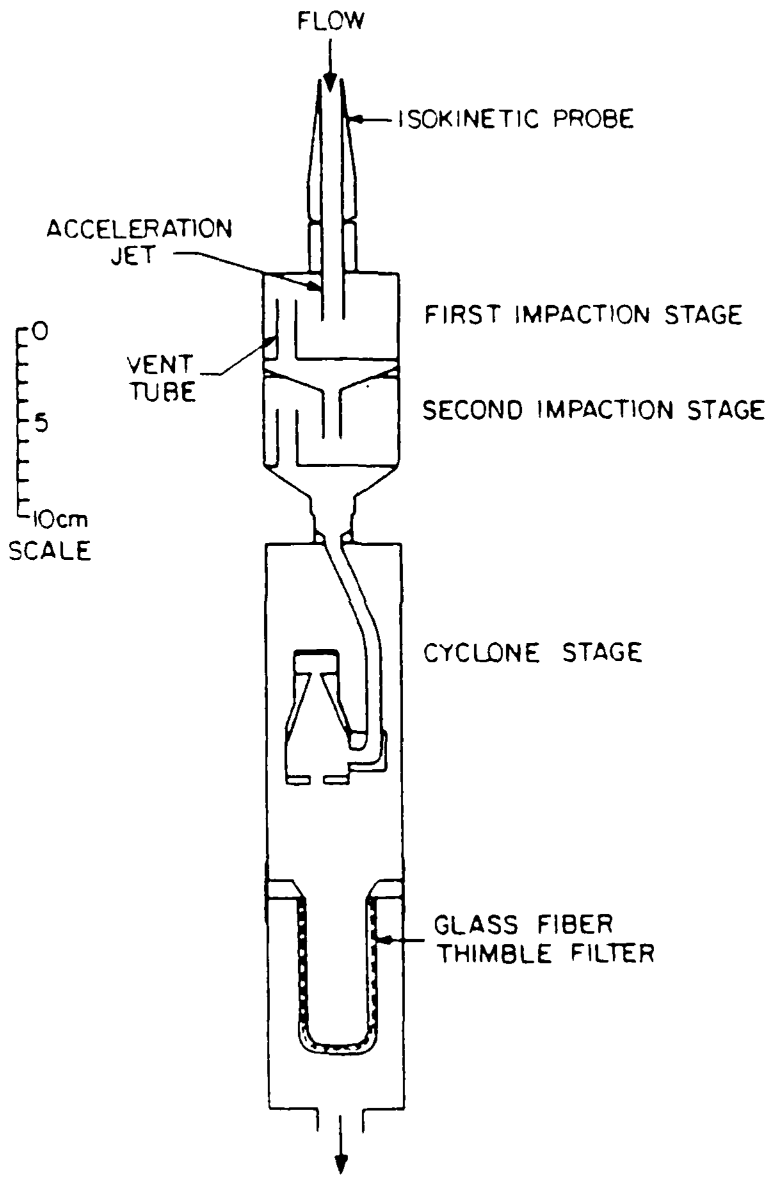

SCHEMATIC OF THE ANDERSEN MODEL HCSS HIGH GRAIN-LOADING IMPACTOR

APPARATUS USED FOR MINERAL CHARACTERIZATION

- Zeiss Petrographic Microscope
- Phillips (Norelco) Diffractometer
- Phillips Four-Position Vacuum Spectrograph
- Debye-Scherrer Camera

RESULTS OF SIEVE ANALYSES

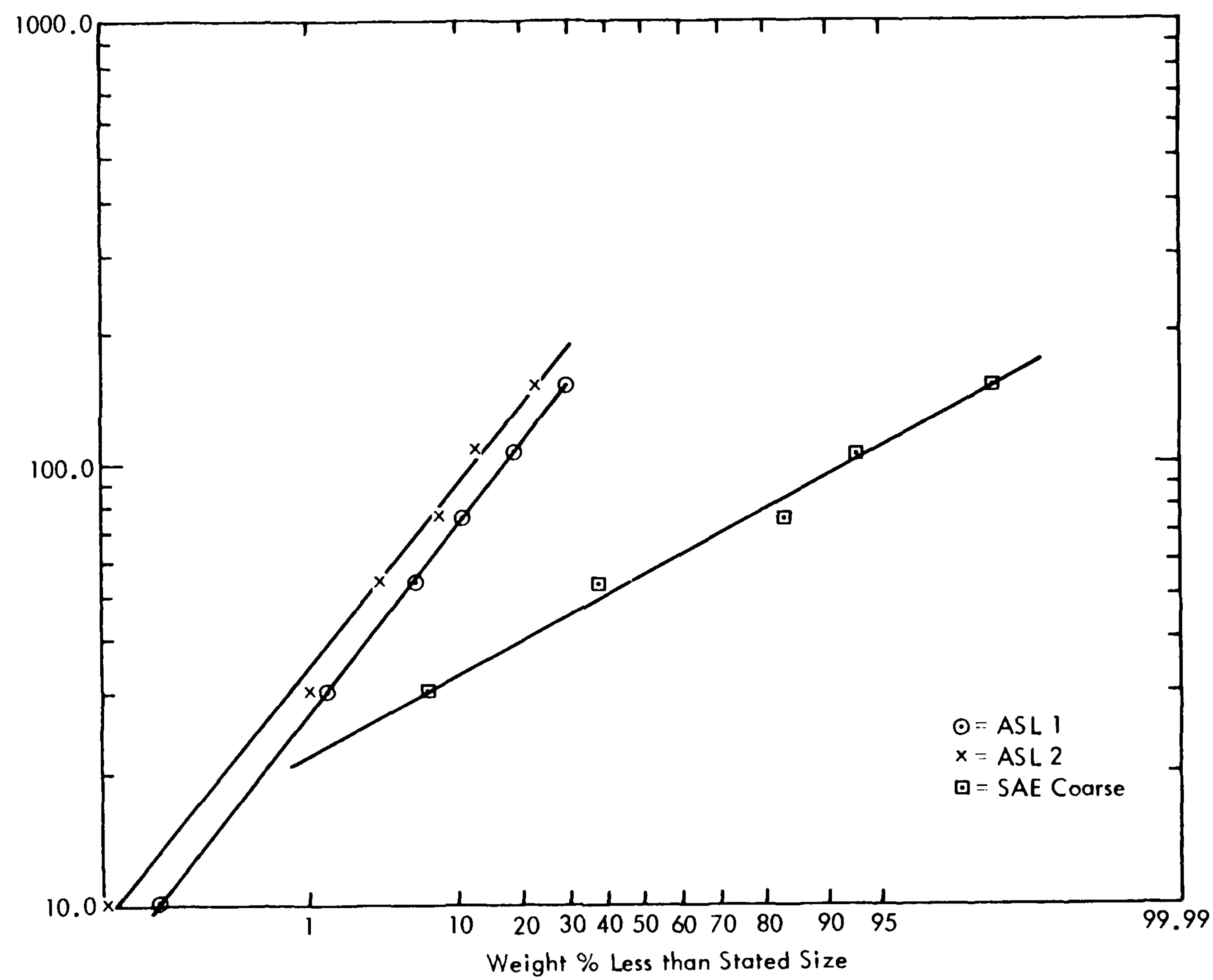

RESULTS OF FLUID BED/IMPACTOR ANALYSES

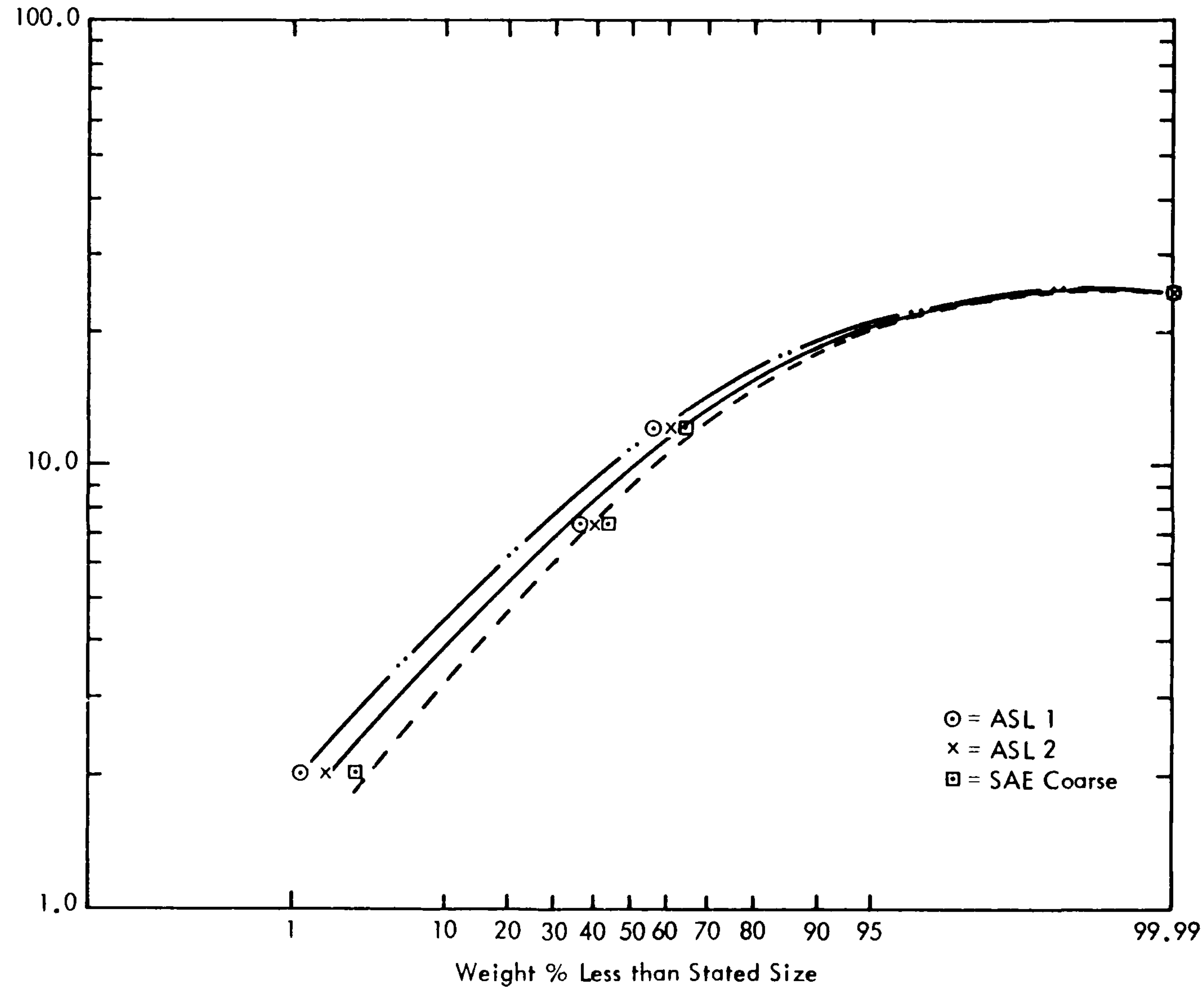

RESULTS OF MINERAL ANALYSES

1. Most samples consist chiefly of sialic minerals such as quartz, microcline, orthoclase, and plagioclase feldspars with lesser quantities of micas, amphiboles, and pyroxenes which is typical of desert soils.

RESULTS OF MINERAL ANALYSES

2. Significant quantities of clay and sericite minerals were found in the smaller particle size ranges with slight increases in the amount of iron oxide minerals (e.g., limonite minerals) in the intermediate size fractions.

RESULTS OF MINERAL ANALYSES

3. A ''coating'' of limonite and phyllosilicate particles was found on other silicate mineral grains in the coarse and intermediate size ranges. This ''coating'' can, and probably will, have an effect on the optical properties of the soil particles existing as an aerosol.

PERCENTAGE OF GRAIN SURFACE COATED BY LIMONITE AND SERICITE-CLAY MIXTURES FOR SOIL SAMPLE NO. 1 (By Visual Estimate)

Size Fraction	Surface % Limonite	Surface % Sericite
Bulk Soil	10-20	30-40
Silt (< 74 μmP)	10-20	20-30
53-74 μmP	10-15	20-30
30-53 μmP	10-15	20-30
10-30 μmP	5-10	30-40
12.3-24 μmA	1-5	10-20
7.3-12.3 μmA	1-5	5-10
2.0-7.3 μmA	1	Nil

RESULTS OF MINERAL ANALYSES

4. The tendency to form "coatings" of clay/sericite minerals was only significant in two out of three cases. The SAE test dust did not exhibit the same tendency to produce agglomerates as was found for the other two samples analyzed.

CONCLUSIONS/RECOMMENDATIONS

1. Size classification by mechanical and sonic sieving was effective for two of the three soil samples analyzed. Aerodynamic techniques, on the other hand, were applicable to all soil types evaluated.

CONCLUSIONS/RECOMMENDATIONS

2. The mineralogy of the two samples submitted for analysis are generally typical of desert soils found in the southwestern United States.

CONCLUSIONS/RECOMMENDATIONS

3. For the two soils analyzed, a "coating" of limonite and phyllosilicate minerals was found on the surface of other mineral grains in the coarse and intermediate particle size ranges. This "coating" could have a significant effect on the optical properties of the soil particles existing as an aerosol. Such was not as prevalent for the SAE test dust.

CONCLUSIONS/RECOMMENDATIONS

4. Because of its importance to the optical properties of the dust aerosol, further investigation should be conducted on the nature of the "coating" of iron oxide minerals found on the larger particles making up soil texture. Appropriate experimentation should be conducted to determine, if possible, how this "coating" is formed, its exact composition, and its overall effect on refractive index.

OVERVIEW OF DNA'S NUCLEAR DUST RE-ANALYSIS PROGRAM

BY

GLEN RAWSON

RDA CONSULTANT

LOW AIR BURST SHOWING TOROIDAL FIREBALL AND DIRT CLOUD FORMING

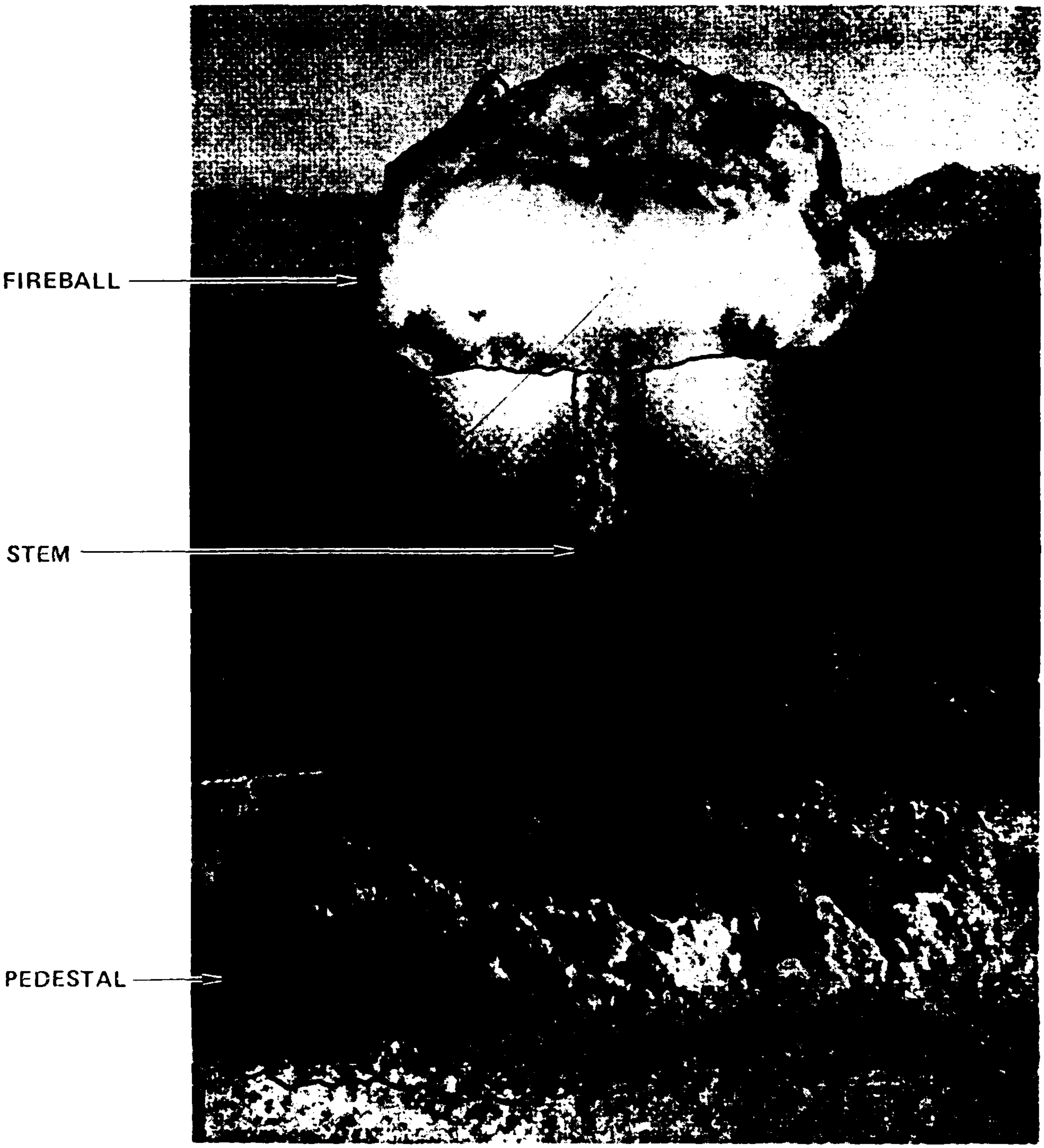

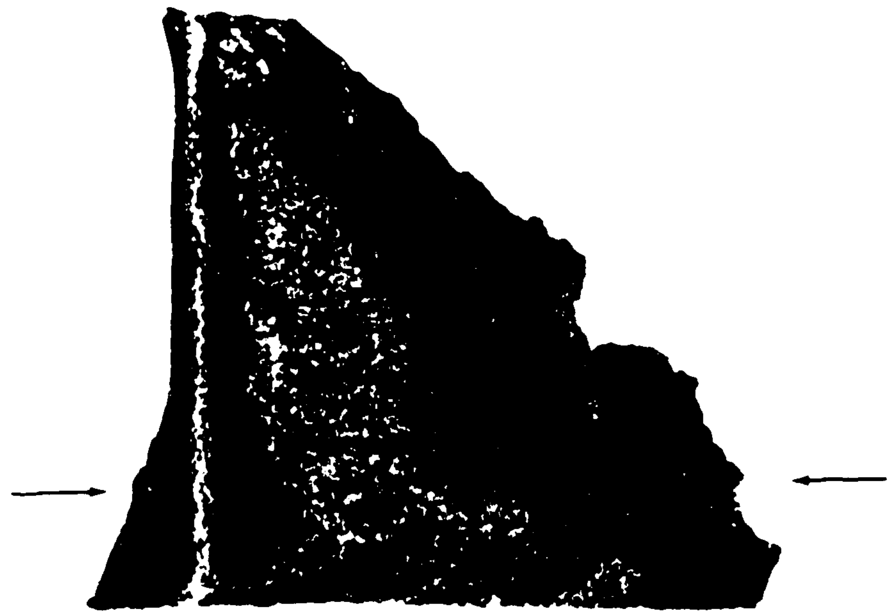

Plane of
thin-section
FIG 1.

Figure 4. Glass Deposit on Stator blade
Mt. St. Helens/C-130 incident
Sample MSH#1

1 INCH

GLASS DEPOSIT ON STATOR BLADE
C-130 ENCOUNTER AT MT. ST. HELENS MAGNIFIED 3.75 x

NORTH-SOUTH PROFILE OF THE ESTIMATED C-130 AIRCRAFT ENCOUNTER NEAR MT. ST. HELENS
(2 HOURS AND 10 MINUTES POST ERUPTION)

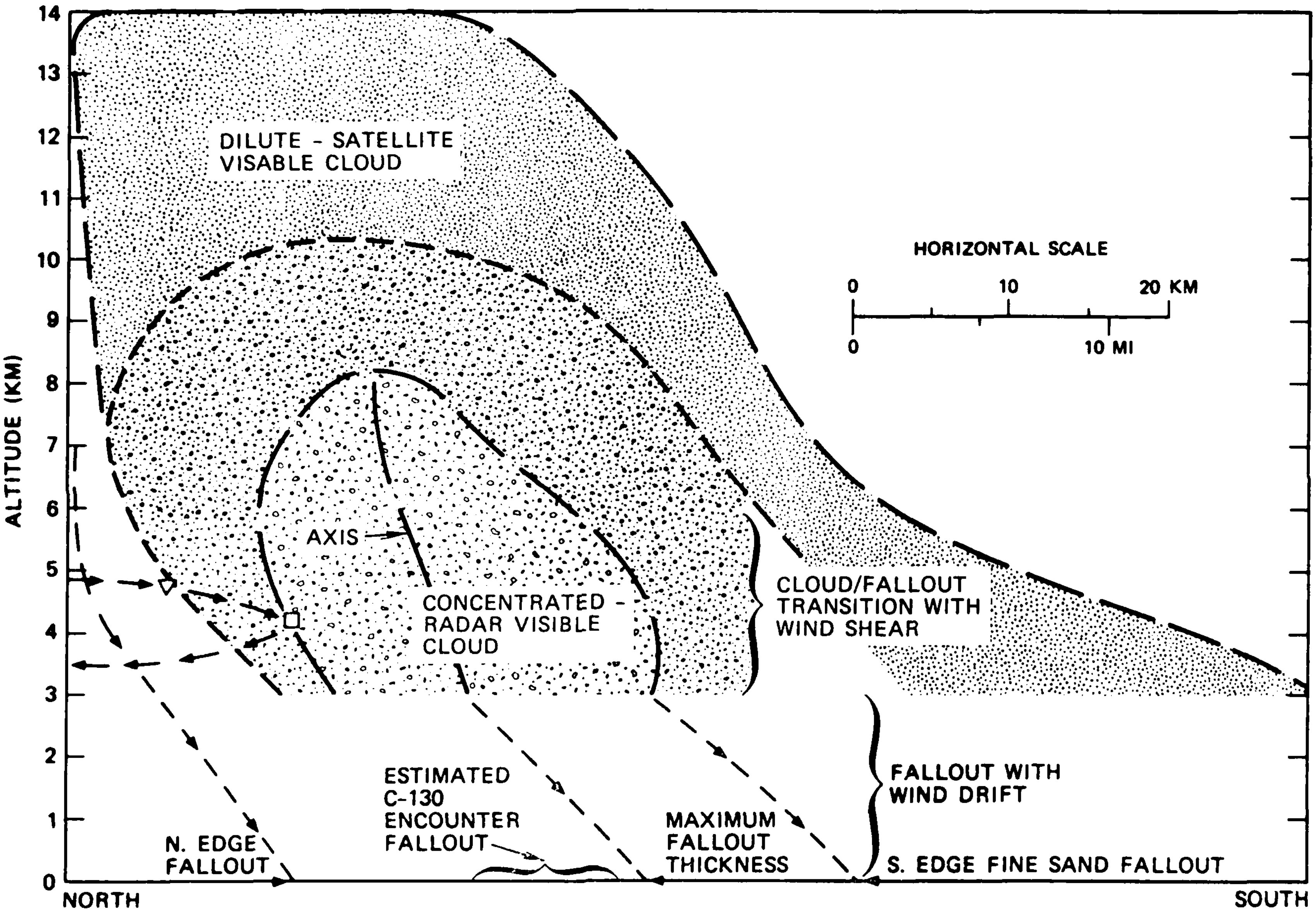

C-130 AIRCRAFT/MT. ST. HELENS ASH CLOUD ENCOUNTER

- RANGE DOWNWIND ~ 57 KM (35 MI)
- TIME - 2 HR AND 10 MIN POST ERUPTION
- ALTITUDE - 4-5 KM - WINDS TO SOUTH
- ALTITUDE MAIN CLOUD 5-14 KM - WINDS TO NW
- 15 MIN CLOUD - INITIAL CONDITIONS*
  - ~ 8000 KM^3 VOLUME
  - ~ 850 KM^2 AREA
  - ~ 4 G/M^3 MASS CONCENTRATION
- 2 HR:10 MIN CLOUD - UPPER BOUND
  - ~ 1000 KM^3 OR AREA OF RADAR DETECTABLE CLOUD
  - ~ 1.3 G/M^3 AT 5 KM ALTITUDE
- 2 HR:10 MIN CLOUD - LOWER BOUND
  - ~ 8600 KM^3 OR 50% AREA OF SATELLITE DETECTABLE CLOUD
  - ~ 0.1 G/M^3
- PARTICLE SIZE MEAN OF ENCOUNTER
  - 200 ± 50 μM

*R. TURCO - RDA 1-D DUST SEDIMENTATION MODEL 12/6/82

KEY CLOUD CHARACTERISTICS

- MASS LOADING
- PARTICLE SIZE DISTRIBUTION
- COMPOSITION & PROPERTIES
  - GLASS TO CRYSTALLINE RATIO
  - HARDNESS & DENSITY
  - RADIOACTIVITY
  - CONDUCTIVITY

PROPERTIES & ESTIMATED AVERAGE WEIGHT PERCENTAGES OF DUST FORMING MINERALS

MINERAL	HARDNESS (MOHS)	FUSION -- °C (DISSOCIATION)	GLOBAL AVG. SEDIMENTS	GENERIC NE DUST CLOUD
QUARTZ & CHERT	7	1713	38	30-40
FELDSPARS & MICAS	2-6	1100-1550	17	10-15
CLAY MINERALS	1-2.5	1000-1400	24	20-25
CALCITE & DOLOMITE	3-4	(800-900)	14	5-10
GYPSUM	2	(~1050)	2	1-2
ACCESSORY MINERALS	1-7	1200-1700	5	2-5
GLASS	~6	~700-1150*	1	10-30

*GLASS-LIQUID TRANSITION

ADDITIONAL WORK NEEDED FOR NUCLEAR CLOUD CHARACTERIZATION

OCTOBER 1982

- CONDUCT MORE DETAILED ANALYSIS OF MASS LOADING DATA BASE
  - COMPARE DATA INTERPRETATION METHODS
  - ADD JOHNNY BOY & FOREIGN TESTS
- IMPROVE ESTIMATES OF GLASS/CRYSTALLINE RATIOS
  - CRATERING AND HOB CALCULATIONS
  - NUCLEAR TEST SAMPLES
- ASSESS GLASSIFICATION POTENTIAL FOR REPRESENTATIVE TARGET SOILS
- EVALUATE HAZARDS OF EXTREME CONDITIONS: WATER SATURATION, FOREST COVER, ETC
- IMPROVE ESTIMATES OF MASS LOADING AND PARTICLE SIZES BY
  - REVIEWING SOIL EROSION DATA & NUCLEAR TEST SAMPLES
- REFINE ESTIMATES OF TRANSPORT DISPERSION & FALLOUT FROM NUCLEAR CLOUDS
  - IMPROVE DISPERSION COEFFICIENTS
  - INCLUDE AGGLOMERATION
  - INCLUDE NONADDITIVE MULT-BURST EFFECTS

MASS LOFTED ESTIMATES

- TYPICALLY AVERAGE ESTIMATES FROM ANALYSES OF CLOUD SAMPLES OBTAINED FROM CLOUD EDGES--AFTER ONE HOUR

- ONLY SMALL BOY AVERAGE IS FROM CLOUD-FALLOUT SAMPLE COUPLETS

- BETA DATA NORMALIZED TO VERY FEW ANALYSES AND TESTS
  --DATA SCATTER HAS LARGE DIFFERENCES IN INVESTIGATOR METHODS---

- GENERALIZED MASS LOFTED RELATIONS DON'T HAVE YIELD SCALING--EXPECTED TO DECREASE WITH INCREASED YIELD AS IS DOCUMENTED FOR SURFACE BURSTS ON WATER

LOFTED MASS FROM NUCLEAR SURFACE BURSTS

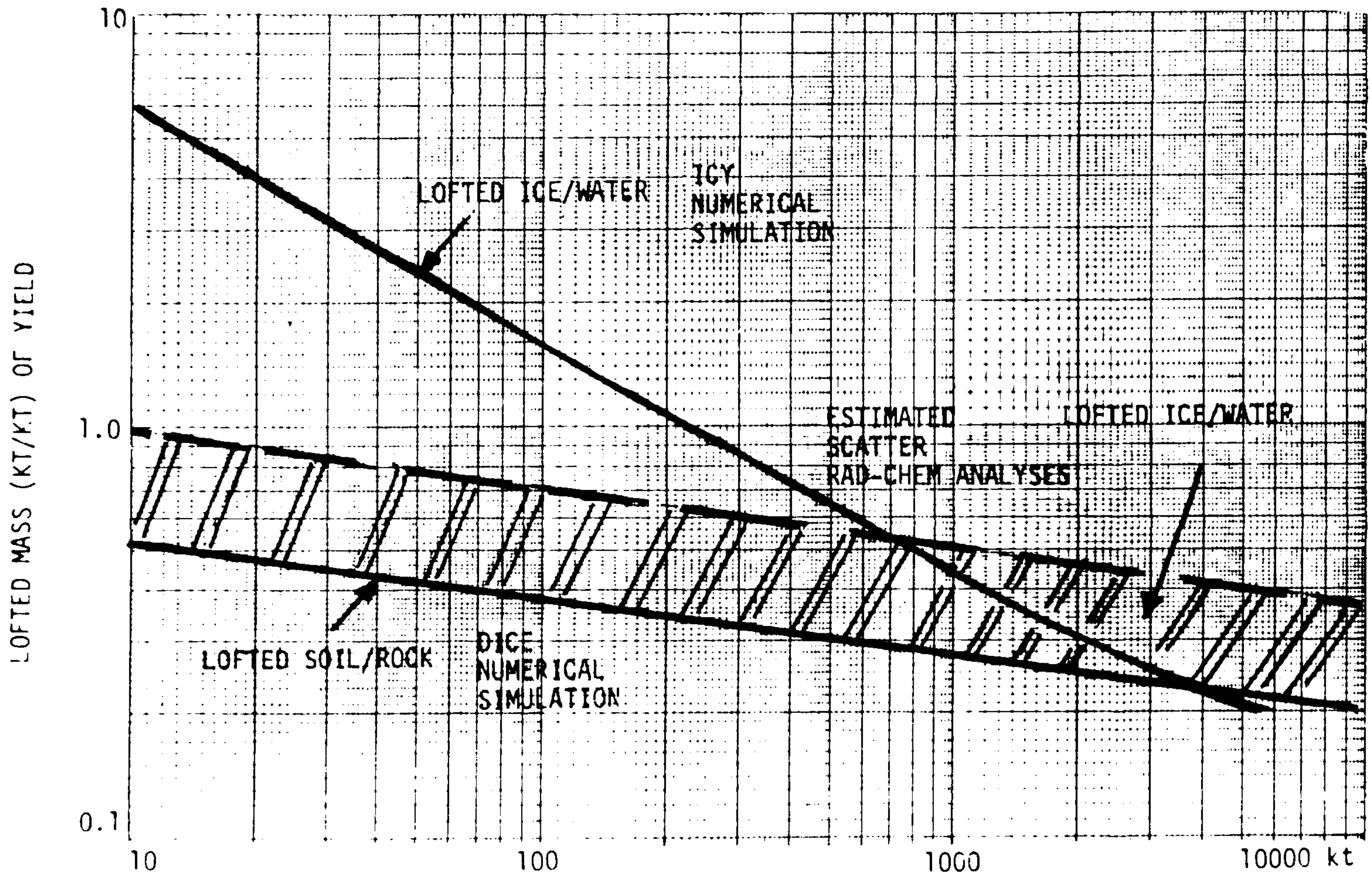

SAMPLES SOUGHT OF U.S. TESTS

NAME	YIELD (KT)	+/- SHOB (FT)	TYPE	DATA (REPORTED)
ANNIE	17	+ 116	TOWER	BETA
NANCY	24	+ 104	TOWER	CLOUD
BADGER	23	+ 102	TOWER	BETA CLOUD
SIMON	43	+ 84	TOWER	BETA CLOUD
ENCORE	27	+ 810	AIR DROP	BETA
HARRY	32	+ 94	TOWER	CLOUD
TURK	43	+ 142	TOWER	CLOUD
PRISCILLA	37	+ 211	BALLOON	BETA
HOOD	74	+ 362	BALLOON	CLOUD
DIABLO	17	+ 195	TOWER	FALLOUT
SHASTA	17	+ 195	TOWER	BETA FALLOUT
SMOKY	44	+ 198	TOWER	CLOUD
SMALL BOY	LOW	+ 8.5	TOWER	FALLOUT CLOUD
JOHNNIE BOY	0.5	- 2.2	PIT	(CLOUD)

BRITISH AND FRENCH SAMPLES IMPORTANT

- MOST OF OUR FALLOUT SAMPLES EITHER:
  - DESTROYED (NRDL)
  - VERY LIMITED LABELING OF REMAINING SAMPLES (UCLA)

- FRENCH--- 1 SURFACE BURST AND 4 TOWER SHOTS OF INTEREST

- BRITISH--- 1 SURFACE BURST AND 8 TOWER SHOTS OF INTEREST

ANALYSES OF SAMPLES

- TRACER AND ACTIVATION METHODOLOGY
- ON FILTER (IN-SITU BUT IMPACTED) PARTICLE SIZE AND SHAPE DISTRIBUTIONS
- DISAGGREGATED PARTICLE SIZE AND SHAPE DISTRIBUTIONS
- DETERMINE GLASS AND CRYSTALLINE FRACTIONS
- CHARACTERIZE MINERALOGICAL AND CHEMICAL COMPOSITIONS
- OTHER POSSIBILITIES--SPECIFIC ACTIVITY AND REFRACTIVE INDICES WITH PARTICLE SIZE; SURFACE AREA OF FINES; ETC.

TRACER AND ACTIVATION METHODOLOGY

- TRACER ELEMENTS ARE SELECTED FOR LOW BACKGROUNDS IN SOIL AND HIGH SENSITIVITY FOR DETECTION BY INSTRUMENTAL NEUTRON ACTIVATION ANALYSIS (INAA). TRACERS ARE EMPLACED IN THE CHARGE AND IN OTHER REGIONS OF INTEREST IN THE TEST BED.
- FOR HISTORIC NUCLEAR TESTS, FISSION PRODUCTS SUCH AS 137 Cs TAKE THE PLACE OF ELEMENTAL TRACERS.
- FILTER COLLECTED CLOUD AND FALLOUT SAMPLES ARE ANALYZED BY INAA FOR TRACERS, OR BY RADIOACTIVITY COUNTING FOR FISSION PRODUCTS. THE FRACTION OF THE CHARGE OR BOMB REPRESENTED BY THE FILTER IS CALCULATED.
- SOIL SAMPLES TO REPRESENT THE TEST SITE ARE ANALYZED BY INAA AND A SET OF REFRACTORY SOIL ELEMENTS IS SELECTED.
- INAA RESULTS FOR THE SOIL ELEMENTS IN THE CLOUD AND FALLOUT ARE USED TO CALCULATE THE DUST LOADING USING THE TEST SITE SOIL RESULTS FOR CALIBRATION.
- THE FILTER DUST LOADING IS DIVIDED BY THE BOMB FRACTION TO OBTAIN THE APPARENT VALUES OF DUST LOFTED PER UNIT OF EXPLOSIVE ENERGY.

TRACER AND ACTIVIATION METHODOLOGY (CONCLUDED)

- EARLY AND LATE TIME CLOUD AND FALLOUT SAMPLE/RESULTS ARE SYSTEMATICALLY COMBINED TO PROVIDE INITIALLY STABILIZED CLOUD VALUES OF LOFTED DUST.
- HAS BEEN TESTED WITH HISTORIC NUCLEAR TESTS AND WITH THE HE TEST-MINOR SCALE.
- MAY WISH TO CONSIDER FOR FIRE STORM SIMULATION EXPERIMENTS.
- A SELECTION OF TRACERS CAN BE DISTRIBUTED IN BURN FUEL IGNITION REGIONS.
- ADDITIONAL TRACERS CAN BE IMBEDDED IN THE AFFECTED ENVIRONMENT--INDUCED BURN REGION, ETC.
- DETAILS CAN BE PREDICTED USING NUMERICAL SIMULATION METHODS AND CHECKED AGAINST A WELL TAGGED EXPERIMENT.

NUCLEAR EXCHANGE TRENDS

- INCREASED ACCURACY
- LOWER YIELDS
- MORE SURFACE BURSTS RELATIVE TO HIGH (FIRE STARTING) AIR BURSTS
- INCREASED TARGET HARDENING
- INCREASED RELIANCE ON GROUND SHOCK (IN CONTRAST TO AIR BLAST) AS A MAJOR KILL RELATED NUCLEAR EFFECT
- EARTH PENETRATING WEAPONS PROBABLE

RESULTS LEAD TO LESS GLOBAL CLIMATIC IMPACTS FROM SMOKE AND AN INCREASED NEED TO UNDERSTAND DUST AND EJECTA EFFECTS. COLLATERAL DAMAGE EFFECTS ARE CHANGED DRAMATICALLY.

DISTRIBUTION LIST

DEPARTMENT OF DEFENSE

ARMED FORCES RADIOBIOLOGY RSCH INST
ATTN: V BOGO

ASSISTANT TO THE SECRETARY OF DEFENSE
ATOMIC ENERGY
ATTN: COL T HAWKINS

DEFENSE INTELLIGENCE AGENCY
ATTN: N BARON
ATTN: RTS-2B

DEFENSE NUCLEAR AGENCY
ATTN: DFRA
ATTN: DFSP G ULLRICH
ATTN: RAAE K SCHWARTZ
ATTN: RAAE L WITTWER
ATTN: RAAE T WALSH
ATTN: RAEE G BAKER
ATTN: RAEE R WEBB
ATTN: SPAS M FRANKEL
ATTN: TDRP D AUTON
ATTN: TDTD/C CORSETTI
4 CYS ATTN: TITL

DEFENSE TECHNICAL INFORMATION CENTER
12 CYS ATTN: DD

NATIONAL DEFENSE UNIVERSITY
ATTN: G FOSTER MOBIL CONCEPTS DEV CTR

OFFICE OF THE SEC OF DEFENSE
ATTN: LTCOL G BETOURNE
ATTN: R RUFFIN

OFFICE OF THE SECRETARY OF DEFENSE
ATTN: COL A RAMSAY

DEPARTMENT OF THE ARMY

NATIONAL WAR COLLEGE
ATTN: COL S GARDINER
ATTN: H ALMOND

U S ARMY ATMOSPHERIC SCIENCES LAB
ATTN: R SUTHERLAND
ATTN: SLCAS-AR-M MR RUBIO

U S ARMY CORPS OF ENGINEERS
ATTN: DAEN-RDM R GOMEZ
ATTN: DR CHOROMOKOS DAEN-RDM

U S ARMY CORPS OF ENGINEERS
ATTN: L ZIEGLER
ATTN: R BECKER

U S ARMY ENGR WATERWAYS EXPER STATION
ATTN: L LINK

U S ARMY MISSILE INTELLIGENCE AGENCY
ATTN: J GAMBLE

U S ARMY NATICK RSCH DEV & ENGRG CENTER
ATTN: H M EL-BISI

U S ARMY STRATEGIC DEFENSE COMMAND
ATTN: DR J LILLY
ATTN: G EDLIN
ATTN: J VEENEMAN
ATTN: M CAPPS
ATTN: R BRADSHAW

DEPARTMENT OF THE NAVY

CNO EXECUTIVE PANEL
ATTN: CAP L BROOKS

NAVAL RESEARCH LABORATORY
ATTN: R JEK

NAVAL SURFACE WEAPONS CENTER
ATTN: K-44 S MASTERS

DEPARTMENT OF THE AIR FORCE

AF/INYXC
ATTN: LTCOL N BARRY

AIR FORCE GEOPHYSICS LABORATORY
ATTN: D CHISHOLM
ATTN: LS/R MURPHY
ATTN: LSI/H GARDINER
ATTN: LYC/R BANTA
ATTN: LYP H S MUENCH

AIR FORCE INSTITUTE OF TECHNOLOGY/EN
ATTN: AFIT/ENP MAJ S R BERGGREN

AIR FORCE OFFICE OF SCIENTIFIC RSCH
ATTN: D BALL

AIR FORCE OPERATIONAL TEST & EVAL CTR
ATTN: MAJ N RODRIGUES

AIR FORCE SPACE DIVISION
ATTN: YNC CAPT K O'BRYAN

AIR FORCE TECHNICAL APPLICATIONS CTR
ATTN: J MARSHALL

AIR FORCE WEAPONS LABORATORY, NTAAB
ATTN: CAPT LEONG
ATTN: J JANNI
ATTN: J W AUBREY, NTED
ATTN: LT LAHTI
ATTN: LTCOL V BLISS

AIR UNIVERSITY
ATTN: LTCOL F REULE

AIR WEATHER SERVICE, MAC
ATTN: MAJ J SCHLEHER

BALLISTIC MISSILE OFFICE/DAA
ATTN: LT ROTHCHILD
ATTN: MYSP/CAP TOMASZEWSKI

DEPUTY CHIEF OF STAFF/XOX
ATTN: AFXOX

STRATEGIC AIR COMMAND
ATTN: CAP CONNERY

STRATEGIC AIR COMMAND/XPXF
ATTN: T BAZZOLI

DEPARTMENT OF ENERGY

ARGONNE NATIONAL LABORATORY
ATTN: H DRUCKER
ATTN: M WESLEY
ATTN: P BECKERMAN

BROOKHAVEN NATIONAL LABORATORY
ATTN: B MANOWITZ
ATTN: E WEINSTOCK

DEPARTMENT OF ENERGY
ATTN: I NEDDOW
ATTN: T HARRIS

DESERT RESEARCH INSTITUTE
ATTN: J HALLETT
ATTN: J HUDSON

LAWRENCE BERKELEY NATIONAL LAB
ATTN: H ROSEN

UNIVERSITY OF CALIFORNIA
LAWRENCE LIVERMORE NATIONAL LAB
ATTN: C R MOLENKAMP
ATTN: C SHAPIRO
ATTN: F LUTHER
ATTN: G BING
ATTN: G SIMONSON
ATTN: J PENNER
ATTN: J POTTER
ATTN: L-10 A GROSSMAN
ATTN: L-262 A BROYLES
ATTN: L-262 J KNOX
ATTN: L-453 L ANSPAUGH
ATTN: M MACCRACKEN
ATTN: R MALONE
ATTN: R PERRET
ATTN: S GHAN

LOS ALAMOS NATIONAL LABORATORY
ATTN: D SAPPENFIELD
ATTN: E J CHAPYAK
ATTN: E JONES
ATTN: E SYMBALISTY
ATTN: G GLATZMAIER
ATTN: G M SMITH
ATTN: L H AUER
ATTN: L CLOUTMAN
ATTN: P HUGES
ATTN: T YAMATTA

OAK RIDGE NATIONAL LABORATORY
ATTN: D FIELDS

SANDIA NATIONAL LABORATORIES
ATTN: A L JOHNSON
ATTN: B ZAK
ATTN: D DAHLGREN
ATTN: D FORDHAM
ATTN: D WILLIAMS
ATTN: K D BERGERON
ATTN: L TROST
ATTN: M D BENNETT
ATTN: R C BACKSTROM

OTHER GOVERNMENT

CENTRAL INTELLIGENCE AGENCY
ATTN: A WARSHAWSKY
ATTN: R NELSON

DEPARTMENT OF AGRICULTURE
ATTN: D HAINES

DEPARTMENT OF TRANSPORTATION
ATTN: COL M ROESCH

ENVIRONMENTAL PROTECTION AGENCY
ATTN: R COTHERN
ATTN: W E FALLON

FEDERAL EMERGENCY MANAGEMENT AGENCY
ATTN: B W BLANCHARD
ATTN: D BENSON NP-CP-MR
ATTN: D KYBAL
ATTN: J POWERS
ATTN: J RUMBARGER
ATTN: S ALTMAN

GENERAL ACCOUNTING OFFICE
ATTN: A PIERCE
ATTN: P J BOLLEA
ATTN: V BIELECKI

NASA
ATTN: N CRAYBILL
ATTN: W R COFER

NASA
ATTN: R HABERLE
ATTN: O TOON
ATTN: R YOUNG
ATTN: T ACKERMAN

NATIONAL BUREAU OF STANDARDS
ATTN: G MULHOLLAND
ATTN: R LEVINE
ATTN: R REHM
ATTN: R SCHRACK

NATIONAL BUREAU OF STANDARDS
ATTN: H BAUM

NATIONAL CENTER ATMOSPHERIC RESEARCH
ATTN: J KIEHL
ATTN: S SCHNEIDER
ATTN: S THOMPSON
ATTN: V RAMASWAMY

NATIONAL CLIMATE PROGRAM OFFICE
ATTN: A HECHT
ATTN: M YERG

NATIONAL OCEANIC & ATMOSPHERIC ADMIN
ATTN: F FEHSENFELD
ATTN: J DELUISI
ATTN: R DICKINSON
ATTN: R PUESCHEL
ATTN: V DERR

NATIONAL OCEANIC & ATMOSPHERIC ADMIN
ATTN: B HICKS

NATIONAL RESEARCH COUNCIL
ATTN: K BEHR
ATTN: R DEFRIES

NATIONAL SCIENCE FOUNDATION
ATTN: B BEASLEY
ATTN: E BIERLY
ATTN: H VIRJI
ATTN: L HAMATY
ATTN: R SINCLAIR
ATTN: R TAYLOR
ATTN: S KEENY

NUCLEAR REGULATORY COMMISSION
ATTN: R ALEXANDER

OFFICE OF SCIENCE AND TECH POLICY
ATTN: B HEALY
ATTN: COL S WYMAN

OFFICE OF TECHNOLOGY ASSESSMENT
ATTN: R WILLIAMSON

U S ARMS CONTROL & DISARMAMENT AGCY
ATTN: B DOENGES NWC-DPA
ATTN: CDR P JAMISON
ATTN: COL H HERTEL
ATTN: G PITMAN
ATTN: H SCHAEFFER
ATTN: LTCOL S LAWRENCE
ATTN: R GODESKY
ATTN: R HOWES
ATTN: R O'CONNELL NWC-DPA

U S DEPARTMENT OF STATE
ATTN: A CORTE
ATTN: C CLEMENT
ATTN: COL M SEATON
ATTN: S CLEARY
ATTN: T VREBALOVICH

U S GEOLOGICAL SURVEY
ATTN: R DECKER

U S GEOLOGICAL SURVEY
ATTN: E SHOEMAKER

U S HOUSE OF REPRESENTATIVES
ATTN: C BAYER
ATTN: COMMITT ON SCI & TECH J DUGAN

U S HOUSE OF REPRESENTATIVES
ATTN: J FREIWALD
ATTN: M HERBST

US DEPARTMENT AGRICULTURE
ATTN: D WARD

DEPARTMENT OF DEFENSE CONTRACTORS

AERO-CHEN RESEARCH LABS, INC
ATTN: D B OLSON

AERODYNE RESEARCH, INC
ATTN: C KOLB
ATTN: J LURIE

AEROJET ELECTRO-SYSTEMS CO
ATTN: A FYMAT
ATTN: S HAMILTON
ATTN: R PAN

AEROSPACE CORP
ATTN: C RICE
ATTN: L R MARTIN

AEROSPACE CORPORATION
ATTN: G LIGHT

ALLEN RESEARCH CORP
ATTN: R ALLEN

AMERICAN ASSN ADVANCEMENT OF SCIENCE
ATTN: D M BURNS

ANALYTIC SERVICES, INC (ANSER)
ATTN: R BROFFT
ATTN: R ELLINGSON

APPLIED RESEARCH CORP
ATTN: A ENDAL

ASSN. DIST. AMERICAN SCIENTISTS
ATTN: J HUBBARD

AT&T DEFENSIVE SYSTEMS STUDIES
ATTN: R JANOW

ATMOSPHERIC AND ENVIRONMENTAL RES
ATTN: N SZE

AUDIO INTELLIGENCE DEVICES INC
ATTN: H BAUM

AVCO SYSTEMS DIVISION
ATTN: G GRANT

BALL AEROSPACE SYSTEMS DIVISION
ATTN: B CUMMINGS
ATTN: C BRADFORD

BDM CORP
ATTN: D SHAEFFER
ATTN: E L COFFEY
ATTN: J LEECH

BERKELEY RSCH ASSOCIATES, INC
ATTN: S BRECHT

BOEING AEROSPACE COMPANY
ATTN: N GERONTAKIS

BOEING TECHNICAL & MANAGEMENT SVCS, INC
ATTN: G HALL

C L CONSULTING SERVICES
ATTN: F FEER

CALIFORNIA RESEARCH & TECHNOLOGY, INC
ATTN: M ROSENBLATT
ATTN: R GAJ
ATTN: S KRUEGER

CALSPAN CORP
ATTN: R MAMBRETTI
ATTN: R MISSERT

CARNEGIE CORPORATION OF NEW YORK
ATTN: D ARSENIAN

CASSIDY AND ASSOCIATES
ATTN: J JACOBSON

CHARLES STARK DRAPER LAB, INC
ATTN: A TETEWSKI

COLORADO STATE UNIVERSITY
ATTN: D KRUEGER
ATTN: W COTTON

COMPUTER SCIENCES CORP
ATTN: G CABLE

DARTSIDE CONSULTING
ATTN: A FORESTER

DELTA RESEARCH
ATTN: L WEINER
ATTN: M RADKE

DYNAMICS TECHNOLOGY, INC
ATTN: D HOVE

ENW INTERNATIONAL, LTD
ATTN: J CANE

EOS TECHNOLOGIES, INC
ATTN: B GABBARD
ATTN: N JENSEN
ATTN: W LELEVIER

FACTORY MUTUAL RESEARCH CORP
ATTN: M A DELICHATSIOS

FEDERATION OF AMERICAN SCIENTISTS
ATTN: J STONE

GENERAL ELECTRIC CO
ATTN: R E SCHMIDT

GENERAL ELECTRIC CO
ATTN: H ROBSON

GENERAL RESEARCH CORP
ATTN: B BENNETT
ATTN: J BALTES

HAROLD ROSENBAUM ASSOCIATES, INC
ATTN: G WEBER

HORIZONS TECHNOLOGY INC
ATTN: A EDWARDS
ATTN: J A MANGO
ATTN: J AMBROSE

HORIZONS TECHNOLOGY, INC
ATTN: R W LOWEN
ATTN: W T KREISS

HUGHES AIRCRAFT
ATTN: E DIVITA

INFORMATION SCIENCE, INC
ATTN: W DUDZIAK

INSTITUTE FOR DEFENSE ANALYSES
ATTN: C CHANDLER
ATTN: E BAUER
ATTN: F ALBINI

JOHNS HOPKINS UNIVERSITY
ATTN: M LENEVSKY
ATTN: R FRISTROM
ATTN: W BERL

KAMAN SCIENCES CORP
ATTN: J RUSH
ATTN: J SCRUGGS

KAMAN SCIENCES CORP
ATTN: P GRIFFIN
ATTN: P TRACY

KAMAN TEMPO
ATTN: B GAMBILL
ATTN: D FOXWELL
ATTN: DASIAC
ATTN: E MARTIN
ATTN: R RUTHERFORD
ATTN: R YOUNG
ATTN: S FIFER
ATTN: W KNAPP

KAMAN TEMPO
ATTN: D ANDERSON
ATTN: DASIAC

LOCKHEED MISSILES & SPACE CO, INC
ATTN: ATTN J HENLEY
ATTN: J GLADIS
ATTN: J PEREZ

LOCKHEED MISSILES & SPACE CO, INC
ATTN: P DOLAN
ATTN: W MORAN

M I T LINCOLN LAB
ATTN: S WEINER

MARTIN MARIETTA DENVER AEROSPACE
ATTN: D HAMPTON

MAXIM TECHNOLOGIES, INC
ATTN: J MARSHALL

MCDONNELL DOUGLAS CORP
ATTN: R C ANDREWS
ATTN: T CRANOR
ATTN: T TRANER

MCDONNELL DOUGLAS CORP
ATTN: A MONA
ATTN: F SAGE
ATTN: G BATUREVICH
ATTN: J GROSSMAN
ATTN: R HALPRIN
ATTN: S JAEGER
ATTN: W YUCKER

MERIDIAN CORP
ATTN: E DANIELS
ATTN: F BAITMAN

MIDWEST RESEARCH INSTITUTE
ATTN: J S KINSEY

MISSION RESEARCH CORP
ATTN: R ARMSTRONG

MISSION RESEARCH CORP
ATTN: C LONGMIRE
ATTN: D ARCHER
ATTN: D KNEPP
ATTN: D SOWLE
ATTN: F FAJEN
ATTN: K R COSNER
ATTN: M SCHEIBE
ATTN: R BIGONI
ATTN: R CHRISTIAN
ATTN: R GOLDFLAM
ATTN: R HENDRICK
ATTN: T OLD
ATTN: W WHITE

MITRE CORPORATION
ATTN: J SAWYER

MRJ INC
ATTN: D FREIWALD

NATIONAL ADVISORY COMMITTEE
ATTN: J ALMAZAN
ATTN: J BISHOP

NATIONAL INST FOR PUBLIC POLICY
ATTN: K PAYNE

NICHOLS RESEARCH CORP, INC
ATTN: H SMITH
ATTN: J SMITH
ATTN: M FRASER
ATTN: R BYRN

NORTHROP SERVICES INC
ATTN: T OVERTON

ORLANDO TECHNOLOGY INC
ATTN: R SZCZEPANSKI

PACIFIC-SIERRA RESEARCH CORP
ATTN: G ANNO
ATTN: H BRODE, CHAIRMAN SAGE
ATTN: M DORE
ATTN: R SMALL

PALOMAR CORP
ATTN: B GARRETT
ATTN: C FELDBAUM

PHOTOMETRICS, INC
ATTN: I L KOFSKY

PHOTON RESEARCH ASSOCIATES
ATTN: J MYER

PHYSICAL RESEARCH CORP
ATTN: A CECERE

PHYSICAL RESEARCH INC
ATTN: H FITZ

PHYSICAL RESEARCH INC
ATTN: D MATUSKA

PHYSICAL RESEARCH INC
ATTN: A WARSHAWSKY
ATTN: J WANG
ATTN: W SHIH

PHYSICAL RESEARCH INC
ATTN: R JORDANO

PHYSICAL RESEARCH, INC
ATTN: D WESTPHAL
ATTN: D WHITENER
ATTN: H WHEELER
ATTN: R BUFF
ATTN: R DELIBERIS
ATTN: T STEPHENS
ATTN: W C BLACKWELL

PHYSICAL RESEARCH, INC
ATTN: G HARNEY
ATTN: J DEVORE
ATTN: J THOMPSON
ATTN: R STOECKLY
ATTN: W SCHLEUTER

PHYSICAL RESEARCH, INC
ATTN: H SUGIUCHI

POLYTECHNIC OF NEW YORK
ATTN: B J BULKIN
ATTN: G TESORO

PRINCETON UNIVERSITY
ATTN: J MAHLMAN

QUADRI CORP
ATTN: H BURNSWORTH

R & D ASSOCIATES
ATTN: A KUHL
ATTN: F GILMORE
ATTN: G JONES
ATTN: J SANBORN
ATTN: R TURCO

R & D ASSOCIATES
ATTN: B YOON

R J EDWARDS INC
ATTN: R SEITZ

RADIATION RESEARCH ASSOCIATES, INC
ATTN: B CAMPBELL
ATTN: M WELLS

RAND CORP
ATTN: G L DONOHUE
ATTN: P ROMERO

RAND CORP
ATTN: J GERTLER

ROCKWELL INTERNATIONAL CORP
ATTN: S I MARCUS

ROCKWELL INTERNATIONAL CORP
ATTN: J KELLEY

S-CUBED
ATTN: B FREEMAN
ATTN: K D PYATT, JR
ATTN: R LAFRENZ

S-CUBED
ATTN: C NEEDHAM
ATTN: S HIKIDA
ATTN: T CARNEY

SCIENCE APPLICATIONS INC
ATTN: R EDELMAN

SCIENCE APPLICATIONS INTL CORP
ATTN: C HILL

SCIENCE APPLICATIONS INTL CORP
ATTN: D HAMLIN

SCIENCE APPLICATIONS INTL CORP
ATTN: B MORTON
ATTN: B SCOTT
ATTN: D SACHS
ATTN: G T PHILLIPS
ATTN: J BENGSTOM

SCIENCE APPLICATIONS INTL CORP
ATTN: D BACON
ATTN: DR L GOURE
ATTN: F GIESSLER
ATTN: J COCKAYNE

ATTN: J SHANNON
ATTN: J STUART
ATTN: M SHARFF
ATTN: W LAYSON

SCIENCE APPLICATIONS INTL CORP
ATTN: J SONTOWSKI

SCIENCE APPLICATIONS INTL CORP
ATTN: T HARRIS

SCIENTIFIC RESEARCH ASSOC, INC
ATTN: B WEINBERG

SPARTA INC
ATTN: R HARPER

SRI INTERNATIONAL
ATTN: C WITHAM
ATTN: D GOLDEN
ATTN: D MACDONALD
ATTN: D ROBERTS
ATTN: E UTHE
ATTN: G ABRAHAMSON
ATTN: J BACKOVSKY
ATTN: W CHESNUT
ATTN: W JOHNSON

SRI INTERNATIONAL
ATTN: R BRAMHALL
ATTN: R WOOLFOLK
ATTN: W VAIL

STAN MARTIN ASSOCIATES
ATTN: S B MARTIN

STANTON CONSULTING
ATTN: M STANTON

SWETL, INC
ATTN: T Y PALMER

SYSTEM PLANNING CORP
ATTN: J SCOURAS
ATTN: M BIENVENU
ATTN: R SCHEERBAUM

SYSTEMS AND APPLIED SCIENCES CORP
ATTN: M KAPLAN

TECHNOLOGY INTERNATIONAL CORP
ATTN: W BOQUIST

TELEDYNE BROWN ENGINEERING
ATTN: D ORMOND
ATTN: F LEOPARD
ATTN: J FORD

TELEDYNE BROWN ENGINEERING
ATTN: D GUICE

TEXAS ENGR EXPERIMENT STATION
ATTN: W H MARLOW

TOYON RESEARCH CORP
ATTN: C TRUAX
ATTN: J GARBARINO
ATTN: J ISE

TRW
ATTN: H BURNSWORTH
ATTN: J BELING

TRW ELECTRONICS & DEFENSE SECTOR
ATTN: F FENDELL
ATTN: G KIRCHNER
ATTN: G MROZ
ATTN: H CROWDER
ATTN: J FEDELE
ATTN: M BRONSTEIN
ATTN: R BACHARACH
ATTN: S FINK
ATTN: T NGUYEN

TRW ELECTRONICS & DEFENSE SECTOR
ATTN: M HAAS

VISIDYNE, INC
ATTN: H SMITH
ATTN: J CARPENTER

WASHINGTON, UNIVERSITY OF
ATTN: J I KATZ

FOREIGN

AERE ENVIRONMENTAL AND MEDICAL SC
ATTN: S PENKETT

ATOMIC WEAPONS RESEARCH ESTABLISHMENT
ATTN: P F A RICHARDS

ATOMIC WEAPONS RESEARCH ESTABLISHMENT
ATTN: D L JONES
ATTN: D M MOODY

AUSTRALIA EMBASSY
ATTN: DR LOUGH
ATTN: MAJ GEN H J COATES
ATTN: P PROSSER

BRITISH DEFENCE STAFF
ATTN: C FENWICK
ATTN: J CRANIDGE
ATTN: J EDMONDS
ATTN: M NORTON
ATTN: P WEST

CANADIAN FORESTRY SERVICE
ATTN: B STOCKS
ATTN: T LYNHAM

CSIRO
ATTN: I GALBALLY

CSIRO: ATMOSPHERIC RESEARCH
ATTN: A PITTOCK

EMBASSY OF BELGIUM
ATTN: L ARNOULD

ISRAEL EMBASSY
ATTN: N BELKIND

MAX-PLANCK INSTITUTE FOR CHEMISTRY
ATTN: P J CRUTZEN

MINISTRY OF DEFENCE
ATTN: R RIDLEY

NATIONAL DEFENCE HEADQUARTERS
ATTN: H A ROBITALLE

TRINITY COLLEGE
ATTN: F HARE

DIRECTORY OF OTHER

ATMOS. SCIENCES
ATTN: G SISCOE

BROWN UNIVERSITY
ATTN: R K MATTHEWS

BUCKNELL UNIVERSITY
ATTN: O ANDERSON

CALIFORNIA, UNIVERSITY
ATTN: R WILLIAMSON

CALIFORNIA, UNIVERSITY OF
ATTN: L BADASH/DEPT OF HISTORY

COLORADO, UNIVERSITY LIBRARIES
ATTN: J BIRKS
ATTN: R SCHNELL

DREXEL UNUVERSITY
ATTN: J FRIEND

DUKE UNIVERSITY
ATTN: F DELUCIA

GEORGE MASON UNIVERSITY
ATTN: PROF S SINGER
ATTN: R EHRLICH

GEORGE WASHINGTON UNIVERSITY
ATTN: R GOULARD

GEORGIA INST OF TECH
ATTN: E PATTERSON

HARVARD COLLEGE LIBRARY
ATTN: W PRESS

HARVARD UNIVERSITY
ATTN: G CARRIER

HARVARD UNIVERSITY
ATTN: D EARDLEY

IOWA, UNIVERSITY OF
ATTN: HISTORY DEPT/S PYNE

MARYLAND UNIVERSITY OF
ATTN: A ROBOCK DEPT METEOROLOGY
ATTN: A VOGELMANN DEPT METEOROLOGY
ATTN: R ELLINGSON DEPT METEOROLOGY

MIAMI LIBRARY UNIVERSITY OF
ATTN: C CONVEY

MIAMI UNIV LIBRARY
ATTN: J PROSPERO ATMOS SC

NEW YORK STATE UNIVERSITY OF
ATTN: R CESS

OAK RIDGE ASSOCIATED UNIVERSITIES
ATTN: C WHITTLE

PENNSYLVANIA STATE UNIVERSITY
ATTN: D WESTPHAL

SOUTH DAKOTA SCH OF MINES & TECH LIB
ATTN: H ORVILLE

TENNESSEE, UNIVERSITY OF
ATTN: K FOX

UNIVERSITY OF SOUTH FLORIDA
ATTN: S YING

UNIVERSITY OF WASHINGTON
ATTN: C LEOVY
ATTN: L RAOKE
ATTN: P HOBBS

VIRGINIA POLYTECHNIC INST LIB
ATTN: M NADLER

WASHINGTON STATE UNIVERSITY
ATTN: DR A CLARK

WISCONSIN UNIVERSITY OF
ATTN: P WANG

END
11-87
DTIC